ISBN 978-82-326-2508-6 (printed ver.)
ISBN 978-82-326-2509-3 (electronic ver.)
ISSN 1503-8181

Dragan Gecan

Doctoral thesis

Doctoral theses at NTNU, 2017:218

Dragan Gecan

Techniques for Linearity and Efficiency Improvement by Biasing Gate and/or Drain as Functions of Envelope Power and Introduction of a Novel FOM for Linearity, Applied on GaN PA's

NTNU
Norwegian University of Science and Technology
Thesis for the Degree of
Philosophiae Doctor
Faculty of Information Technology and Electrical Engineering
Department of Electronic Systems

NTNU
Norwegian University of Science and Technology

Doctoral theses at NTNU, 2017:218

NTNU

NTNU
Norwegian University of Science and Technology

Dragan Gecan

Techniques for Linearity and Efficiency Improvement by Biasing Gate and/or Drain as Functions of Envelope Power and Introduction of a Novel FOM for Linearity, Applied on GaN PA's

Thesis for the Degree of Philosophiae Doctor

Trondheim, August 2017

Norwegian University of Science and Technology
Faculty of Information Technology and Electrical Engineering
Department of Electronic Systems

NTNU
Norwegian University of
Science and Technology

NTNU
Norwegian University of Science and Technology

Thesis for the Degree of Philosophiae Doctor

Faculty of Information Technology and Electrical Engineering
Department of Electronic Systems

ISBN 978-82-326-2508-6 (printed ver.)
ISBN 978-82-326-2509-3 (electronic ver.)
ISSN 1503-8181

Doctoral theses at NTNU, 2017:218

Printed by NTNU Grafisk senter

Abstract

Over the past years, a digital cellular system evolved from the GSM providing the voice and text services over the GPRS and EDGE to the 3G and 4G services providing the video and broadband mobile services, and it is now moving forward to the 5G. Consequently, the demand for the wireless data has been dramatically increasing which has led to the development of the more spectral efficient modulation with the increased peak-to-average power ratio (PAPR).

In order to maintain the original information carried by the RF signal, the RF power amplifiers (PAs) have to assure the linear amplification. Traditionally, the class A PA has been used to satisfy the high linearity requirement. Unfortunately, modern modulation schemes with the high PAPR force the class A PA to operate well in back-off to avoid nonlinear amplification of the high signal peaks. This leads to the extremely poor average efficiency and the efficiency decays rapidly as the envelope of the signal decreases. This linearity-efficiency trade-off challenges the PA designers to develop various efficiency and linearity enhancement techniques to satisfy the linearity requirements with as high as possible efficiency.

This dissertation investigates linearization capabilities of a dynamic gate bias technique applied to a 10 W GaN HEMT PA and introduces a Power Gate Tracking (PGT) technique for the PA linearization. It is important to find an optimal matching networks for the PA operating under the dynamic gate bias conditions, so the 10 W GaN HEMT load sensitivity is investigated. Furthermore, a new linearity measure and figure of merit (FOM) is developed, which evaluates the nonlinear distortion both inside and outside of the output signal bandwidth, making it convenient for the linearity evaluation and optimisation. This dissertation also shows that the bandwidth of the dynamic bias or supply voltage can be limited and well defined if the power of the signal is used instead of its envelope like in an envelope tracking (ET) technique. Based on the power tracking principle, a Power Envelope Tracking (PET), 2nd order Power

Envelope Tracking (2nd order PET) and an Auxiliary Power Tracking (APT) techniques for dynamic drain supply operation are also presented. In addition, the PET and the 2nd order PET techniques are combined with the PGT technique in order to improve linearity.

A load-pull measurement of the 10 W GaN HEMT shows that the fundamental load for the maximum output power and the maximum efficiency does not change much with varying the gate bias voltage. There is also an overlapping impedance area for the second and third harmonics tuned for the maximum power added efficiency (PAE). The PA subjected to the dynamic gate bias operation is designed with the selected optimal matching impedances from the load-pull results. The results are showing the improvement of the PA linearity performance if the transfer phase is flattened with the PGT technique while flattening the gain does not provide any linearity improvement. The PET technique results in the simultaneous linearity and efficiency improvement compared to the reference static bias PA with further improvement in the linearity if it is combined with the PGT technique optimised for the presented FOM. The 2nd order PET technique used for the approximation of the ET tracking function shows the comparable efficiency enhancement as the ET technique but with the significantly narrower and well defined drain supply voltage bandwidth. The APT technique shows slightly higher linearity improvement capabilities compared to the auxiliary envelope tracking (AET) technique with significantly narrower drain supply voltage bandwidth due to the power tracking. If the APT technique works in combination with the PGT technique the dynamically biased PA shows further improvement in the linearity performance.

Preface

This dissertation has been submitted in partial fulfilment of the requirement for Philosophiae Doctor (PhD) degree at the Norwegian University of Science and Technology (NTNU) in Trondheim, Norway. The work has been carried out at the Department of Electronic Systems (IES), under the supervision of Associate Professor Morten Olavsbråten and co-supervision of Karl Martin Gjertsen, Senior RF & Microwave Architect at Disruptive Technologies AS. The dissertation is part of the project "Mikrobølgeradio med nettverksfunksjonalitet og teknologi for mobil internett infrastruktur" with the project number 210716, founded by the Research Council of Norway.

Acknowledgments

I would like to thank my supervisor Associate Professor Morten Olavsbråten for his support, guidance and valuable advice helping me to accomplish this goal. I also want to thank my co-supervisor Karl Martin Gjertsen for his valuable contribution. His creative ideas and advice have been of significant importance for this project. I would also like to thank Terje Mathiesen for his guidance and help in the laboratory.

I am also thankful to Cardiff University, especially to Professor Paul J. Tasker, Michael Cabson and Dr James Bell for conceding the laboratory and measurement equipment as well as for their advice and help. I would also like to thank Dr Tudor Williams and Dr Randeep Saini from Mesuro Ltd for their help with the measurement system, Mesuro software and the Cardiff model.

I would also like to thank fellow PhD students for help and advice. Special thanks also goes to my friends for their support and for making everyday life interesting.

Finally, I am most thankful to my father Željko, my mother Karlica and my sister Martina for constant encouragement and support. It would not be possible to do it without you. I would also like to thank my brother in law Josip for his support, to my new born nephew Karlo for bringing the joy to the Skype conversations and to the rest of my family for their role during this valuable adventure.

Dragan Gecan

Trondheim, January 2017

Table of Contents

Abbreviations

ACPR	Adjacent channel power ratio
AET	Auxiliary envelope tracking
APT	Auxiliary power tracking
AM-AM	Amplitude-to-amplitude conversion (distortion)
AM-PM	Amplitude-to-phase conversion (distortion)
BJT	Bipolar junction transistor
CCDF	Complementary cumulative distribution function
CDF	Cumulative distribution function
DDR	Dynamic deviation reduction
DPD	Digital predistortion
DSP	Digital signal processing
DUT	Device under test
EER	Envelope elimination and restauration
ET	Envelope tracking
EVM	Error vector magnitude
FET	Field effect transistor
GMP	Generalized memory polynomial
HBT	Heterojunction bipolar transistor
HEMT	High electron mobility transistor
LP	Load-pull
LUT	Look up table
MESFET	Metal semiconductor field effect transistor
NLPR	Nonlinear-to-linear power ratio

PA	Power amplifier
PAE	Power added efficiency
PAPR	Peak-to-average power ratio
PDF	Probability density function
PEP	Peak envelope power
PET	Power envelope tracking
STDR	Signal-to-total distortion ratio
VNA	Vector network analyser

List of Figures

List of Tables

Chapter 1

Introduction

1.1 Motivation

Over the last years, deployment of wireless communications has increased tremendously and the demand for the higher data rate is growing. One way to achieve higher data rate is to increase the spectrum of a modulated signal. Unfortunately, the spectrum is limited resource and nowadays it is quite occupied. This leads to the usage of the more spectrally efficient modulation schemes, which are capable to "carry" more bits per *Hz* like m-QAM in OFDM, LTE, etc. These modulation schemes are based on the usage of several subcarriers in order to achieve higher spectral efficiency. As a consequence, the envelope variation of the signal becomes larger with the number of subcarriers i.e. the peak to average power ratio (PAPR) of the signal is larger. A power amplifier (PA) that amplifies such signal has to be linear in order to satisfy the spectral mask requirement and in order not to affect an information carried by the signal. The PA also has to be efficient to reduce the power consumption and the cooling hardware size to comply with the environmental and the required space challenges. These requirements are creating huge challenges for the PA designers. For example, the most linear conventional static bias PA is the class A PA. It has a theoretical maximum efficiency of *50 %* at the peak envelope power (PEP). When the class A PA amplifies the signal with varying envelope, its average efficiency decreases as the PAPR of the signal increases due to the back-off operation, and it can be as low as *5 %* for the PAPR of *10 dB* [1].

Today we have a number of different linearization techniques (e.g. feedforward, feedback, predistortion) and efficiency enhancement techniques like envelope elimination and restauration (EER), envelope tracking (ET), and Doherty [2]. Here, the EER and the ET are the

bias modulation schemes, while Doherty is an example of the load modulation scheme. One of the challenges in the ET technique is the design of the supply voltage amplifier (supply voltage modulator or tracker). It must be efficient, so the overall efficiency of the ET system is high. Namely, the efficiency of both the RF PA and the supply voltage amplifier defines efficiency of the overall ET system. This is especially difficult to realise for the modulated signals with wide bandwidth since it becomes more challenging to achieve high linearity and efficiency of the supply voltage amplifier.

The answer to the wide bandwidth requirements of the signal envelope could lie in using the signal power instead. The bandwidth of the signal power is limited to the RF bandwidth which is significantly narrower compared to the envelope bandwidth which is infinite in theory. The power of the signal for the dynamic supply voltage calculation can be applied to the drain/collector as well as to the gate/base. Dynamic bias at the input (gate/base) of the PA can potentially linearize the AM-AM and/or AM-PM characteristics of the PA while it operates in the back-off region. Intuitively, when the PA operates in the compression nothing can be achieved with the input bias voltage. Linearization of the PA in saturation can be done with a recently presented auxiliary envelope tracking (AET) technique [3]. These observations make a lot of room for the experimentation with dynamic bias at the input and/or the output of the PA. One of the challenges in designing the PA for dynamic biasing operation is an optimal matching of the transistor for such operation. Namely, the input and output impedances of the transistor vary with the bias. This means that it is important to analyse the input and output impedances of the transistor under dynamic bias condition and to find the optimal matching networks.

It has been shown that dual dynamic biasing can be used in order to achieve only efficiency enhancement, only linearity enhancement or find an optimal trade-off between the efficiency and linearity [4], [5]. The graphical and analytical approach to find or simultaneously optimise various input (base/gate) and output (collector/drain) tracking functions are presented in several publications by Juan F. Miranda Medina et al, [4]–[7] and Walter Caharija et al. [8]. In this work approach to the dual dynamic biasing is somewhat different. Tracking function at the drain of the HEMT is analytically defined, and the gate tracking functions are optimised for a signal to total distortion ratio (STDR) explained in Chapter 3.

This PhD thesis is funded by Norwegian Research Council (Forskningsrådet) and started as a part of the project at Ceragon Networks AS, Bergen, Norway. The research is focused to the

PAs with high efficiency and linearity for 4th generation mobile networks, exploration of GaN device capabilities and dynamic bias technique based on previous company's exploration.

1.2 The Overview, Scope and Contribution

As mentioned previously, the main challenges in the RF PA design are to achieve both high linearity and high efficiency. This is especially difficult to achieve simultaneously since the linearity and efficiency are conflicting requirements [9]. In this work focus is on dynamic supply voltage techniques applied to the input (gate), the output (drain) or simultaneously to both the input and the output of the 10 W GaN HEMT [10] PA in order to improve its linearity and/or efficiency. Furthermore, the focus is on using the power of the modulated signal instead of the signal envelope for defining/calculating the supply voltage waveforms. This way the bandwidth of the supply voltage is analytically defined and much narrower. This simplifies the design of the voltage amplifier (modulator/tracker).

Outline of the thesis is as follows:

Chapter 2 covers basic background which is important for this work. It introduces different transistor technologies, modulated signal properties and RF PA parameters. Theoretical analysis of the power tracking technique is presented as well. It also explains the concept of various classes of the PA operation as well as various linearization and efficiency enhancement techniques. The measurement techniques important for this work are also presented in this chapter.

Chapter 3 shows the theoretical development of a novel linearity measure and the corresponding figure of merit (FOM). The nonlinear measure is defined as the nonlinear power of the modulated signal and the FOM is defined as a signal to total distortion ratio (*STDR)*. Presented FOM can be used for optimisation of different PA linearization techniques.

Chapter 4 describes the design of the 10 W GaN HEMT power amplifier with the optimal output matching network for the dynamic gate bias operation. It also describes the measurement of the PA for making a behavioural model. Data collected from the measurements later used in the Matlab simulation.

Chapter 5 presents how the dynamic gate biasing (gate tracking) technique can be used for the linearity improvement. It shows that flattening the phase of the RF PA with dynamic gate biasing technique improves its linearity. It also evaluates the behavioural model of observed 10 W GaN HEMT PA. The model is based on one-tone static measurements and used for the gate

tracking function estimation and the CAD simulation with a digitally modulated signal (16-QAM signal in this work). It also presents measured results of the power gate tracking (PGT) PA with the coefficients of the gate tracking function optimised for the *STDR*.

Chapter 6 has a focus on the power tracking i.e. using the power of the modulated signal for the drain supply voltage calculation instead of its envelope like in the envelope tracking (ET). It points out the importance of the gate bias selection for optimal efficiency and linearity operation of the PAs with dynamic drain bias (supply voltage) variation. Next, it presents the ideal power envelope tracking (PET) technique and compares it with the ET technique. The dual dynamic bias operation where dynamic gate bias PGT technique is combined with the PET for the additional linearity improvement is also shown. Section 6.4 shows the 2nd order PET tracking functions with more degrees of freedom, which can closely follow the ET tracking function achieving similar performance with narrower supply voltage waveform bandwidth.

Chapter 7 shows the results of the auxiliary power tracking (APT) linearization technique and compares it with the auxiliary envelope tracking (AET) linearization technique. It also shows the results of the dual dynamic bias operation where the APT technique is combined with the PGT technique (dynamic gate biasing) for additional improvement of the linearity performance.

Contributions of this thesis:

- **Reduced and analytically defined bandwidth of the dynamic gate supply voltage waveform**

  In Chapter 5 it is shown that using the power of the modulated signal for calculation of the dynamic supply voltage results in analytically defined supply voltage bandwidth which is significantly narrower compared to the supply voltage calculated according to the signal envelope.

- **Power Envelope Tracking and 2nd order Power Envelope tracking**

  These two techniques are based on power tracking. Ideal power envelope tracking (PET) PA shows higher linearity and efficiency compared to the static bias PA while its efficiency is lower compared to the ET technique. The 2nd order power envelope tracking has more degrees of freedom so its tracking function can be adjusted to fit much closer to the ET tracking function which results in the similar linearity and the efficiency performance with well-defined and reduced voltage waveform compared to the ET technique.

- **Nonlinear distortion measure and figure of merit (Signal to Total Distortion Ratio – STDR)**

  A novel measure of the nonlinear distortion as total nonlinear power is presented in Chapter 3. Furthermore, a figure of merit STDR as linear to nonlinear power ratio is defined. The STDR evaluates nonlinear distortion inside and outside of the signal bandwidth. Optimisation for STDR can be beneficial for linearity improvement of the total spectral content of the signal. It simultaneously improves ACPR and EVM.

- **Linearity improvement with dynamic gate bias variation**

  Chapter 5 shows that flattening the phase of the 10 W GaN HEMT PA with dynamic gate bias variation significantly improves linearity with maintained efficiency.

- **Linearity dependence of the PAs with dynamic drain bias variation on static gate bias conditions**

  Chapter 6 and 7 are showing that linearity performance of the PAs with dynamic drain supply voltage operation is highly dependent on the static gate bias value. It is possible to find optimal gate bias condition that results in high linearity and preserved efficiency.

- **Load impedance sensitivity of the 10 W GaN HEMT on gate bias variation**

  It is shown that optimal load impedance of the 10 W GaN HEMT for maximum output power and power added efficiency does not vary much for the wide range of the static gate bias voltage values (from deep class AB to the class A). That makes this device suitable to be subjected to the dynamic gate bias operation.

- **Validation of the behavioural model of the 10 W GaN HEMT PA**

  It is shown that behavioural model of the 10 W GaN HEMT PA based on the one-tone static time-domain waveform measurement can be used for simulation in the CAD tool with the digitally modulated signal (16-QAM in this work)

Chapter 2

Background and Theory

2.1 Transistor materials, technologies and types

There is a number of traditional materials and technologies used for the high-frequency solid-state transistors available on the market like III-V materials (gallium-arsenide (GaAs), indium-phosphide (InP)) and silicon (Si). The choice of a material depends on the application and device specification. Recently, only the III-V materials (GaAs) were able to satisfy the required performance at the RF frequencies. However, technology development on the silicon devices changed that, and today we have a variety of the RF silicon devices. Recently, a rather new gallium-nitride (GaN) HEMT transistor, which is the scope of this work, has been increasing its dominance in the high-frequency solid-state power amplifiers. Table 2.1 shows some important semiconductor materials and their properties. The main advantages of the GaN

Table 2.1: Semiconductor material properties

Semiconductor		**Si**	**GaAs**	**InP**	**SiC**	**GaN**
Characteristic	**Unit**					
Bandgap	eV	1.1	1.42	1.35	3.25	3.49
Electron mobility at 300 °K	Cm^2/Vs	1.500	8,500	5,400	700	1,000-2,000
Saturated Electron Velocity	$\times 10^7 cm/s$	1	1.3	1	2	2.5
Breakdown Field	MV/cm	0.3	0.4	0.5	3	3.3
Thermal Conductivity	W/cm °K	1.5	0.5	0.7	4.5	> 1.5
Relative Dielectric Constant	ε_r	11.8	12.8	12.5	10	9

in the high frequency and high power operation is wide bandgap as well as its high saturated electron velocity. Due to its performance benefits and the increase in the market for the wireless communication and defence applications (prediction is that it will double in next few years) the GaN is used and tested in this research.

2.1.1 GaN RF Technology

The GaN is a rather new material, which appeared in the early 1990s. Modern RF applications (defence and commercial) demand more power and wider bandwidths at higher frequencies, and that is where the GaN technology finds its place for competition [11]–[13]. Since there is currently no commercially available native GaN substrates with good mechanical, thermal and electrical properties, the GaN is usually grown on a foreign substrate like silicon-carbide (SiC) or silicon (Si). However, there is continuous research on promising native GaN substrates [14]. Wide bandgap of 3.49 eV which is much higher than 1.42 eV in GaAs and 1.1 eV in Si (Table 2.1) assures a high breakdown voltage for the GaN devices. Due to the high breakdown voltage, GaN can operate at higher voltages which makes it suitable for the high power applications. High saturation velocity of 2.5×10^7cm/s (Table 2.1) assures a higher current density which in combination with the high voltage results in the high power density. The GaN on SiC has excellent thermal properties due to the high thermal conductivity of the SiC (which is much higher than Si). This means that, with a proper cooling, the GaN on SiC does not get nearly as hot as GaN on Si while dissipating the same amount of power which improves its reliability. Because of the high power density, the GaN devices can deliver more power with the same surface area. This property assures lower parasitic capacitance making it suitable for the wide bandwidth applications. Furthermore, smaller devices have lower combining loss so higher efficiency, gain, and power are achievable. Although the GaN on Si does not have as good thermal properties as the GaN on SiC, it is sometimes used in low cost applications.

2.2 Transistor types

Transistors can generally be divided in the bipolar (current is carried by major and minor carriers) and unipolar (current is carried only by major carriers) transistors. In the bipolar junction transistors (BJTs) the output current is controlled by the input current, while in the unipolar field effect transistors (FETs) the output current is controlled by the input voltage.

Both types, BJTs and FETs, can be further divided into the different types [15], [16]. In this section, some of these transistor types are briefly be presented.

2.2.1 Heterojunction Bipolar Transistor, HBT

Due to the demand for higher frequency operation, thinner base regions and higher doping levels are required in the traditional BJT transistors. This results in a higher electric field across the narrow depletion regions and in the rise of leakage effects. Thus, a lot of attention has been devoted to development of more advanced vertical architectures like HBT [15]. Operation of the HBT is generally the same as of the BJT (it has similar vertical structure), but the implementation is essentially different. In the HBT transistor, the base-emitter junction is not the simple *p-n* junction, in one material, as in the BJT. Instead, it uses heterojunction which employs dissimilar materials to provide a barrier between the emitter and the base, allowing heavy base doping, which minimises the base resistance and maximises cut-off frequency. The band diagram of the HBT is shown in Figure 2.1. Increase in the emitter bandgap ($\Delta E_C + \Delta E_V$) increases the barrier between the base and the emitter. That reduces the hole injection from the base to the emitter and results in an increase in the current gain. The most of the HBTs are realised in the III-V technology, but Si HBTs like SiGe HBT are also possible [15]. The HBTs based on the AlGaAs/GaAs and InGaAs/GaAs materials are widely used in the wireless handsets and the GaAs HBTs up to 20 GHz in Monolithic-Microwave-Integrated-Circuit (MMIC) technology [16]. The silicon-germanium (SiGe) HBTs can also be found on the market for the low GHz communication area, although they are not as efficient as the GaAs HBTs [15]. Use of the InP in an HBT results in even higher operation frequencies, higher gain and efficiency due to the low turn-on and the knee voltage [16].

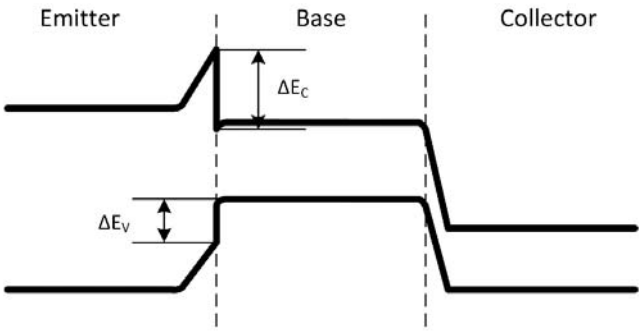

Figure 2.1: Band diagram of a HBT

2.2.2 Metal-Semiconductor Field Effect Transistor, MESFET

In contrast to the bipolar devices, the current flow in an MESFET is parallel (horizontal) i.e. it flows from the source to the drain through the channel placed under the gate of the device. Due to the higher mobility of the electrons compared to the holes, the MESFETs for RF applications are in general manufactured as *n-type* devices [15].

The MESFET transistor is biased with two voltage sources; the gate-to-source voltage V_{gs} and the drain-to-source voltage V_{ds}. With the reverse gate voltage V_{gs}, the depletion region in the channel starts to form, and the channel becomes narrower reducing the current through the channel (from source to drain). If the V_{gs} is constant and the drain voltage V_{ds} starts to increase linearly, the current through the channel starts to increase. Since the electric field at the drain side is higher than on the source side, due to the V_{ds}, the depletion region becomes wider on the drain side making the channel narrower. Although the channel conductive region becomes narrower, the electric field along the channel is higher making electrons to move faster keeping the current to increase further. When the V_{ds} becomes so large that the depletion region spreads across the whole channel, the current becomes constant with further increase of the V_{ds}, due to the electric field increase along the channel. This is so called linear (active) region and current strength in this region can be controlled with the V_{gs} voltage changing the channel width. We can say that MOSFET is the voltage controlled current source [17] in the active region.

The GaAs MESFETs have higher mobility than the Si devices which makes them suitable for the operation at higher frequencies. The SiC MESFET has high mobility and high breakdown voltage. This means that it has the comparable frequency response as the GaAs MESFET, but with much higher power density. High thermal conductivity of the SiC makes it suitable for the high power applications [16].

2.2.3 High Electron Mobility Transistor, HEMT

The operation of the HEMT is similar to that of the MESFET. In order to improve the mobility of the electrons, the HEMT uses different material layers in the vertical architecture. An additional layer separates the conducting channel from its donor parent, which reduces ionised scattering impurity in the channel allowing electrons to achieve higher mobility. In addition, a large electron concentration layer is formed at the well-defined plane, close to the surface of the material structure. In the AlGaAs/GaAs HEMT the *n-doped* AlGaAs layer provides the electrons for the channel, while the undoped AlGaAs spacer layer beneath is introduced to improve the channel mobility and separate donor atoms from the electron

accumulation layer. The high mobility channel formed in the undoped GaAs channel layer results from the fact that the AlGaAs has a larger bandgap than the GaAs, and thus the electrons in the doped AlGaAs donor layer naturally accumulate at the AlGaAs/GaAs interface as it is energetically favourable for them to reside in the GaAs channel layer. The current flows from the source to the drain through the electron accumulation layer usually known as the 2DEG layer [15]. The band diagram of an AlGaAs-GaAs HEMT showing the 2DEG layer is shown in Figure 2.2.

The GaAs HEMTs with f_T as high as 158 GHz are reported. PAs based upon these HEMTs exhibit 15W output as 12 GHz with a power added efficiency (PAE) of 50 %. The outputs of 100 W are available at S band from package devices [16].

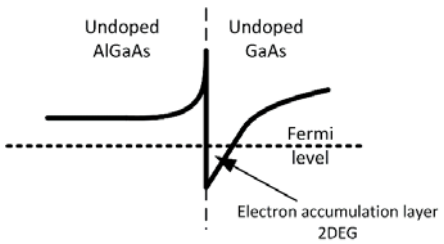

Figure 2.2: Band diagram of an AlGaAs-GaAs HEMT showing the 2DEG channel.

Pseudomorphic HEMT, pHEMT

The channel of the pHEMT is formed from the InGaAs. The addition of Indium increases the channel mobility and, for concentrations in the range of 20-60 %, also slightly increases the effective velocity. Both of these factors are improving the high-frequency performance of the device [15]. The increased mobility of Indium with respect to the GaAs increases the bandgap discontinuity and therefore the number of carriers in the 2DEG layer. The pHEMTs can operate up to the frequency of 80 GHz with the power of 40W in the L band and 100 mW at the V band [16].

The InP HEMT places an AlInAs/GaInAs heterojunction on an InP substrate resulting in even higher mobility and increased velocity. The InP HEMT has higher gain and efficiency compared to the GaAs pHEMT, where the efficiency is beginning to drop at the frequencies around 60 GHz. The thermal resistance is 40 % lower than for the devices built on the GaAs. The drawback is the low breakdown voltage which reduces the maximal operating drain

voltage. This results in the lower output power. Amplification at frequencies up to 190 GHz has been demonstrated [16].

GaN HEMT

As it is described in Section 2.1.1 and reported in Table 2.1, the GaN has advantages like wider bandgap and higher saturation velocity compared to the Si and the GaAs. This results in the higher operating frequencies and the higher power density for the GaN HEMT. In the GaN HEMT, the barrier which isolates the gate and the channel is usually fabricated in the aluminium-gallium-nitride (AlGaN). Aluminium concentration level makes the barrier level higher and, as the consequence, the charge capacity of the channel is higher. This allows larger currents to flow from the source to the drain. The channel is fabricated in the GaN which has high mobility and saturation velocity which provides higher current density. Since there is no native GaN substrate of high quality that is commercially available, the GaN HEMTS are fabricated on the Si or the SiC substrate. Anyway, producing the native GaN substrate with good mechanical and thermal properties is an active area of research. Due to the high thermal conductivity of the SiC, which increases reliability, it is the preferred material. However, the Si based devices are used for low power and low-cost applications. The GaN devices have higher impedances due to the high operating voltages and the high power density. High input and output impedance allow lower transformation ratio in the matching networks. This together with lower output capacitance results in the lower loss and wider bandwidths [11], [18].

A W-band GaN PA based on the new broadband GaN MMIC chip with the 37 W CW (Continuous Wave) across the 75-100 GHz band with the average computed combining the efficiency of 84.5 % has been reported recently [19].

2.3 Microwave Monolithic Integrated Circuit, MMIC

The characteristic of the MMICs is that the complete circuit (active components, passive components, and interconnections) is fabricated on the same piece of the substrate (monolithic architecture). The frequency range of operation spans from 300 MHz to 300 GHz. The benefit of the monolithic architecture is low loss and the dimension in the order of microns. The whole chip size can be a couple of square millimetres in size which is significantly smaller than the equivalent package transistor (microwave integrated circuit, MIC). The small dimension of the MMICs also means low weight [20].

Setting up the MMIC fabrication facility for the mass production is almost prohibitively expensive and time consuming. The functionality of the circuit cannot be checked until the whole process is completed. For these reasons, it is important that the design of the chip is accurate and functional when it is fabricated for the first time. Although setting up a fabrication facility is very expensive, the mass production is cheaper than the circuits with hybrid MICs. The fabricated MMICs require minimal assembly work and manual tuning. Reproducibility is better compared to the MIC since the active and passive components are produced by the same, well controlled fabrication steps. The MMIC reproducibility can be very high in the case of the matured processes. MMICs are more reliable compared to the hybrid circuits, as long as the fabrication process is carefully controlled and quantified [15], [20].

2.4 Signal Properties

The aim of the radio communication systems is to deliver any information carried by the RF signal from the point A to the point B. In digitally modulated signals the information is coded as a binary sequence i.e. string of the bits that are called symbols. Those symbols are then often modulated with the quadrature amplitude modulation (QAM). The QAM modulation uses two separate discrete signals *I(t)* and *Q(t)*, which are orthogonally modulated. The transition time between the symbols cannot be instantaneous due to the infinite bandwidth requirement. Hence, the modulated signal is usually oversampled and filtered with a raised-cosine filter (RC). Oversampling means that the signal is sampled with the sampling rate that is equal or higher than the Nyquist sampling rate (Nyquist sampling rate is the minimum sampling rate that

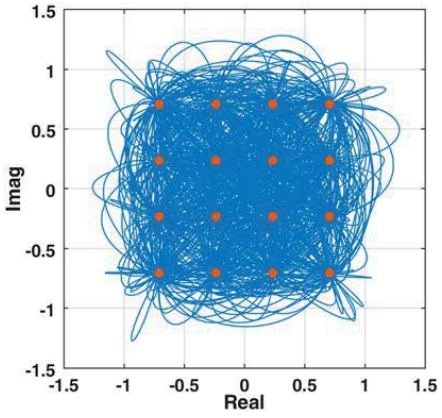

Figure 2.3: 16-QAM signal after oversampling and filtering with the RC filter with the roll-off α=0.22.

preserves the signal information within a limited bandwidth). Oversampling the signal at the rate greater than the Nyquist sampling rate provides the larger frequency zone between wanted and unwanted spectral components, making alias filtering much simpler. An example of the 16-QAM with the RF bandwidth of 1 MHz and trajectories between the symbols is shown in Figure 2.3. In communication systems, that kind of the signal is then upconverted to the carrier frequency, and it consequently varies the envelope of the RF signal.

Every signal can be characterised by parameters like the power spectral density, occupied bandwidth, probability density function and the spectral efficiency. These parameters are described below.

Power Spectral Density

Power spectral density describes the distribution of the signal power within a certain bandwidth. It is an individual property of the signal which is strongly dependent on the modulation applied [21]. An example of the power spectral density is shown in Figure 2.4.

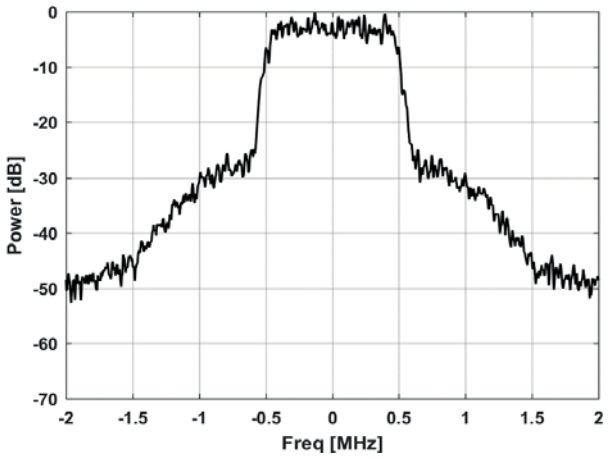

Figure 2.4: Power spectral density (normalised) of the 16-QAM signal with the RF bandwidth of 1 MHz.

Occupied Bandwidth

Occupied bandwidth is usually defined as the frequency range that contains *99 %* of the signal's power. This means that *0.5 %* of the power is radiated below the minimum signal's frequency and *0.5 %* above the maximum signal's frequency [22]. However, the signal bandwidth can be separated into two categories. One is the necessary bandwidth based on the

signal itself, and it is the total bandwidth of the transmitted signal that must be applied to the demodulator for proper demodulation of the signal. Another one is the bandwidth allocated by the government or other regulations. The latter tells us how much of the signal bandwidth including spurious components (spectral regrowth) is allowed to be transmitted through the channel [21].

Spectral Efficiency

Spectral or bandwidth efficiency of the modulated signal is the measure of how many bits can be transmitted per second within the signal bandwidth in *Hz* and it is measured in *bit/s/Hz*.

Peak to Average Power Ratio, PAPR

The peak to average power ratio (PAPR) is an important parameter of the signals with the varying envelope. It is defined as the ratio of the peak envelope power and the average power of the signal (2.1). In other words, it gives information about how much higher the peak power is compared to the average power of the signal. In general, the efficiency of the PA decreases as the PAPR increases due to the increased back-off.

$$PAPR_{dB} = 10log_{10}\frac{P_{peak}}{P_{rms}} \tag{2.1}$$

Probability Density Function, PDF

When the signal has varying envelope power, each power level of such signal has its occurring probability. That probability can be presented as the PDF function showing the

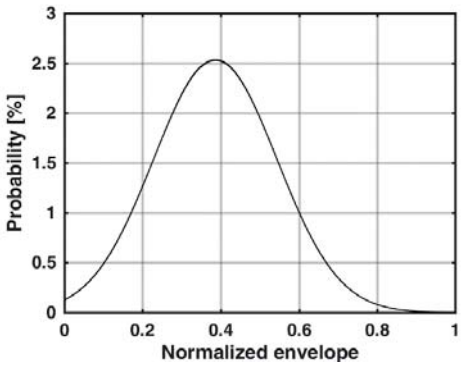

Figure 2.5: Probability density function (PDF) of the finite 16-QAM signal envelope.

probability over the power or envelope dynamic range of the observed signal. Figure 2.5 shows an example of the PDF function of the finite 16-QAM signal. Another way of presenting probability is a cumulative distribution function (CDF) and complementary cumulative distribution function (CCDF). The former shows the probability that the envelope is less than or equal to the particular value, while the latter shows the probability that the envelope of the signal is above its average level. Probability functions are useful tools in the PA design for avoiding compression of the envelope peaks.

More detailed reading about modulated signals and parameters can be found in [21].

2.5 Power Tracking

2.5.1 Power Tracking vs. Envelope Tracking

Let's consider a complex, time varying signal *v(t)* with the RF bandwidth B_{RF} in the form

$$v(t) = v_r(t) + jv_i(t). \tag{2.2}$$

Envelope of the signal (2.2) can be defined as

$$v_e(t) = |v(t)| = \sqrt{v_r(t)^2 + v_i(t)^2} \Rightarrow B \to \infty. \tag{2.3}$$

It can be seen from the equation (2.3) that the envelope of a complex signal has an infinite bandwidth since it is the function of the square root. This means that the bandwidth of the drain supply voltage shaped according to the signal envelope also has the infinite bandwidth. The drain voltage in the ET system is defined as shown in (2.4).

$$V_{ddET}(t) = k'_1 v_e(t) + k'_0 \tag{2.4}$$

The power of the signal (2.2) is defined as

$$p(t) = v(t) \cdot v^*(t) = v_r(t)^2 + v_i(t)^2, \tag{2.5}$$

and the power envelope of the (2.5) can now be defined as

$$p_e(t) = {v_e}^2 = v_r(t)^2 + v_i(t)^2 \Rightarrow B = B_{RF}. \tag{2.6}$$

From the equation (2.6) it can be seen that the signal power bandwidth is analytically well-defined and limited to the value of the RF bandwidth B_{RF}. This means that the bandwidth

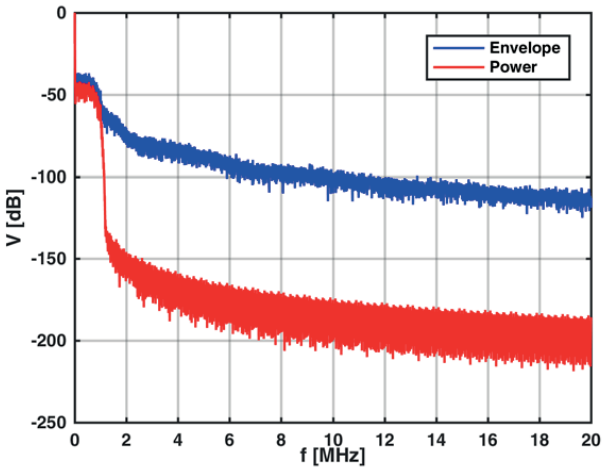

Figure 2.6: Bandwidth of the envelope and the power or the 16-QAM signal with 1 MHz RF bandwidth.

requirement of the voltage tracking amplifier (modulator) is significantly lower if one uses the power tracking instead of the envelope tracking technique. As an example, Figure 2.6 shows the bandwidth of the envelope and the power of the 16-QAM signal with *1 MHz* RF bandwidth filtered with the raised cosine filter ($\alpha = 0.22$), applied to the test amplifier. It can be clearly seen that the power has well-defined bandwidth which is significantly narrower compared to the envelope bandwidth.

As it is shown in the next section, the power envelope tracking (PET) [23] technique, by its nature, results in the lower efficiency than the ET technique due to the poorer fitting of the PET drain voltage waveform to the envelope of a signal. However, there is a possibility to use the 2nd order polynomial function with the power as the variable which can approximate the envelope tracking function closely and still have a significantly narrower bandwidth of the drain voltage waveform [23] and comparable efficiency to the ET technique.

2.5.2 Power Envelope Tracking and Second Order Power Envelope Tracking

Power tracking of the signal envelope can be extended to the higher order power tracking as shown by equation (2.7).

$$V_{dd,nPET}(t) = \sum_{n=1}^{N} k_n p(t)^n + k_0 = \sum_{n=1}^{N} k_n v_e(t)^{2n} + k_0 \tag{2.7}$$

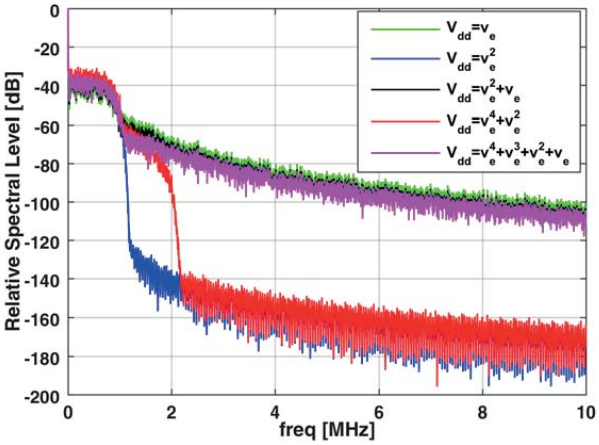

Figure 2.7: Spectral bandwidth of the drain voltage for up to the 4th order envelope tracking with and without the odd order power elements.

It is important to note that the order *n* of the power tracking corresponds to the order *2n* of the envelope tracking containing only even powers. Consequently, the square root function from (2.3) is cancelled in (2.7) since the odd powers of *n* are removed from the equation and the bandwidth of the drain voltage $V_{dd,nPET}(t)$ is nB_{RF}. The spectral bandwidth of the drain voltage $V_{dd}(t)$ for up to 4th order envelope tracking with and without the odd power elements is shown in Figure 2.7. It can be clearly seen that the drain voltages calculated without the odd power elements *n* in the equation (2.7) have much narrower and well-defined bandwidth. Note that the 2nd order envelope tracking without the first order power element (coefficient) corresponds to the power tracking and the 4th order envelope tracking without the odd order powers (the first and the second order element/coefficient) corresponds to the 2nd order power tracking.

With the power of the modulated signal defined as in the equation (2.5) the PET [23] drain voltage waveform is defined as shown in the equation (2.8).

$$V_{ddPET}(t) = k_1 p(t) + k_0 = k_1 v_e{}^2(\mathrm{t}) + k_0 \tag{2.8}$$

There are also some requirements that have to be defined in addition to the equation (2.8) for the ideal PET. The first requirement is that the drain supply voltage $v_{dd}(t)$ should never exceed the maximum value at the maximum drive level as in the ET technique (2.9).

$$V_{ddPET,max} = V_{ddET,max} = k_1 {v_{e,max}}^2 + k_0,$$
$$V_{ddET,max} = {k'}_1 v_{e,max} + {k'}_0 \tag{2.9}$$

The second requirement is that the drain supply voltage of the PET follows the drain voltage of the ET as close as possible. That is, for the ideal case, when the derivative of the PET and the ET voltage is equal at the maximum drive level (2.10).

$$\frac{dv_{ddPET}}{dv_e}(v_{e,max}) = \frac{dv_{ddET}}{dv_e}(v_{e,max}) \tag{2.10}$$

The PET tracking function (2.8) with satisfied requirements (2.9) and (2.10) significantly differs from the ET tracking function as shown in Figure 2.8. In order to follow the ET tracking curve more closely, the order of the equation (2.8) is increased, resulting in the second order power envelope tracking (2nd order PET). The 2nd order PET tracking function is defined by equation (2.11).

$$V_{dd,2ndPET}(t) = k_2 p^2(t) + k_1 p(t) + k_0 = k_2 {v_e}^4(\mathrm{t}) + k_1 {v_e}^2(\mathrm{t}) + k_0 \tag{2.11}$$

The 2nd order PET provides more degrees of freedom than the PET allowing better fitting to the ET tracking function. It is also important to be aware that the bandwidth of the $v_{dd}(t)$ of the 2nd order PET is twice the bandwidth of the PET bandwidth or twice the RF bandwidth i.e. B_{2ndPET}

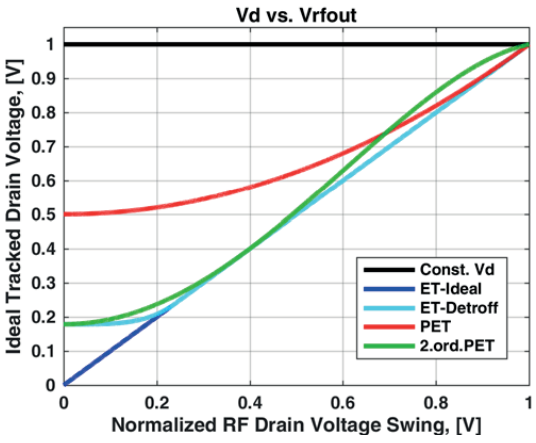

Figure 2.8: Ideal drain tracking functions as the function of the signal envelope [23].

$= 2B_{PET} = 2B_{RF}$. This is the consequence of the second order coefficient in (2.11). However, this is still analytically well-defined and narrower bandwidth compared to the ET technique.

The tracking functions of the ET, detroughed ET, PET and the 2nd order PET are shown in Figure 2.8 [23]. Voltages of the output signal (drain voltage swing) and the drain supply voltage are normalised. Detroughing of the ET function (clipping at the certain minimum drain voltage value) is common in the ET technique in order to avoid the gain collapse below the knee voltage of the transistor. The 2nd order PET tracking function coefficients can be chosen so that it has the same minimum and maximum $v_{dd}(t)$ value and the same derivative (2.10) at these points as the detroughed ET tracking function. The midpoint of the 2nd order PET tracking function is selected so that the $v_{dd}(t)$ is never lower than for the ET case in order to get the closest approximation of the detroughed ET tracking function. Note that if $v_{dd}(t)$ would have values lower than the ET function for some drive levels, it would lead to the deeper compression of the RF PA which may be unwanted behaviour.

2.6 RF PA Parameters

The task of the RF PAs is to increase the power of the signal by converting the DC power to the RF power. The amplified version of the signal should not be distorted in order to preserve the original information i.e. the amplification has to be linear. In order to maintain the battery life in the handsets, reduce the cooling requirement and finally reduce the expense, the linear amplification has to be done with high efficiency. To evaluate these characteristics of the PAs, some important parameters like the linearity, efficiency, gain, bandwidth, etc. have to be defined. This section presents some of these parameters.

2.6.1 Linearity

According to the energy conservation principle, the power that enters the PA (power of the input signal and the DC power) has to be equal to the power that comes out of the PA (the power of the output signal and the dissipated power). Since the DC power is limited, the power at the output of the PA is limited. Because of this limitation, the gain has to drop for the high input signal level i.e. the gain compression occurs, which leads to the nonlinear amplification of the signal.

In the memoryless PAs the nonlinear behaviour can be modelled with the AM-AM and the AM-PM conversions. The AM-AM conversion describes how is the amplitude of the output

signal related to the amplitude of the input signal, while the AM-PM conversion describes how is the phase transfer from the input to the output of the PA related to the amplitude of the input signal [2], [24].

When the signal bandwidth is comparable to the inherent bandwidth of the PA, the frequency dependent behaviour occurs, and output signal is not dependent only on the instantaneous input signal, but it also depends on the previous states of the signal. The time lag or the phase shift of the signal passing through the amplifier is different for the individual frequency components inside the signal bandwidth i.e. the AM-AM and the AM-PM characteristics are different for different spectral components of the signal, resulting in the asymmetric intermodulation components generated with the odd order nonlinearities. These bandwidth dependent phenomena are called the *memory effects*. The memory effects are not usually detrimental for the linearity of the PA, but they add to the total distortion and can decrease the effect of the linearization technique applied to the PA [24], [25]. The memory effects can be divided into the short- and long-term memory as well as to the nonlinear and linear memory effects. The most difficult to cope with are the long-term nonlinear memory effects because the duration is longer than the period of the carrier or even the symbol duration of the signal [26]. The sources of the long-term memory are the bias networks, the self-heating, and the trapping phenomena in the semiconductor.

There are several measurement standards for the PA linearity evaluation for the multitone or modulated signals. Most common are the adjacent channel power ratio (ACPR) and the error

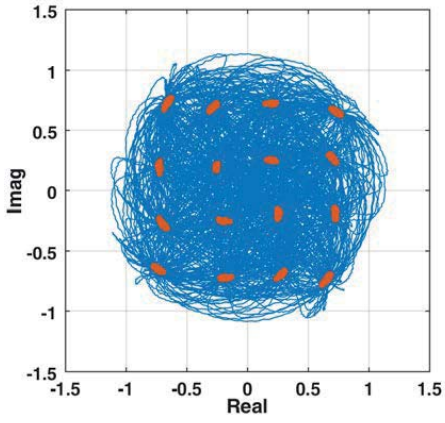

Figure 2.9: Distorted 16-QAM signal.

vector magnitude (EVM) and these are described below. A distorted version of the 16-QAM signal from Figure 2.3 is shown in Figure 2.9.

Adjacent Channel Power Ratio – ACPR

The ACPR is the linearity measure of how much the signal spreads into the adjacent (neighbouring) channels i.e. it evaluates the linearity outside of the signal bandwidth (outside the main channel). The power of the signal in the main channel appears in the adjacent channels due to the spectral regrowth caused by the odd order nonlinearities in the PA and that power, if it is too high, can affect the signal in the neighbouring channel. From these reasons the maximum amount of the signal that can appear in the adjacent channel has to be defined. The ACPR can be defined for the lower and the upper adjacent channel ($ACPR_l$ and $ACPR_h$) and it is defined as the ratio of the power contained inside the adjacent channel and the power contained inside the main channel (2.12).

$$ACPR = \frac{P_{adjacent}}{P_{main}} \tag{2.12}$$

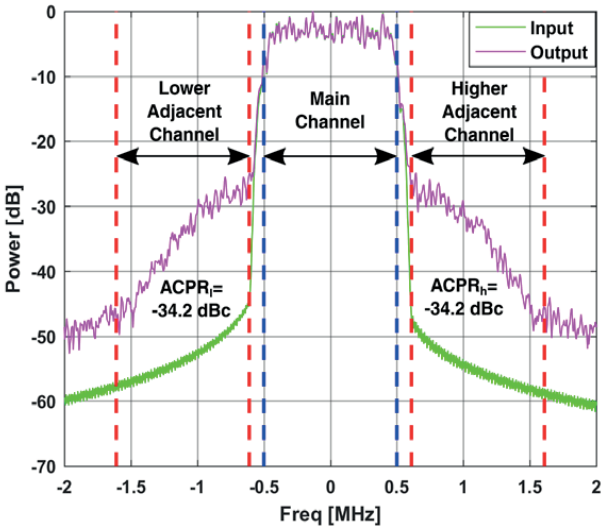

Figure 2.10: Adjacent channel power ratio (ACPR) for the lower and higher neighbouring channels of the distorted output 1 MHz 16-QAM signal.

Figure 2.10 shows the power bandwidth of the 16-QAM signal at the input and the output of the PA with the defined main and adjacent channels and the lower and the higher *ACPR* values. The input and the output powers are normalised i.e. the gain is set to 1.

Error Vector Magnitude – EVM

For the modulation schemes based on the quadrature amplitude modulation like the m-QAM, the symbols of the distorted signal are displaced from their ideal position in the I-Q constellation diagram (see Figure 2.9). The distortion that appears inside of the signal's bandwidth can be evaluated with the error vector magnitude (EVM). The concept of the EVM measure is shown in Figure 2.11. The AM-AM or the amplitude distortion and the AM-PM or the phase distortion are displacing the symbol from its ideal I-Q position in the constellation. That displacement can be evaluated by the error vector (Figure 2.11).

For the signal sequence of the *N* symbols, the RMS EVM is defined as:

$$EVM_{RMS} = \sqrt{\frac{\sum_{k=1}^{N}(e_k)}{\sum_{k=1}^{N}\left(I_k^{ref\,2} + Q_k^{ref\,2}\right)}} \cdot 100. \tag{2.13}$$

$$e_k = (I_k^{ref} - I_k^{meas})^2 + (Q_k^{ref} - Q_k^{meas})^2, \tag{2.14}$$

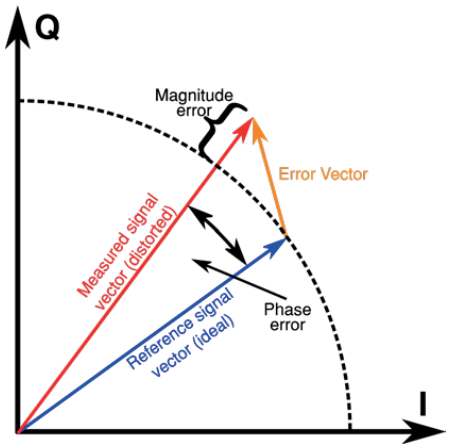

Figure 2.11: Error vector magnitude (EVM) concept illustration.

where I_k is the in-phase (real) value of the *k-th* symbol in the sequence, Q_k is the quadrature phase (imaginary) value of the *k-th* symbol in the sequence. The EVM can be calculated for each individual symbol as:

$$EVM_k = \sqrt{\frac{e_k}{\frac{1}{N}\sum_{k=1}^{N}\left(I_k^{ref^2} + Q_k^{ref^2}\right)}} \cdot 100. \tag{2.15}$$

The maximum EVM for the sequence can be found as the $EVM_{max}=max\{EVM_k\}$ where $k \in [1\ldots N]$ [27].

Signal to Total Distortion Ratio, STDR

The STDR is a novel linearity measure [28] which simultaneously evaluates nonlinear distortion inside and outside of the signal bandwidth caused by any distortion source including the memory effects. It can be a powerful tool as a figure of merit (FOM) for optimisation of transmitters and the power amplifiers for the linearity and the output power performance [28]. The STDR is explained in detail in Chapter 3.

2.6.2 Efficiency

The efficiency tells as how efficiently the DC power is used for the amplification and it has high importance for the RF PAs. For example, in the handsets where the PAs are powered by batteries, the higher efficiency means longer battery lifetime. Efficiency is also important for the high power stationary equipment due to the cost of the electrical energy, the cooling requirement (size and cost), and the lifetime of the equipment (less dissipation means the lower

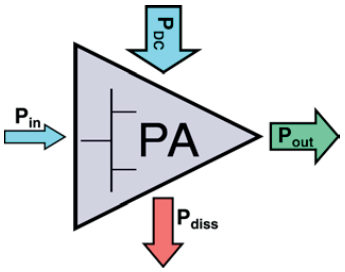

Figure 2.12: Power flow in the RF PAs.

temperature of the active device). Generally, efficiency can be defined as the usable power coming out of the PA divided by the power coming into the PA. Since power is delivered to the PA and it comes out of the PA in more than one way, we can define several different types of the efficiency. Figure 2.12 shows the input and the output power flow of the PA used for various efficiency definitions. Most common definitions are the drain efficiency, the power added efficiency and the overall efficiency [29].

Drain Efficiency

The drain efficiency is defined as the ratio of the output power of the PA (dissipated at the load) and the DC power from the DC power supply

$$\eta = \frac{P_{out}}{P_{DC}} \tag{2.16}$$

where $P_{DC}=V_{DC}I_{DC}$ and P_{out} is the power of the fundamental harmonic i.e. usable power (Figure 2.12). In the case of the PAs based on the bipolar technology that type of efficiency is called collector efficiency.

Power Added Efficiency – PAE

Designers often like to take into account the input RF power in addition to the DC power because it can be significant in the RF PAs. This type of the efficiency is called power added efficiency (PAE)

$$PAE = \frac{P_{out} - P_{in}}{P_{DC}} = \frac{P_{out} - \frac{P_{out}}{G}}{P_{DC}} \tag{2.17}$$

where $G=P_{out}/P_{in}$ is the power gain of the PA. Generally, if the RF gain is less than 10 dB, then the drive power requirements starts to take a serious bite out of the drain efficiency of the PA, and the higher the efficiency, the more severe the effect [30].

Overall Efficiency

The overall efficiency includes the drive power of the PA into efficiency equation in a different way

$$\eta_{overall} = \frac{P_{out}}{P_{DC} + P_{in}} = \frac{P_{out}}{P_{DC} + \frac{P_{out}}{G}}. \tag{2.18}$$

In general, the RF PAs designed for the high drain efficiency tend to achieve low power gain, which is a disadvantage for the overall power budget. As for the PAE, if the gain is low, the drive power can significantly influence the overall efficiency despite the drain efficiency. Note that overall efficiency cannot be less than 0 as it can be the case for the power added efficiency.

2.7 Linear Classes of the Power Amplifiers

The basic RF power amplifiers can be classified in the most common classes as the class A, AB, B, C, D, E and F. The class A is a linear class, the classes AB, B and C are the classes with the reduced conduction angle [30]. The classes D and E are the switching mode classes, while the class F can be designed around the switching transistor, as it is done originally, or designed around the class B PA. It is also important to note that the classes E and F are harmonically tuned PA classes. In this section, the non-switching classes are presented. The basic concepts of the single ended power amplifier for the classes A, AB, B, and C are illustrated in Figure 2.13. Figure 2.14 shows the set of the I-V curves for the FET transistor with the quiescent bias points for the classes A, AB, B, and C with the corresponding loadlines.

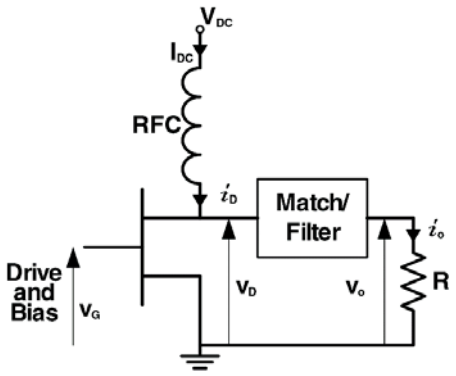

Figure 2.13: Basic circuit of the single ended power amplifier (from [2]).

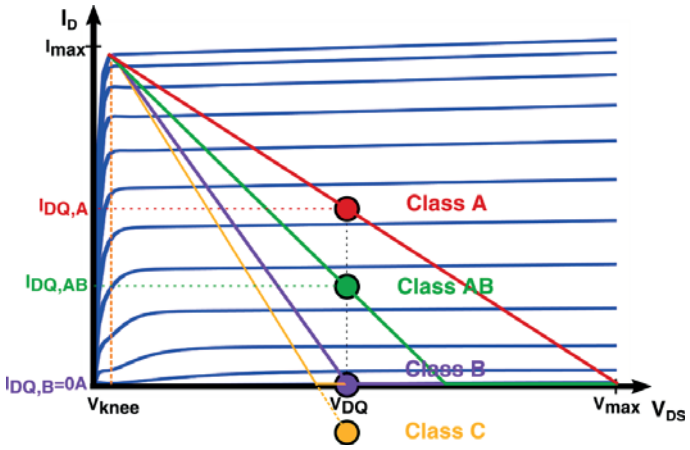

Figure 2.14: I-V curves, the Class A, AB, B and C bias points with the corresponding load-lines.

2.7.1 Class A

The class A power amplifier is biased so that the quiescent bias point (the quiescent drain current I_{DQ} in combination with the quiescent drain bias voltage V_{DD}=V_{DQ}) is placed as shown in Figure 2.14. The transistor is in the active region during the entire RF cycle i.e. the conducting angle of the amplifier is 360°. Consequently, the output current and voltage are ideally sinusoidal for the sinusoidal input as it is shown in Figure 2.15. If we assume that all the components of the circuit in Figure 2.13 are ideal with no losses, the transistor is an ideal voltage controlled current source with a linear transfer curve; the output power can be expressed as

$$P_{out} = \frac{V_o I_o}{2} = \frac{V_o^2}{2R}, \tag{2.19}$$

and the DC power from the power supply can be expressed as

$$P_{DC} = V_{DC} I_{DC}. \tag{2.20}$$

For the ideal class A PA maximum output current with full swing is $I_{o,max}$=I_{max}, and the maximum output voltage is $V_{o,max}$= V_{DC} giving the maximum output power

$$P_{out,max.} = \frac{V_{DC} I_{max}}{2} = \frac{V_{DC}^2}{2R}. \tag{2.21}$$

Now we can express drain efficiency of the ideal class A PA as:

$$\eta = \frac{P_o}{P_{DC}} = \frac{V_o I_o}{2 V_{DC} I_{DC}} = \frac{1}{2}\frac{V_o^2}{V_{DC}^2}. \tag{2.22}$$

The maximum theoretical efficiency can be calculated from the expression (2.22) by substituting P_o with $P_{o,max.}$ (2.21) or V_o with $V_{o,max} = V_{DC}$, and it is $\eta = 1/2 = 50\ \%$. The maximum efficiency is achieved only for the peak envelope power (PEP). For the practical circuits, the drain efficiency is usually *40-45 %* [29]. If it operates in the back-off or with a digitally modulated signal with varying envelope, the average drain efficiency is significantly lower. For the example, it can drop to $\eta = 5\ \%$ when operating 10 dB in the back-off [1].

The class A PA presents the linear transfer characteristic and the high power gain. However, because of the low efficiency, the class A amplifiers are most often used as low-level drivers for the more efficient PAs. In such applications, the class A amplifier consumes only a small portion of the total DC power, and the overall efficiency is not significantly affected [29].

2.7.2 Class B

The gate bias for the class B PA is set so that the quiescent drain current does not flow ($I_{DQ} = 0$ *A)* (Figure 2.14). Consequently, the transistor is in its active region only during half the cycle of the RF signal (the conduction angle is 180°) and for the sinusoidal drive the output current is half the sinusoid (see Figure 2.15). Since the output power of the class B PA is proportional to the drive power, the instantaneous efficiency also changes with the drive power. The output power is defined as shown in the equations (2.19) and (2.21). Due to the reduced conduction angle, the necessary DC power for the maximum output power is:

$$P_{DC} = V_{DC} I_{DC} = \frac{2}{\pi}\frac{V_{DC}}{R} V_D. \tag{2.23}$$

Drain efficiency is then:

$$\eta = \frac{P_o}{P_{DC}} = \frac{\pi}{4}\frac{V_D}{V_{DC}}. \tag{2.24}$$

The maximum theoretical drain efficiency of the class B PA for the PEP when $V_D = V_{DC}$ is $\eta = 4/\pi = 78.5\ \%$. The drain efficiency of the practical class B PA can be between *60* and *70 % [29]*. The class B PA is significantly more efficient than the class A PA. According to [1], the

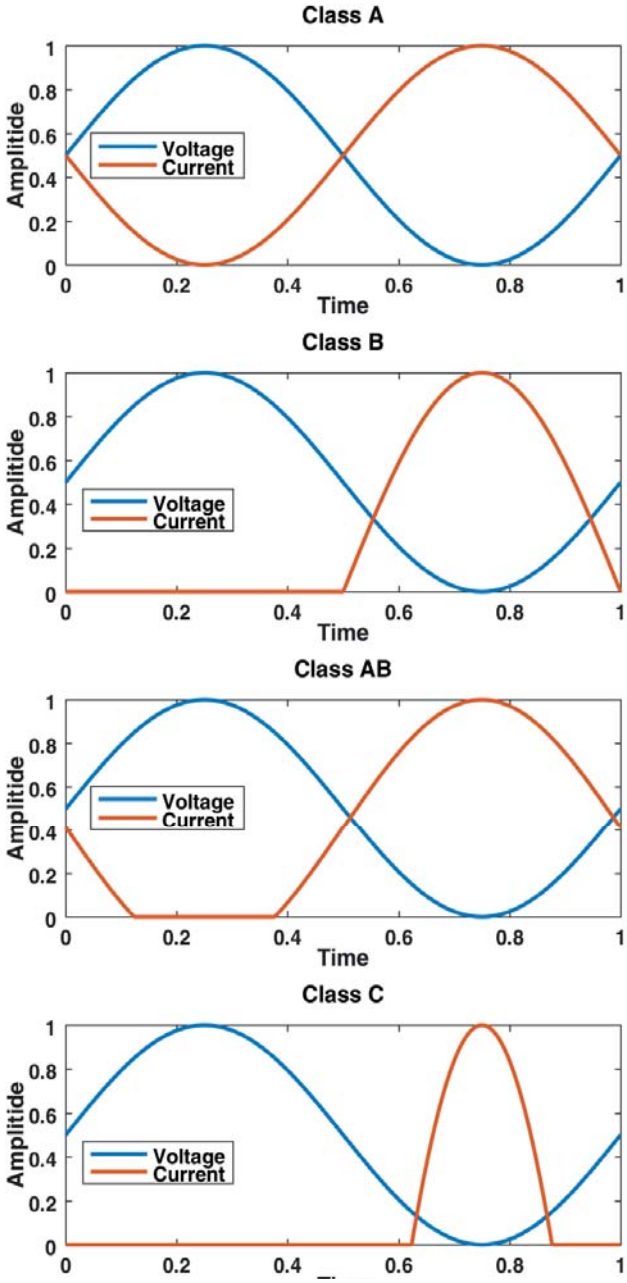

Figure 2.15: Normalized output voltage and current waveforms for the PA classes A, B, AB, and C.

efficiency of 28 % can be achieved when the class B PA operates 10 dB in the back-off, which is a significantly higher efficiency compared to the 5 % with the class A. In order to achieve the maximum efficiency performance; the class B PAs must have a significantly higher drive than the class A PAs. This results in the lower power gain.

With the assumption that the circuit is ideal and that all the high harmonics are short-circuited, the class B PA may be considered as the linear power amplifier. However, there is some serious distortion going on [30]. Furthermore, the real transistor does not change abruptly from the cut-off region to the active region. The transition is gradual, nonlinear and involves the offset/knee voltage [29]. Therefore, the linearity of the class B PA is worse compared to the class A PA. That is the price paid for the higher efficiency.

2.7.3 Class AB

The transistor in the class AB PA is biased between the class A and the class B so that it conducts for more than half of the RF cycle but less than the full RF cycle i.e. the conduction angle is between *180°* and *360°* (see Figure 2.14). Since the conduction angle is between the class A and the class B, the distortion is consequently greater than in the class A PA, but less than in the class B PA. Conversely, the efficiency is less than that of the class B but greater than that of the class A PA. Linearity versus efficiency trade-off depends on the static bias which can be closer to the class A PA or to the class B PA (Figure 2.14) [2]. Normalised voltage and current waveforms are shown in Figure 2.15.

2.7.4 Class C

The class C PA is biased below the threshold voltage (Figure 2.14) so that the transistor stays in its active region for less than half of the RF cycle (the conduction angle is less than 180°). Consequently, the drain efficiency gets higher, but the linearity is getting worse. Therefore, the class C PAs are convenient for the applications where linearity is not important. The efficiency can be increased toward *100 %* by decreasing the conduction angle toward zero. Unfortunately, this causes the output power to decrease toward zero and the drive power to increase toward infinity. A typical compromise is the conduction angle of *150°* with the theoretical efficiency of *85 % [1]*. Normalised voltage and current waveform are shown in Figure 2.15.

2.7.5 Harmonically Tuned Class F

The class F amplifier [30] increases efficiency and the output power by terminating the higher voltage and current harmonics to shape a square voltage waveform, and a half sine rectified current waveform. Generally, presenting the open termination to the odd harmonics shapes the voltage as the square wave, while presenting the short termination to the even harmonics shapes the current as the half sine rectified wave (like class B). Originally, it has been developed from the switching mode class E type of amplifier, but today it is usually developed around the class B PA.

Since harmonics with very high order do not significantly contribute to the waveform shaping because the power of these harmonics is too low, it is common to use harmonics up to 3rd or 5th order. Adding the odd harmonics with correct amplitude to the voltage waveform

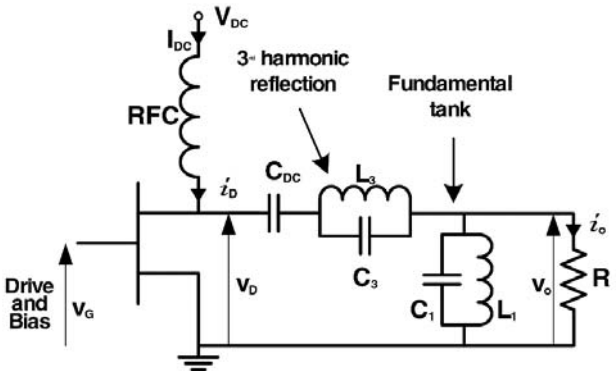

Figure 2.16: Class F power amplifier basic configuration (from [2]).

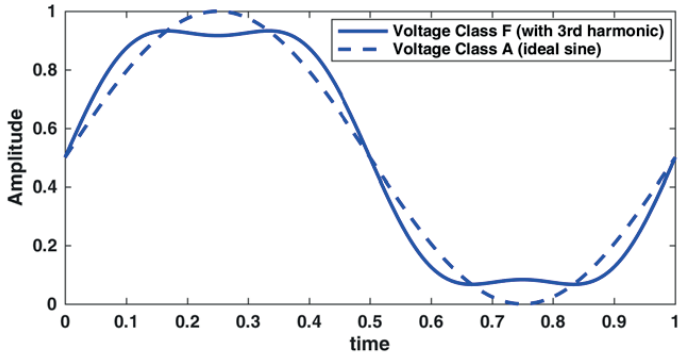

Figure 2.17: Class F power amplifier voltage waveform with the 3rd harmonic and the ideal sine voltage waveform (Class A).

approximates the square wave while adding the even harmonics with correct amplitude to the current waveform approximates the half sine wave. The half sine current waveform can also be achieved with the PA biased in the class B. Shaping the class F waveforms (voltage and current) at the internal current source of the transistor minimises the overlap of the voltage and the current waveforms. Minimising that overlap means less dissipation of the power inside of the device and leads to the higher efficiency. As the number of the harmonics increases, the efficiency of an ideal PA increases from *50 %* (class A) to *100 %* (class-D) [1]. The basic configuration of the class F PA with reflected 3rd harmonic is shown in Figure 2.16. The 3rd harmonic reflection, with correct amplitude and phase, squares up the voltage waveform. Figure 2.17 shows voltage waveform of the class F PA with added optimal amount of the 3rd harmonic and ideal sinusoidal voltage. It is important to note that squaring the voltage waveform allows the amplitude of the fundamental harmonic to be higher. Consequently, the class F PA achieves higher output power performance.

2.8 Efficiency enhancement techniques

The maximum efficiency of the power amplifier is achieved when the input drive is large enough for the PA to operate at the peak envelope power (PEP). The problem arises when the PA amplifies the signals with varying envelope. Namely, while the PA amplifies the signal with varying envelope, it is not saturated all the time (it operates in the back-off for the low signal levels). That significantly reduces efficiency and increases the power dissipation. This problem has been more or less solved over the years by applying different efficiency enhancement techniques.

2.8.1 Doherty

The basic concept of the Doherty PA [31] is shown in Figure 2.18. The Doherty efficiency enhancement technique is based on a dynamic load operation. The RF load impedance changes dynamically by introducing an additional current source in the PA's circuit. The main PA is employed to amplify the lower power, and the peak PA is employed to amplify the high power levels of the signal. That way both PAs are operating at the PEP with the maximum efficiency. The peak PA is usually biased in the class C so it is turned off until the power of the signal is increased to the certain level.

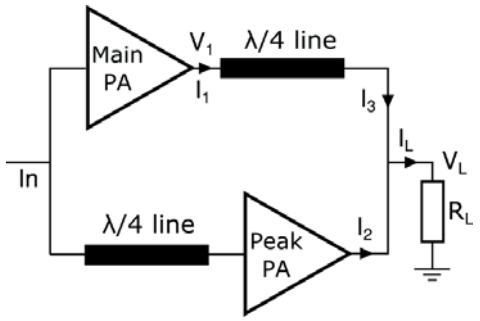

Figure 2.18: Doherty amplifier.

For the low power levels, only the main PA is active, and it delivers the RF power to the load. As power increases and the main PA reaches saturation operating at its maximum efficiency, the peak PA turns on, and that is the point when the main action occurs. It is common that the peak PA turns on with the *6 dB* input signal back-off. The impedance that is presented to the main PA is dependent on the current I_2 from the peaking PA. By modulation of the load, the main PA stays saturated and acts as the voltage source operating at the maximum efficiency, while the currents I_2 and I_3 are increasing. At the PEP both power amplifiers are saturated and with the maximum efficiency [30]. Figure 2.19 shows the efficiency versus input power of the Doherty PA with the auxiliary PA (the peak PA) biased in the class B. The dip that appears in the upper part of the input power would be smaller if the auxiliary PA would be more efficient i.e. if it would be biased in the class C [30].

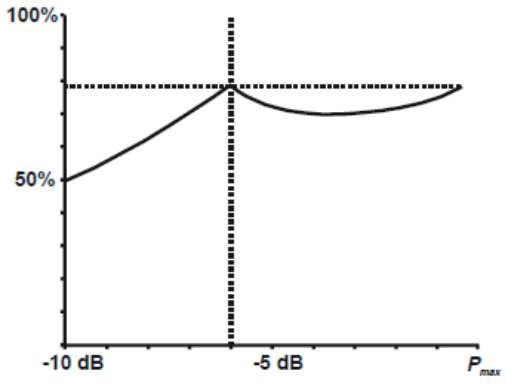

Figure 2.19: Doherty amplifier, efficiency versus input power back-off [30].

The Doherty technique can be a good choice for the efficiency enhancement, but the requirement for the transmission lines makes it narrowband. The linearity of the Doherty is not good, but in modern Doherty systems, the digital signal processing (DSP) can be used to control the drive and the bias of the PAs as well as implementing the digital predistortion (DPD) systems improving linearity [16].

2.8.2 Outphasing

Although the outphasing technique presented by Henric Chireix [32] is known for 80 years now, in recent years it has got a new attention from researchers. The main idea of this technique is to use nonlinear but efficient amplifiers to achieve the linear output signal. The simplified outphasing transmitter architecture is presented in Figure 2.20. Both PAs are amplifying signals with only the phase information i.e. the signals with the constant envelope. That allows usage of the saturated class C, switching classes D or E or the class F PAs which are highly efficient [1]. The phase control of the signal in each branch, which is the function of the envelope of the input signal, controls the amplitude (envelope) of the output signals. In other words, it uses two constant-envelopes, the phase-modulated signals (2.25) to produce a complex modulated output signal. At the combining network in the outphasing system, the interaction between currents from the PAs in each path results in the load modulation.

$$x_1 = V_0 e^{j(\varphi(t)+\emptyset(t))}$$
$$x_2 = V_0 e^{j(\varphi(t)-\emptyset(t))} \tag{2.25}$$

Due to the modulated load, at certain outphasing angles, the reactive part of the impedance can occur which decreases the efficiency. Chireix proposed a combining network with two

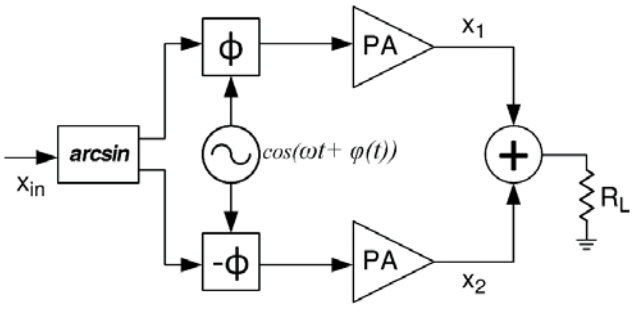

Figure 2.20: Outphasing architecture.

reactive lumped components that cancel the reactive component of the load impedances presented to the PAs. However, that approach works only for the low dynamic range and narrow bandwidth. It is important to note that the power-combining network, in combination with the branch PA operating class, determines the achievable efficiency performance and the bandwidth of the outphasing system. General Chireix design results in good efficiency in the upper *6 dB* of the output range. The Chierix efficiency curve is similar to that in Figure 2.21. Recently, several solutions of the wideband power-combining networks are presented in [33] making it competitive technique for the linear-efficient PAs.

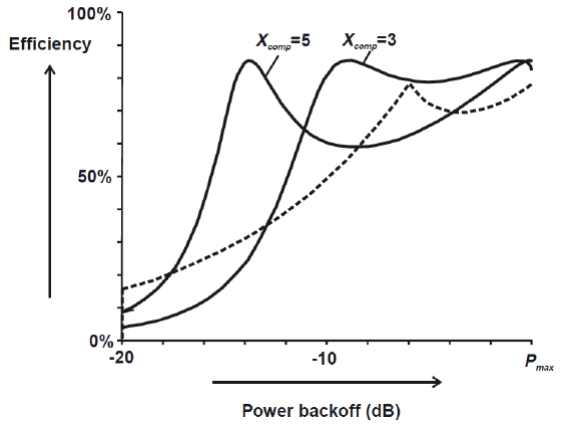

Figure 2.21: Outphasing amplifier efficiency for two values of the compensation reactance, compared to the Doherty amplifier (dotted) [30].

2.8.3 Envelope Tracking

The envelope tracking (ET) technique is in a way similar to the Khan's envelope elimination and the restoration (EER) technique [30]. In the ET technique, the PA operates in the linear manner (not as a switch as in the EER technique) while the DC supply voltage is dynamically varied to minimise the dissipated power.

Modern mobile communication systems are using complicated digital modulation schemes with large bandwidths and high PAPR. Since varying the envelope of such signal leads to the back-off operation of the PA, the average efficiency drops as the PAPR increases. In order to maintain the efficiency for the low levels of the envelope, the supply voltage of the PA is decreased so that PA operates at its PEP with maximum efficiency for the given input drive.

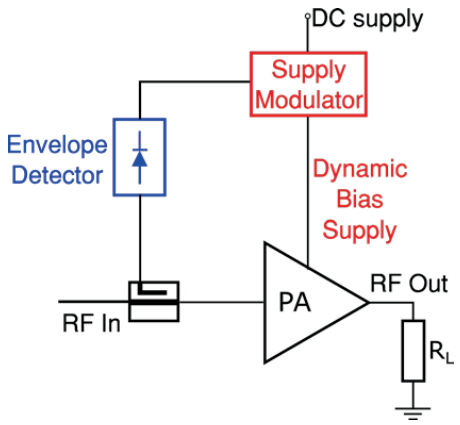

Figure 2.22: Envelope Tracking (ET) PA

The concept of the ET power amplifier is shown in Figure 2.22. A sample of the input signal is taken with the directional coupler, and the envelope is detected by the envelope detector. Alternatively, the envelope can be taken directly from the digital modulator. The supply modulator (supply voltage amplifier/tracker) then delivers the supply voltage that is modulated according to the envelope of the signal reducing dissipation power of the PA and improving the efficiency [30], [34]. The critical part of the ET system is the supply modulator (amplifier) which should have a bandwidth equal to the envelope and high efficiency over that bandwidth. The bandwidth of the envelope is infinite in theory, but it can be approximated to the 4-10x the bandwidth of the signal.

2.9 Linearization techniques

The purpose of the linearization techniques is to improve the linearity of PAs but can also be used to recover linearity after applying one of the efficiency enhancement techniques. It is, for example, common to use a digital predistortion (DPD) with envelope tracked PAs. This section presents a short overview of the three most common linearization techniques [2] and one recently presented (auxiliary envelope tracking - AET) which is subject of the research in this thesis.

2.9.1 Feedback

Disadvantage of the feedback is a sacrifice of the gain for the linearity and bandwidth limitation. Nevertheless, it is popular because it is easy to implement in audio frequency

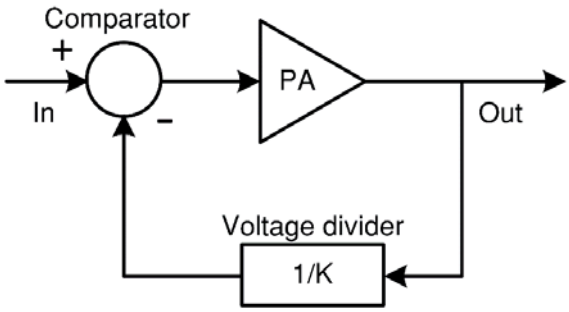

Figure 2.23: The Feedback principle (from [2])

applications where the gain is inexpensive. When it comes to the RF frequencies where the gain is expensive, that factor has to be taken into account [2].

In principle, the feedback technique takes a small portion of the output signal, compares it with the input signal and generates the error signal which is injected back to the input of an amplifier. The basic principle is shown in Figure 2.23. More detailed study about the feedback can be found in [1] and [2].

RF Feedback

Since the gain is much more expensive at the RF frequencies than at the audio frequencies, the usage of the feedback in discrete circuits is limited to the HF and the lower VHF frequencies. It can also be applied in the MMIC architectures well into the microwave region. In order to reduce power dissipation in the feedback branch, an active amplifier can be used instead of a voltage divider.

Envelope Feedback

Replacing the RF signal with its envelope in the feedback loop, the delay that can cause instability can be significantly minimised. That is due to the fact that in the RF feedback the delay is associated with the RF frequency, while in the envelope feedback the delay is associated with the modulated signal (baseband) bandwidth. The envelope feedback will reduce a distortion inside of the signal bandwidth associated with the amplitude distortion. Only the amplitude distortion (AM-AM) is corrected since the envelope is associated with the amplitude of the signal. Therefore, this technique is beneficial only for the PAs where the amplitude distortion is dominant.

Polar-Loop Feedback

In the polar-loop feedback technique two functions are employed; one is the envelope feedback and another is the phase feedback realised with a phase-locked loop. The advantage of the polar-loop feedback is the correction of both, the amplitude and the phase distortion. Disadvantage is different bandwidth requirement for the amplitude and the phase correction which leads to a different level of improvement in the amplitude and the phase distortion.

Cartesian Feedback

The Cartesian feedback overcomes the problems associated with the wide bandwidth of the signal phase by applying modulation feedback in the I and Q components. The I and Q error signals are applied to the I and Q subcarriers of the input signal and then upconverted to the PA.

2.9.2 Feedforward

In contrast to the feedback system which often requires high feedback bandwidths, the feedforward gain-bandwidth is limited to the band of interest. The basic configuration of the feedforward system is shown in Figure 2.24. The input signal is split into two paths where the signal in the top path is amplified by the PA and a portion of the amplified signal is then taken to the parallel path. A sample of the input signal in the parallel path is then subtracted from the sample of the amplified signal. The resulting error signal is equal to the distortion added by the PA. The error signal is then phase-shifted for 180° and added to the output signal so it cancels distortion in the main path, ideally making amplified replica of the original input signal. It is very important to time-delay and amplify error signals precisely in order to have the phase and amplitude match. The wider bandwidths can increase the difficulty with the delay lines due to the loss and the line bandwidth resulting in the lower degree of linearization

One of the drawbacks of the feedforward system described above is the non-ideal error amplifier which adds distortion to the output signal. This problem can be alleviated by adding additional feedforward loop to the existing feedforward system correcting the residual error or only around the error amplifier cancelling the distortion of the error signal [2]. The number of additional loops is not limited.

The PAPR of the error signal can be much higher than that of the desired signal, making the amplification of the error signal inherently much less efficient than that of the main signal. This drawback may significantly decrease the overall efficiency of the feedforward system [1].

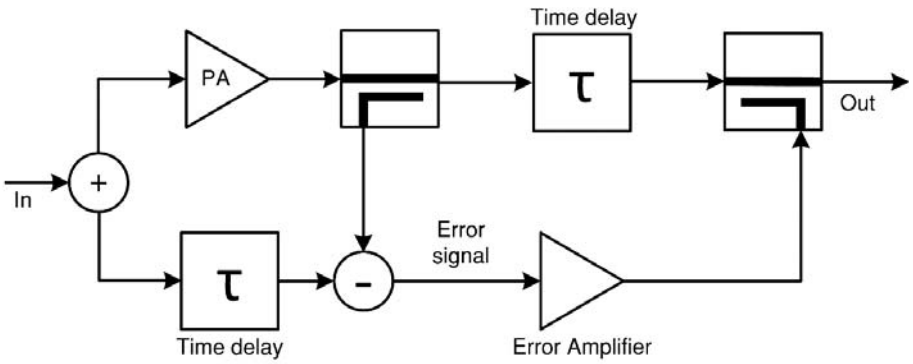

Figure 2.24: Basic feedforward configuration (from [2]).

2.9.3 Predistortion

The basic idea of the predistortion system is to apply the distortion to the signal prior amplification which is exactly the inverse of the distortion from the PA. The predistortion can be done at the RF frequency, the intermediate frequency (IF) or the baseband frequency. Today, digital processing makes the digital predistortion (DPD) at the baseband frequency a very useful linearization tool. The concept of the predistortion system is shown in Figure 2.25 where G_p is the predistorting function which is a complement to the gain function G of the PA. The signal at the output of the PA is the then exact amplified replica of the input signal. Another way of looking at the predistortion is in terms of the intermodulation products IMDs. If the IMD components generated by the predistorter are equal in magnitude and 180° out of phase compared to those generated by the PA, the IMDs will be cancelled.

The predistorting function is often a cubic function which compensates the third order nonlinearity. It is not usual to predistort the even order nonlinearities in the PA since those can easily be removed by filtering. Another approach is to fit the distortion characteristic of the PA and compensate for the higher order nonlinear distortion. There is a number of different solutions for that types of distortion [2].

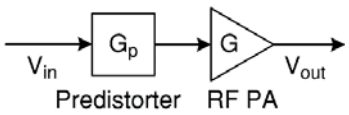

Figure 2.25: Concept of the predistortion (from [2]).

Digital Predistortion

Evolution of digital signal processing (DSP), which is commonly used in the modern transmitters, has made the usage of the digital predistortion (DPD) easy to utilise. Nowadays, the DPD technique is widely used from radio transmitters to mobile base stations.

The model of the AM-AM and the AM-PM characteristics of the PA can be stored in the lookup tables (LUTs) where the data is usually stored according to the input power. The input signal is then corrected according to the PA's response stored in the LUTs. This technique has good performance results, but it also requires a lot of memory to store the data and good processing capabilities to update the data due to the changes caused by time, temperature, etc. [1]. The LUT technique is often static or memoryless so it cannot correct the distortion caused by the memory effects.

The functions describing nonlinearities and dynamics can solve the problem with the memory effects. The Volterra series polynomial can model the nonlinear dynamic behaviour quite well. The drawback of the Volterra series is increasing the number of necessary coefficients as the order of the nonlinearity and the memory depth increases [26]. One solution for that problem are the memory polynomials [35]. As the bandwidth and the number of the channels increase in the modern communication systems, the memory polynomial is not good enough. There are techniques to overcome wide bandwidth like the generalized memory polynomial (GMP) [36] and the dynamic deviation reduction (DDR) [37] which are quite widely adopted for the DPD [38].

Due to the change of the PA's transfer characteristic over time, temperature, and power, the modern DPD systems are adaptive. The adaptive DPD system is essentially a feedback system where the correction is applied at the digital baseband [38].

2.9.4 Auxiliary Envelope Tracking

The auxiliary envelope tracking (AET) architecture is recently presented as the linearization technique by Z. Yusoff et.al. on the GaN HEMT device [3]. The principle is similar as in the efficiency enhancement ET technique, only here it is used for the linearity enhancement. Namely, in the AET technique, the drain bias voltage is increased for the high levels of the signal and it is decreased for the low levels of the signal. Increasing the voltage expands the gain of the PA which provides the linearization effect. The AET technique linearizes the PA with little or no overall efficiency degradation. The AET is a topic later in the Chapter 7.

2.9.5 Dynamic Gate Biasing

The dynamic gate biasing technique as the PA linearization tool is investigated and reported in this thesis. Namely, the nonlinear distortion in memoryless PAs comes from the AM-AM and the AM-PM transfer functions. These transfer functions are related to the gain and the transfer phase a PA, which are dependent on the gate bias voltage. The gain and the transfer phase (AM-AM and AM-PM transfer functions) of the PA vary the with signal power i.e. the signal envelope. Now, if the gate bias voltage is dynamically changed in dependence of the signal envelope or the signal power in the adequate way, the AM-AM and the AM-PM functions can be flattened and nonlinear distortion is consequently reduced. More detailed description of the dynamic gate biasing and the introduction of power gate tracking (PGT) linearization technique is presented in Chapter 5.

2.10 Measurement Techniques

2.10.1 Load Pull

The performance of the PA in terms of the output power, gain, and efficiency depends on the slope of the dynamic loadline, which on the other hand depends on the output matching (load) impedance “seen” by the active device. The power transistors are often the most expensive parts of the RF PAs and efficiency is of great importance in mobile handsets as well

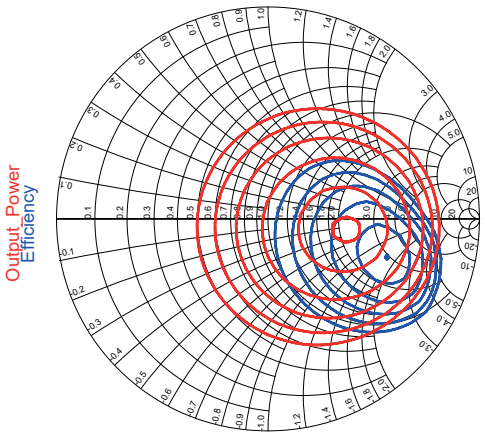

Figure 2.26: Load-pull contours for the output power with the 0.5 dB setp and the drain efficiency with the 5% step.

as in the base-stations. This means that matching condition has to be taken seriously, despite the lower small-signal gain as a trade-off for power or efficiency [30].

The load-pull (LP) measurement technique is used to determine the device capability and matching network requirements. It uses an impedance tuner at the fundamental frequency, and possibly at the higher harmonic frequencies at the output of the device under test (DUT). The performance of the DUT in terms of gain, output power, efficiency and linearity can be measured at several load impedance values. The result are closed "contours" marking the boundaries of the specified measured parameter in the Smith chart from which designer can chose well-defined impedance targets and the trade-off between the parameters of interest (gain, power, efficiency, and linearity). An example of the load pull contours for the output power and

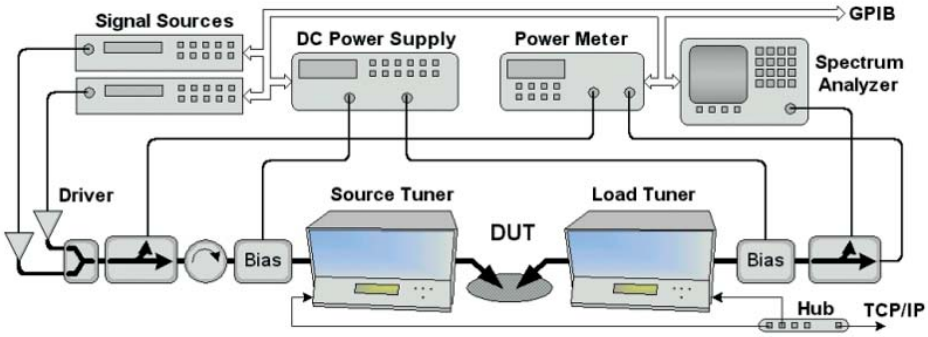

(a) Passive harmonic load-pull measurement setup. Figure from [40].

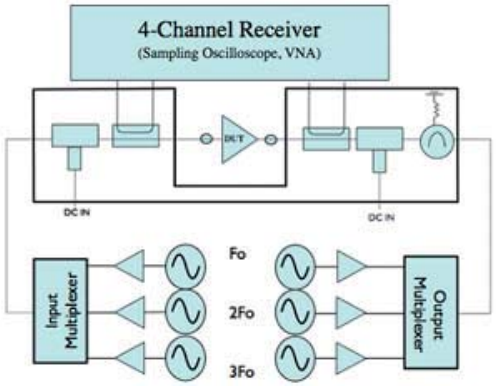

(b) Active harmonic load-pull open loop configuration. Figure from [41].

Figure 2.27: Passive and active load-pull for harmonic tuning.

the efficiency is shown in Figure 2.26. The source-pull is also very important for the PA optimisation since the input (source) matching impedance defines the small-signal gain of the PA.

The load/source-pull measurement can be done with passive or active tuners. The passive tuners are mechanical structures that can be designed in different ways. The mechanical tuners typically have wide matching impedance range but it is limited, and the limitation depends on the loss in the tuner. The active impedance tuning is done by "injecting" the signal at the fundamental and the harmonic frequencies to the output of the DUT with the amplitude and phase that correspond to the amplitude and phase of the signal that would be reflected when certain load impedance is "presented" to the output of the DUT. Therefore, it requires highly accurate phase-locked signal generators and power amplifiers to generate the reflected signals. With the active LP system the complete impedance range can be covered [39]–[41]. The configuration of the passive and the active LP systems are shown in Figure 2.27.

2.10.2 Time-Domain Waveform Measurement

Standard microwave measurements are usually done in the frequency domain using a vector network analyser (VNA) or a spectrum analyser. The VNA measures the S-parameters which are small-signal parameters supporting linear analysis. The spectrum analyser performs scalar measurements of the signal power which provide information about the gain compression, higher harmonics, and intermodulation distortion. Since it measures only the magnitude of the signal power and not the phase, it cannot provide the information about voltage and current waveforms.

Waveform measurement is the ability to observe and quantify the time-varying voltage $v(t)$ and current $i(t)$ present at all terminals of the DUT. It involves all the frequencies including DC, IF, and RF [42]. The waveform measurement can be done by measuring the voltage and current in the time domain with an oscilloscope. That technique is common at low frequencies, but when it comes to the microwave frequency it may be challenging to perform. Alternatively, the waveform measurement can be done in the frequency domain where the VNA or the SWAP [43] is used to measure individual frequency components of the signal with the phase reference or the coherent phase relation. In this case the time varying incident $a(t)$ and reflected $b(t)$ waves are actually measured and not the nod voltages and currents. The RF and the baseband test set is shown in Figure 2.28. For full functionality, any waveform measurement system has to be fully vector calibrated (with absolute power and phase relations) to provide the correct

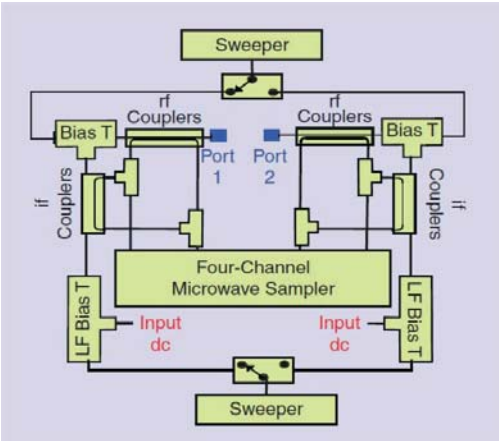

Figure 2.28: Basic schematic of the multi-tone time-domain based RF and IF I-V waveform measurement system. Figure from [42].

measurement of the time varying voltage and current waveforms [42]. Furthermore, if the time-domain waveform measurement is to be used for the waveform engineering purpose (if designer wants to shape the waveforms) or for the output impedance measurement at the intrinsic current source, the measured *a* and *b* waves must be deeembedded from the calibrated measurement reference plane to the intrinsic current source.

2.11 Summary

This section covers a small part of the background theory standing behind this work. Section 2.1 and Section 2.2 discuss main materials, technologies and types used in the transistor design. The focus in this work is on the GaN HEMT device because of its growth on the market, high breakdown voltage and the power density. Namely, the GaN devices are supporting a higher power density compared to the GaAs. High breakdown voltage makes the GaN convenient for the bias voltage variation which is a part of this research.

Section 2.4 presents some of the basic properties of the signals commonly amplified by the power amplifiers like bandwidth, peak-to-average power ratio, probability density function. These properties affect the complexity of the PAs and their performance.

Section 2.5 presents the theoretical analysis of the power tracking technique and it shows definition of the ideal PET and 2nd order PET techniques. The advantage of the power tracking techniques is in the limited and well defined bandwidth of the signal power.

Section 2.6 is dedicated to the linearity and efficiency definitions and different evaluation parameters. Linearity and efficiency are two of the most important parameters in the RF PA design and there is always a compromise that has to be done between them during design [9].

Section 2.7 covers the basic theory about different PA classes that are purely dependent on the DC bias conditions. Some of these classes are more linear but less efficient (class A) and some are more efficient but less linear (class B). That is why there is a number of the linearization and efficiency enhancement techniques developed and investigated over the years. Most common efficiency enhancement and linearization techniques are discussed in Section 2.8 and Section 2.9 respectively. In this research, some of them, like Envelope Tracking (ET) and Auxiliary Envelope Tracking (AET), are part of the scope.

A very important part of the PA design is measurement. The most important measurement techniques used in this work are the load-pull measurement and the time-domain waveform measurement. These are explained in Section 2.10.

Chapter 3

Novel Linearity Measure and Figure of Merit

The signal distortion in the PAs can be described in several ways like the amplitude and phase distortion, intermodulation distortion and spectral regrowth. The amplitude-to-amplitude (AM-AM) and the amplitude-to-phase (AM-PM) nonlinear conversions are common descriptions of the nonlinear behaviour of the memoryless narrow-band PAs. The common metrics for the distortion evaluation of the digitally modulated signals are the adjacent channel power ratio (ACPR) and error vector magnitude (EVM). The ACPR is the measure of the distortion that appears out of the signal bandwidth, and the EVM is the measure of the distortion that appears inside of the signal bandwidth [2]. There is a relationship between the AM-AM and AM-PM conversions and the ACPR as well as the EVM that can be described with the transfer characteristics (AM-AM and AM-PM) [44]–[46]. Although the nonlinear distortion outside (ACPR) and within (EVM) the signal bandwidth can be related to each other, it would possibly require a cost function to make a unique figure off merit (FOM) for the overall distortion that includes in and out of the band distortion. In other words, it would be complicated to evaluate both the ACPR and the EVM simultaneously and find the optimum between these two measures during an optimisation of the PA for the linearity.

This chapter presents a novel metric for the nonlinear distortion that simultaneously evaluates distortion inside and outside of the signal bandwidth. It includes the memoryless nonlinear distortion and distortion caused by the memory effects if present. The novel metric is defined as the total nonlinear power of the distorted signal. Furthermore, the derivation of the FOM from the presented metric, which can be used for the optimisation of various linearity

improvement techniques applied to the PA or the transmitter (Tx) architectures, is also developed as a Signal to the Total Distortion Ratio (STDR).

3.1 Total Nonlinear Power

Assuming a signal *a(t)* which is amplified with a PA which has a nonlinear complex gain *G(·)*, the signal at the output of the PA *b(t)*, can be expressed as follows:

$$b(t) = G(a(t)) \cdot a(t). \tag{3.1}$$

The instantaneous nonlinear power $P_n(t)$ of the output signal *b(t)* can then be defined as

$$P_n(t) = |b(t) - G_l \cdot a(t)|^2, \tag{3.2}$$

Where the G_l is the average complex gain of the PA with no amplitude or phase variation i.e. it is the wanted linear gain of the ideal PA. The $G_l \cdot a(t)$ is then the linear power of the output signal. The linearized PA would minimise the average nonlinear power $P_{n,avg}$ which can be defined as:

$$\begin{aligned} P_{n,avg} &= \frac{1}{T}\int_0^T P_n(t)dt = \frac{1}{T}\int_0^T |b(t) - G_l \cdot a(t)|^2 dt \\ &= \frac{1}{T}\int_0^T \big(b(t) - G_l \cdot a(t)\big)\big(\overline{b(t) - G_l \cdot a(t)}\big)dt \end{aligned} \tag{3.3}$$

In the equation (3.3) it can be noticed that the $P_{n,avg}$ is a function of the linear gain of the PA (G_l). The equation (3.3) can now be rewritten as:

$$P_{n,avg}(G_l) = |G_l|^2 I_a - 2Re(G_l I_x) + I_b. \tag{3.4}$$

In the equation (3.4) the integral I_a is the average input power, the integral I_b is the average total (linear and nonlinear) output power, and the integral I_x is the mixing product of the input and output signals. Note that the mixing product of the input and output signals corresponds to twice the power of the baseband signal. These integrals are shown in the equations (3.5), (3.6), and (3.7) respectively.

$$I_a = \frac{1}{T}\int_0^T |a(t)|^2\, dt, \tag{3.5}$$

$$I_b = \frac{1}{T}\int_0^T |b(t)|^2\, dt, \tag{3.6}$$

$$I_x = \frac{1}{T}\int_0^T b(t)^* \cdot a(t)\, dt. \tag{3.7}$$

The average nonlinear power $P_{n,avg}$ (3.4) changes with the amplitude and the phase of the linear gain G_l, which must be selected. An advanced receiver would align the received signal (it would adjust the amplitude and phase of the signal) so that *EVM* is minimal i.e. it would adjust the constellation of the signal. The selection of the proper G_l is done by minimising $P_{n,avg}$. The first step to achieve this is to look at the phase of the G_l and the term $Re(G_l I_x)$ in the equation (3.4), which must be maximised. This is achieved when the phase of the G_l is opposite (has opposite sign) compared to the I_x giving the expression:

$$P_{n,avg,min}(|G_l|) = |G_l|^2 I_a - 2 \cdot |G_l||I_x| + I_b. \tag{3.8}$$

The minimum of the equation (3.8) can be found from its derivative (3.9):

$$\frac{dP_{n,avg,min}(|G_l|)}{d|G_l|} = 2I_a|G_l| - 2|I_x|. \tag{3.9}$$

Knowing that the minimum of $P_{n,avg}$ (3.8) is achieved when its derivative (3.9) is equal to zero, one gets the minimum of the $P_{n,avg}$ when the $G_l = I_x^*/I_a$. The G_l is an optimal average gain for the given input signal. It is important to note that the optimal average gain varies for different signals and PAs. It is also worth noting that the average minimum nonlinear power $P_{n,avg,min}$ in (3.8) evaluates the total nonlinear power contained in the output signal. The $P_{n,avg,min}$ contains the nonlinear distortion inside and outside of the signal bandwidth and takes into account all the sources of the nonlinear power. Optimising a PA or applying the linearization technique (PGT, DPD or other) for the minimal average nonlinear power $P_{n,avg,min}$ would lead to less distortion, and it would improve both the *ACPR* and the *EVM*. However, it could lead to a trivial solution when the output power $|b(t)|^2$ reduces i.e. the gain of the PA drops. This is certainly an unwanted result. In order to optimise the linearity and the gain of the PA or the PA with applied

linearization technique during the optimisation process, the figure of merit based on the linear and nonlinear power is developed in the next section.

3.2 Nonlinear to Linear Power Ratio NLPR and Signal to Total Distortion Ratio (STDR)

Maximising both, the linearity and the output power level of the PA during optimisation the Nonlinear-Linear Power Ratio (NLPR) is defined as:

$$NLPR(|G_l|) = \frac{P_{n,avg,min}}{P_{lin}} = \frac{|G_l|^2 I_a - 2 \cdot |G_l||I_x| + I_b}{I_a|G_l|^2} = 1 + \frac{I_b}{I_a|G_l|^2} - \frac{2|I_x|}{I_a|G_l|}. \quad (3.10)$$

The nonlinear power $P_{n,avg,min}$ in the equation (3.10) is defined as shown in (3.8), and the linear power is defined as $P_{lin} = I_a|G_l|^2$. The P_{lin} is actually the power of the input signal (integral I_a defined in (3.5) corresponds to the input power) increased by the linear gain G_l of the PA. By minimising the *NLPR*, the nonlinear power is minimised and the linear power is maximised simultaneously. That means that the nonlinear distortion is reduced, with little or no loss in the output power i.e. the gain of the PA.

By calculating the derivative of the above function (3.10), we can find the minimum of the *NLPR* function (3.11).

$$\frac{d}{d|G_l|} NLPR(|G_l|) = \frac{2}{I_a|G_l|^2}\left(|I_x| - \frac{I_b}{|G_l|}\right), \quad (3.11)$$

The minimum of the *NLPR* function is achieved when the $G_l = I_b/I_x$ (the average gain of the PA for the given input signal). The *NLPR* can now be expressed as

$$NLPR = 1 - \frac{|I_x|^2}{I_a I_b}. \quad (3.12)$$

We can now present the FOM as inverse of the *NLPR* or the Signal to Total Distortion Ratio *STDR* in logarithmic scale as

$$STDR = 10log\left(\frac{I_a I_b}{I_a I_b - |I_x|^2}\right)\ [dB]. \quad (3.13)$$

Knowing the input and output signals from the PA we can calculate integrals (3.5), (3.6) and (3.7). The *STDR* will be maximised by minimising the nonlinear power and by maximising the linear power. The former assures the linearity of the PA and the latter assures the high output power i.e. high gain of the PA. This robustness of the presented FOM is a great advantage in an optimisation process of various PA linearity improvement techniques. The presented FOM can be very beneficial for optimisation of the DPD or other linearization techniques like tracking functions of the dynamic bias techniques in the PAs and the Tx systems instead of optimising for the *ACPR/ACLR* and *EVM* which can be complicated to evaluate for the Tx systems.

Moreover, the integrals (3.5), (3.6), and (3.7) could be directly measured with usage of the additional hardware and power meter. Namely, I_a is the average input power, I_b is the average output power, and I_x is the power of the mixing product of the input signal and the output signal. By measuring these three values and applying some digital processing which can be found in every transmitter system the *STDR* could be easily calculated. This would open the possibility of adaptive correction of the DPD system or the coefficients of the tracking functions for the dynamic biasing technique.

3.2.1 Verification of the STDR

Verification of the presented FOM is done by evaluating several measurements. The measurement of the static bias class AB and class A PAs (I_D= 163 mA and I_D= 500 mA

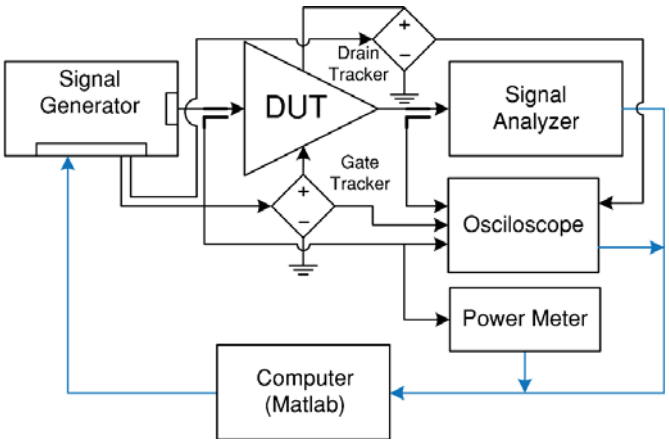

Figure 3.1: Measurement setup with the supply voltage tracker (amplifier) at the gate and drain side of the DUT.

respectively) with the *1 MHz* 16-QAM signal, the Envelope Tracking (ET) PA with the *1 MHz* 16-QAM signal and the class-AB PA with the LTE E-UTRA TM-3.2 *10 MHz* test signal. The measurement of the LTE signal is done with two different input power levels giving the same *ACPR* as the best (class A) and the worst (ET PA) case. The dynamic gate bias operation with the optimised gate tracking function coefficients for the *STDR* are also presented in Section 5.5.

The measurement setup is shown in Figure 3.1. The operation is the same as explained in Section 5.4.1, but here both the gate and drain voltages are calculated in Matlab [27] and sent to the signal generator. These signals are then sent to the gate and drain trackers which are feeding the transistor with the gate bias and drain supply voltages. The gate and drain voltages in the measurement system can be constant DC values or dynamic voltages for the dynamic gate biasing or the ET operation.

The results are presented in Table 3.1. The G_l (linear gain) is the magnitude of the average gain of the PA. The phase of the G_l is relative and it results in *0°* when calculated from the captured data. The *STDR* value increases for the signals with less distortion i.e. with better *ACPR* and/or *EVM*. It can also be noted that the *STDR* value is comparable for the 16-QAM and LTE signals when the ACPR values are comparable for these two modulated signals. These results are showing that presented FOM (*STDR*) is valid for the *1 MHz* 16-QAM and the *10 MHz* LTE signal which verifies its validity and show its robustness.

Table 3.1: Measured results of the *STDR* with the 16-QAM and the LTE signal for the static bias and the ET PA.

PA	$P_{out,avg.}$ [dBm]	G_l [dB]	PAE_{avg} [%]	**STDR [dB]**	ACPR L [dBc]	ACPR R [dBc]	EVM [%]
Static gate bias operation with 16QAM							
I_{DQ}= 500 mA	35.58	17.5	30.57	**24.43**	-38.80	-38.17	4.10
I_{DQ}= 163 mA	35.59	16.7	38.9	**19.57**	-32.68	-32.36	7.85
Envelope Tracking PA with 16QAM							
I_{DQ}= 15 mA	35.59	15.36	65.61	**18.77**	-28.36	-28.74	10.13
Static gate bias operation with LTE							
I_{DQ}= 163 mA	21.43		3.61	**24.84**	-38.30	-38.50	4.27
I_{DQ}= 163 mA	32.93		26.72	**18.88**	-28.10	-29.40	7.78

3.3 Summary

This chapter shows development of the novel PA linearity measure with corresponding FOM. Section 3.1 presents the linearity measure as the total nonlinear power of the distorted signal. The characteristic of this measure is that it evaluates the nonlinear distortion inside and outside of the signal bandwidth. This characteristic is beneficial for the optimisation of different linearity enhancement techniques, however, the drawback is that this measure does not account for the PA's output power and optimisation may lead to a significant drop of gain. Section 3.2 presents the *STDR,* which is the corresponding FOM of the presented linearity measure. This FOM is actually the ratio of linear over total nonlinear power of the distorted signal. In other words, by optimising a linearization technique for the *STDR,* the linear (wanted) power is increasing and the nonlinear (unwanted) power is decreasing. This way the linearity of the linearized PA is improved with no or small output power loss.

Chapter 4

Power Amplifier Design Optimised for Dynamic Gate Bias Variation

As the input and the output impedance of a transistor subjected to the dynamic gate bias operation varies, it is important to find the best matching impedances for the optimal PA performance. According to the load-line theory [30], if the PA is driven so that the drain current peak value is constant for different conduction angles (conduction angle i.e. the class of the operation depends on the gate bias voltage), an optimal impedance for the fundamental frequency does not change between the class A and the class B operation. However, it is a little reduced for the class AB operation, reflecting a slightly higher fundamental current component which results in a little higher output power compared to the class A and the class B PAs. Here, the assumption is that the transistor is an ideal voltage dependent current source, where the transconductance is linear except at the pinch-off and the current saturation area. In such an ideal environment, the optimal load impedance is also constant for all drive levels inside the linear region. Once the device starts to operate in the nonlinear region, waveforms are no longer sinusoidal and the load-line theory, as such, breaks apart. Furthermore, the real device contains parasitic components like the gate to source capacitance, the gate to drain capacitance and the drain to source capacitance as well as the output resistance, inductance, etc. [17]. These parasitic components separate the observable load impedance from the idealised intrinsic reference plane. The value of these parasitic components may be dependent on the gate bias voltage, dissipated power and temperature, changing the observable optimal load impedance. Thus, it is important to test/measure the output impedance sensitivity of the transistor subjected to the dynamic gate bias variation. A commonly used technique for the measurement of the load

impedance is the load-pull measurement technique (see Section 2.10.1), which is used in this work. The load-pull results can be used to determine if a device is suitable for the dynamic bias operation and determination of the optimal matching impedance (e.g. for the output power and/or efficiency). It is also important to find the optimal input impedance, which can be measured with the source-pull measurement technique.

4.1 Device Measurement and Measurement Method

This section presents the measured results showing how much the load impedance changes with the gate bias voltage (from deep class AB to class A) for the case of the maximum output power and the case of the maximum *PAE*. The device used for the experiments is the 10 W GaN HEMT device from Wolfspeed/CREE [10]. The measured results are used for determining whether the device is suitable for the dynamic gate biasing operation, and for finding the optimal matching network of the PA operating under dynamic gate biasing conditions.

The measurement is done using the passive load-pull measurement technique [44] (see Section 2.10.1) at the fundamental frequency of f_0=*2 GHz*. The load impedance is tuned for the fundamental, second and third harmonics in order to find the optimum matching impedances for the maximum output power and the maximum efficiency.

4.1.1 Measured Device and Fixture

The circuit (DUT) subjected to the measurement is shown in Figure 4.1. It consists of the stabilised 10 W GaN HEMT device from Wolfspeed/CREE [10] in the fixture produced on the standard FR-4 substrate. The stabilisation circuit is designed using the transistor model in the Agilent Advanced Design System (ADS) CAD tool [45] biased with the quiescent drain current of I_{DQ}=*163 mA* (class AB) and the quiescent drain voltage V_{DQ}=*28 V* for frequencies from *f* = *100 MHz* and upwards until the transistor is unconditionally stable by itself. The quiescent drain

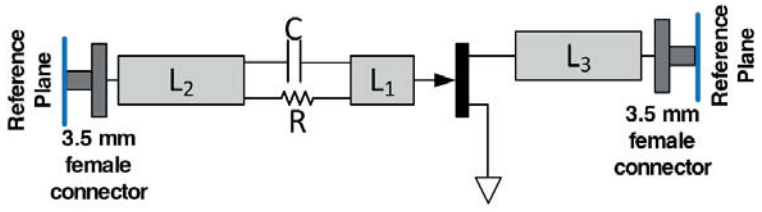

Figure 4.1: Stabilized 10 W GaN HEMT with the fixture for the load-pull measurement.

current for the class A operation of the device is I_{DQ}=*500 mA* and it can be found from its de-rating curve [10]. In the circuit shown in Figure 4.1, the width of the lines is *W=3.05 mm* which yields the characteristic impedance of the transmission line of Z_0 = *50 Ω* at the fundamental frequency of f_0 = *2 GHz*. The lines L_2 and L_3 have a length of *12.9 mm* and the length of the line L_1 is *4.2 mm*. The values of the stabilisation capacitor and the resistor are *R=82 Ω* and C=*6.8 pF*.

4.1.2 Load-Pull Measurement Setup

The load-pull measurement setup is shown in Figure 4.2. It consists of the multi-harmonic tuners (iMPTs) from Focus Microwaves Inc. [40] with fixtures at the input and the output of the DUT, input and output blocks, the driver amplifier and the surrounding measurement equipment. The input and output blocks consist of DC bias tees and directional couplers used for the power measurement. The harmonic tuners are capable of tuning up to three harmonics at the same time. The tuners are calibrated at the *3.5 mm* male connectors at the fixture (reference plane) for the fundamental, second and third harmonic. All impedances, reflection coefficients, and other measured results in this load-pull measurement are referred to these reference planes.

4.1.3 Measurement Method

The measurement system presented above is used to find the optimal matching impedances at the input and the output of the DUT. The quiescent gate voltage V_{GQ} that delivers the

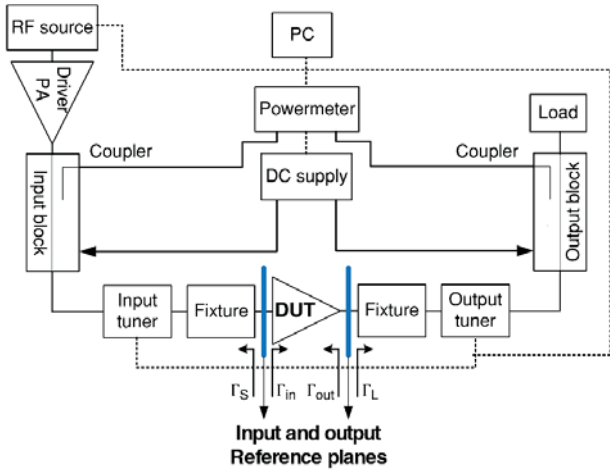

Figure 4.2: Passive load-pull measurement setup.

quiescent drain current I_{DQ}=*163 mA* (class AB) with the nominal drain voltage V_{DQ}=*28 V* is used as the reference static bias.

First, the input and the output matching impedances for the maximised small-signal gain of the DUT with the reference bias (I_{DQ}=*163 mA*) have been found. Tuning the fundamental impedance at the input and the output of the DUT for the maximum small-signal gain is performed with the input power level of P_{in} = *0 dBm*. Impedances for the higher harmonics (second and third) are set to *50 Ω* at the reference planes on both sides of the DUT. After that, the large-signal load-pull measurements for the fundamental frequency for the set of the static gate bias voltage values is performed. The input matching impedance for the fundamental frequency is set to be the impedance for the maximum small-signal gain for the reference bias, while the second and third harmonics maintain at *50 Ω* on both sides of the DUT. The static drain voltage is the nominal voltage of the transistor V_{DQ} = *28 V* [10] and the gate bias is varied to deliver the quiescent drain currents of I_{DQ} = *15 mA*, I_{DQ} = *25 mA*, I_{DQ} = *50 mA*, I_{DQ} = *100 mA*, I_{DQ} = *163 mA*, I_{DQ} = *200 mA*, I_{DQ} = *300 mA*, I_{DQ} = *400 mA* and I_{DQ} = *500 mA*. The quiescent drain current of I_{DQ} = *500 mA* is chosen as the maximum allowed static drain current (the class A bias point) according to the power dissipation de-rating curve of the device [10].

For the large-signal load-pull measurement with the reference bias (I_D = *163 mA*), the input power level is set to the value driving the DUT into *1 dB* compression. In order to keep the same compression level criteria for all the quiescent bias points, the difference *D* between the output power level for the *1 dB* compression $P_{out,\ 1dB}$ and the maximum output power level $P_{out,max}$ with the reference bias is determined as shown in Figure 4.3. Now, in order to keep the same compression criteria for all the other bias conditions, for each measured gate bias the PA

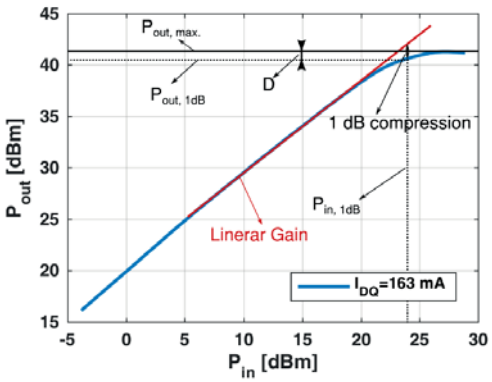

Figure 4.3: Compression level definition for the fundamental harmonic load-pull measurement.

is driven so that it delivers the output power (P_{out}) that has the distance D from its corresponding $P_{out,max}$. The $P_{out,max}$, for each gate bias voltage, is determined from the corresponding CW power sweep measurement driving the PA in deep compression.

For each load-pull measurement (for each bias point) of the fundamental frequency, the impedance at the geometrical midpoint between the impedances for the maximum *PAE* and the maximum P_{out} is found in the Smith Chart as trade-off between the output power and the efficiency. Next step is to find matching impedances for the second and third harmonics resulting with the maximum *PAE* at each bias point while the load impedance for the fundamental is set to the corresponding geometrical midpoint value. The goal of this is to see if all the bias points support a common load impedance area within which the *PAE* is not more than *3* percentage points lower than the maximum *PAE* with the optimal impedance for the second and third harmonics resulting in the maximum *PAE*. The input power during the load-pull measurement of the second and third harmonics is increased until the gain suffers additional *2 dB* compression compared to the compression of the fundamental load-pull measurement. This increment of the input power gives the sufficient amplitude of the higher harmonics for the load impedance tuning. Matching impedances for the second and third harmonics are forced to have a minimum loss (to be at the outer edge of the Smith Chart) as much as possible with the passive tuners.

4.2 Results

In this work, the matching impedances Z are presented as corresponding reflection coefficients Γ. Conversion is done according to the equation (4.1)

$$\Gamma = \frac{Z - Z_0}{Z + Z_0}, \tag{4.1}$$

where Z is matching impedance and $Z_0 = 50\ \Omega$ is the characteristic impedance of the measurement system. Matching reflection coefficients at the input (Γ_S) and the output (Γ_L) of the DUT (see Figure 4.1) for the small-signal gain are presented in Table 4.1. Impedance tuning

Table 4.1: Small-signal gain matching at the input and the output of the DUT. (I_{DQ} = *163 mA*, V_{DQ} = *28 V* and P_{in} = *0 dBm*)

I_{DQ} [mA]	V_{DQ} [V]	P_{in} [dBm]	$\lvert\Gamma_{Sf0}\rvert$	$\angle\Gamma_{Sf0}$ [°]	$\lvert\Gamma_{Lfo}\rvert$	$\angle\Gamma_{Lf0}$ [°]	G [dB]
163	28	0	0.897	14.5	0.73	-49.2	20.42

at the input and the output is performed with the reference bias (I_{DQ} = *163 mA* and V_{DQ} = *28 V*) and with input power level of P_{in} = *0 dBm*.

Next, the comprehensive load-pull measurement at the fundamental frequency f_0 = *2 GHz* is performed for the set of quiescent drain currents (corresponding to the set of the quiescent gate bias voltages V_{GQ}) from *15 mA* to *500 mA*. The input matching reflection coefficient Γ_{Sf0} is set to the value shown in Table 4.1 during the load-pull measurement. Drive level during the load-pull measurement at each bias condition is selected according to the method explained in Section 4.1.3, and it is approximately for *1 dB* compression for all the bias conditions. During the load-pull measurement for the fundamental frequency, impedance for the second and third harmonics at the input and the output of the DUT is set to be *50* Ω. The measurement results for the maximum output power $P_{out,max}$ and the maximum *PAE* are shown in Table 4.2. The results are also presented in the Smith Chart in Figure 4.4.

Table 4.2: Load-pull measurement results for the fundamental frequency for the set of the quiescent drain current values evaluated for the maximum output power and the maximum *PAE*.

I_{DQ} [mA]	V_{DQ} [V]	$\Gamma_{Lf0,max.\ PAE}$	PAE (%)	$\Gamma_{Lf0,\ max.\ Pout}$	P_{out} [dBm]
15	28	0.74∠-66°	78.7	0.74∠-38°	40.3
25	28	0.73∠-64°	78.8	0.74∠-38°	40.3
50	28	0.73∠-65°	72.0	0.65∠-35°	40.5
100	28	0.73∠-65°	74.9	0.65∠-35°	40.9
163	28	0.72∠-64°	80.7	0.65∠-35°	41.0
200	28	0.7∠-65°	81.1	0.65∠-35°	40.9
300	28	0.69∠-62°	70.8	0.65∠-35°	41.2
400	28	0.7∠-65°	78.9	0.65∠-35°	41.0
500	28	0.7∠-65°	75.7	0.65∠-35°	41.1

The impedances resulting with the $P_{out,max}$ and the PAE_{max} are marked with "x" in Figure 4.4 and many are hidden due to the overlap with the other measurement results. Impedances (reflection coefficients) located at the geometrical middle in the Smith Chart between the maximum $P_{out,max}$ and the maximum PAE_{max} with each gate bias are marked with "o". These reflection coefficients are selected as the optimum i.e. the trade-off between the output power and the efficiency for each bias condition. Geometrical midpoint values $\Gamma_{Lf0,\ mid}$ with the corresponding PAE and P_{out} are presented in Table 4.3.

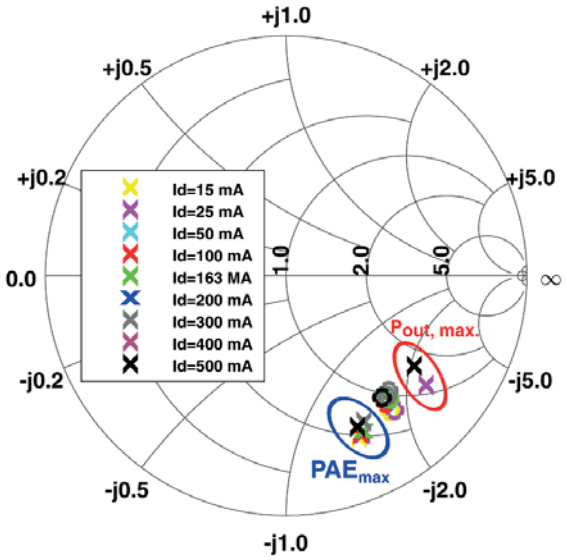

Figure 4.4: Load-pull measurement results for the fundamental frequency for the set of quiescent drain current values evaluated for the maximum output power P_{out} and the maximum power added efficiency *PAE* marked with "x" and the geometrical midpoint results marked with "o".

Table 4.3: Load reflection coefficients at the geometrical midpoint between the maximum P_{out} and maximum *PAE* load, *PAE*, P_{out} and the degradation of the *PAE* and P_{out} compared to the maximum values.

I_D [mA]	V_D [V]	$\Gamma_{Lf0,\,mid.}$	$PAE_{mid.}$ [%]	$P_{out,\,mid.}$ [dBm]	PAE_{max} - PAE_{mid} [%]	$P_{out,\,max.}$ - $P_{out,\,mid.}$ [dB]
15	28	0.711∠-52.6°	69.8	39.7	8.87	0.64
25	28	0.719∠-51.2°	66.7	39.6	12.11	0.65
50	28	0.675∠-51.2°	67.0	39.8	5	0.65
100	28	0.673∠-52.1°	67.2	39.9	7.7	1.0
163	28	0.67∠-50.4°	71.9	40.4	8.86	0.63
200	28	0.654∠-50.1°	64	40.0	17.4	0.91
300	28	0.641∠-48.4°	64.2	40.4	6.67	0.78
400	28	0.654∠-50.1°	66.3	40.4	12.71	0.6
500	28	0.646∠-51.9°	73.7	40.8	2.0	0.35

From the results, it can be seen that the output load impedance of the 10 W GaN HEMT does not show significant sensitivity on the gate bias changing from the deep class AB to the class A. The results also indicate that the measured device is suitable to be subjected to the dynamic gate bias operation and that the optimum load reflection coefficient (impedance) for such operation can be easily selected. In this work, the selected optimal load reflection coefficient

Γ_{Lf0} has an average absolute value $abs(\Gamma_{Lf0})$ and average phase $angle(\Gamma_{Lf0})$ over the reflection coefficients at the geometrical midpoint marked with "o" in Figure 4.4 and presented in Table 4.3. The optimal load for the fundamental frequency $f_0 = 2$ GHz is found to be $\Gamma_{Lf0} = 0.67\angle$-50.8° i.e. $Z_{Lf0} = 45.8\text{-}j*85.3\ \Omega$. The impedance is calculated according to the equation (4.2)

$$Z = Z_0 \frac{1+\Gamma}{1-\Gamma} \tag{4.2}$$

where the characteristic impedance is $Z_0 = 50\ \Omega$.

During the load-pull measurements of the second and third harmonics at the frequencies $f_{2f0} = 2f_0$ and $f_{3f0} = 3f_0$, the source and load reflection coefficients at the fundamental frequency $f_0 = 2$ GHz are set to $\Gamma_{Sf0} = 0.90\angle 14.5°$ (Table 4.1) and $\Gamma_{Lf0} = 0.67\angle$-50.8°. The impedances for the second and the third harmonics at the input (gate) side of the DUT are set to $50\ \Omega$. The magnitude of the reflection coefficients during the harmonic tuning is set to be as close to one as possible, and it is about 0.95 due to the loss in the passive impedance tuner. The phase of the reflection coefficients for Γ_{L2f0} and Γ_{L3f0} that result in the maximum *PAE* is found for the same set of the gate bias values as for the fundamental frequency (see Table 4.2). The phase tuning of the Γ_{L2f0} and the Γ_{L3f0} is done several times alternately until the optimum phase values for both harmonics are changing. The results are presented in Table 4.4.

In order to find the optimal load impedances for the higher harmonics for all the bias conditions, the phase of the reflection coefficients for the second and third harmonics is tuned to find an area where the *PAE* does not drop for more than 3 percentage points from its maximum value. During the phase tuning of the second harmonic, the phase of the third harmonic is set to -60° as the round approximation of the results in Table 4.4. For the 3rd order harmonic phase tuning, the phase of the 2nd harmonic is set to 30° because the most bias

Table 4.4: Load reflection coefficients pairs for the 2nd and 3rd harmonics tuned for the maximum PAE.

I_D [mA]	V_D [V]	Γ_{L2f0}	Γ_{L3f0}
15	28	0.95∠30°	0.95∠-64°
25	28	0.95∠33°	0.95∠-64°
50	28	0.95∠30°	0.95∠-64°
100	28	0.95∠30°	0.95∠-62°
163	28	0.95∠28°	0.95∠-68°
200	28	0.95∠30°	0.95∠-64°
300	28	0.95∠32°	0.95∠-62°
400	28	0.95∠39°	0.95∠-55°
500	28	0.95∠40°	0.95∠-54°

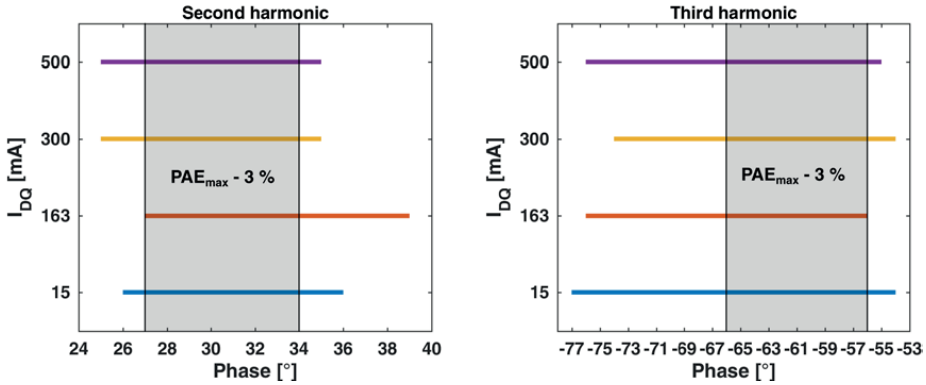

Figure 4.5: Phase area of the 2nd and 3rd harmonics for which the PAE does not drop for more than 3 percentage points. The measurement results for the I_{DQ} = *15 mA, 163 mA, 300 mA* and *500 mA*. Outside of the "safe" grey area the PAE is right at the edge at some points.

conditions in Table 4.4 result in highest *PAE* around that value. The results are shown in Figure 4.5. It can be seen that there is the phase area from *27°* to *35°* for the 2nd harmonic and from *-74°* to *-56°* for the 3rd harmonic where the *PAE* does not drop for more than *3* percentage points from its maximum value. However, some parts of these phase areas are right at the edge of the allowed *PAE* loss limitation (i.e. *3* percentage points) so the "safe" area is defined around initial phase values for the second and the third harmonic i.e. *30°* and *-60°* respectively (the grey area in Figure 4.5) as it is shown in Figure 4.5. Values of the *PAE* at the edges and the centre of the "safe" area for the second and third harmonics are presented in Table 4.5. Selected common load reflection coefficients for the fundamental, second and third harmonics over the measured gate

Table 4.5: PAE values for the 2nd and 3rd harmonics phase values at the edges and in the centre of the "safe" are where the PAE does not decrease for more than 3 percentage points.

I_D (mA)	Γ_{2f0} while Γ_{3f0}= 0.95∠-60°	PAE (%)	Γ_{3f0} while Γ_{2f0}= 0.95∠30°	PAE (%)
15	0.95∠27°	74.5	0.95∠-56°	75.3
	0.95∠30°	76.6	0.95∠-60°	76.6
	0.95∠34°	75	0.95∠-66°	74.8
163	0.95∠27°	76.9	0.95∠-56°	76.4
	0.95∠30°	76.4	0.95∠-60°	76.4
	0.95∠34°	77.9	0.95∠-66°	76.3
300	0.95∠27°	74.2	0.95∠-56°	76.4
	0.95∠30°	76.2	0.95∠-60°	76.2
	0.95∠34°	76.4	0.95∠-66°	76.7
500	0.95∠27°	72.8	0.95∠-56°	72.9
	0.95∠30°	73.3	0.95∠-60°	73.3
	0.95∠34°	73.9	0.95∠-66°	73.2

bias values are shown in Table 4.6 including the reflection coefficients at the gate side of the DUT. The reflection coefficient presented to the input of the DUT at the fundamental frequency Γ_{Sf0} is the small-signal matching for the maximum gain at I_{DQ} = *163 V* and V_{DQ} = *28 V*.

Power sweep measurement of the gain and the *PAE* with matching conditions from Table 4.6 are shown in Figure 4.6. The spread of the gain curves between different bias conditions in Figure 4.6 can be adjusted by changing the input (source) matching impedance for the small-signal gain (it will be discussed in the next section).

Table 4.6: Selected optimal load and source reflection coefficients for the dynamic gate bias operation.

Input			Output		
Γ_{Sf0}	Γ_{S2f0}	Γ_{S3f0}	Γ_{Lf0}	Γ_{L2f0}	Γ_{L3f0}
0.9∠14.5°	0	0	0.67∠50.8°	0.95∠-30°	0.95∠-60°

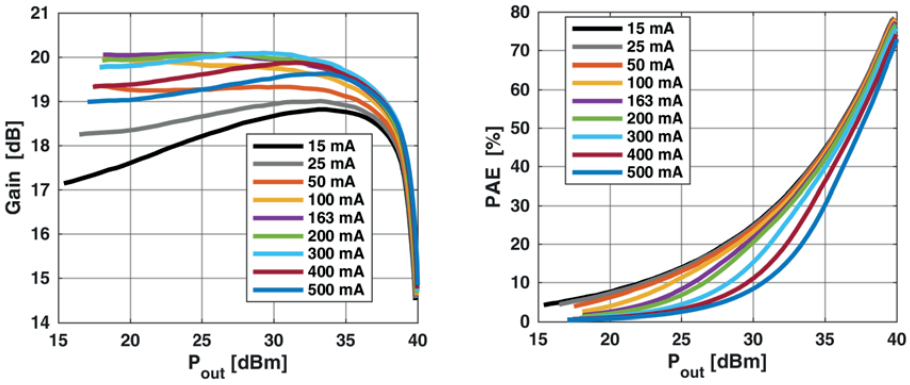

Figure 4.6: Gain and PAE vs. P_{out} of matched DUT for the set of quiescent bias point.

4.3 PA Design for the Dynamic Gate Bias Operation

4.3.1 Large-Signal Gain Measurement with Various Input Matching for Different Bias Conditions

In the previous section, it is shown that the load impedance of the 10 W GaN HEMT [10] is not significantly sensitive to the gate bias variation. According to the load-pull measurement results, the optimal load (trade-off between the efficiency and the output power) is selected, while the input matching is chosen to be the one for the maximum small-signal gain at the defined reference bias condition (I_{DQ} = *163 mA* and V_{DQ} = *28 V*). Changing the input matching

impedance for the small-signal gain, the gain level and the spread between the gain curves in Figure 4.6 can be manipulated. The power sweep measurement results with the input matching conditions $\Gamma_S = 0.90\angle 14.5°$, $\Gamma_S = 0.90\angle 13.5°$, and $\Gamma_S = 0.90\angle 12.5°$ and with the output matching condition presented in Table 4.6 are shown in Figure 4.7.

From the measured results in Figure 4.7 it can be seen that the gain level and the gain spread over the gate bias voltages that are resulting in the quiescent drain currents between the I_{DQ} = *15-500 mA* are varying for these input matching impedances. Thus, the order of the tracking function for the gain flattening can be reduced, and unwanted overlapping of the gain curves for the various bias conditions can be avoided with a careful selection of the input matching.

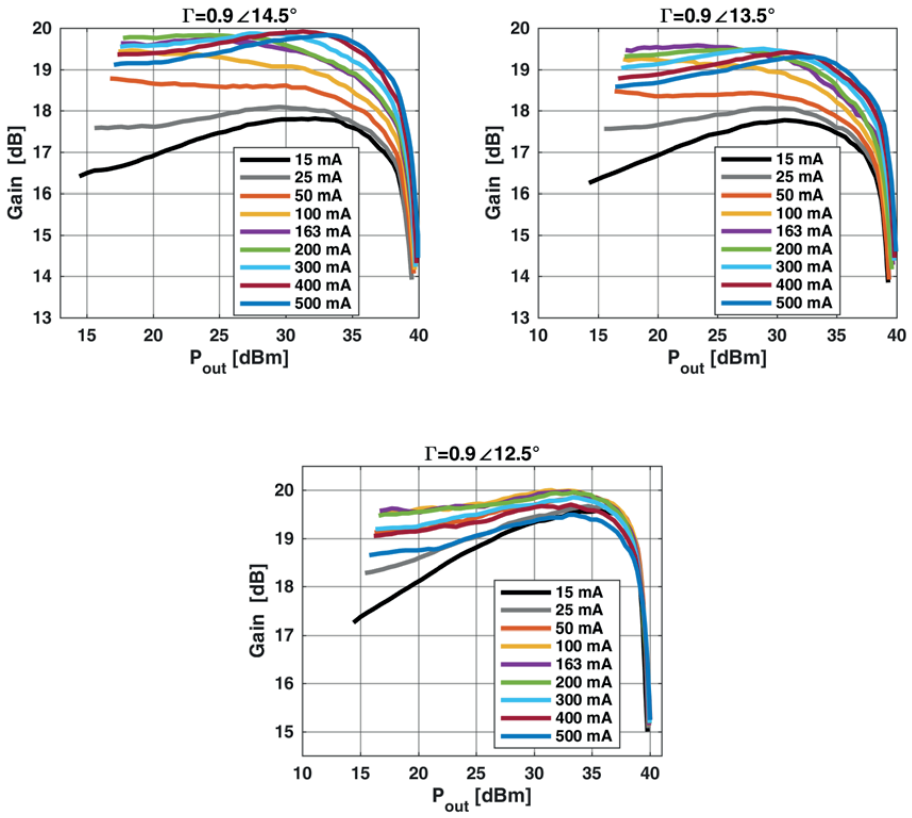

Figure 4.7: The power sweep gain measurements of the stabilized device for the set of the bias points for different input matching impedance values ($\Gamma_S = 0.9\angle 14.5°$, $\Gamma_S = 0.9\angle 13.5°$, and $\Gamma_S = 0.9\angle 12.5°$). Output matching is presented in Table 4.6.

Although the significant change in the optimal output impedance for the maximum output power and maximum PAE is not expected, it is investigated anyway. According to the equation (4.3), the output impedance (the output reflection coefficient) may vary if the device is bilateral. In (4.3) S_{xy} are the S parameters of the device, Z_{out} is the output impedance, and Z_0 is the characteristic impedance.

$$\Gamma_{out} = \frac{Z_{out} - Z_0}{Z_{out} + Z_0} = S_{22} + \frac{S_{12}S_{21}\Gamma_S}{1 - S_{22}\Gamma_S} \tag{4.3}$$

The load-pull measurement of the DUT with the input matching $\Gamma_S = 0.9\angle 12.5°$ and with the reference bias ($I_{DQ} = 163\ mA$) under the same compression level as the load-pull measurement in Section 4.2 is presented in Table 4.7 and compared with the measurement results in Table 4.3 ($\Gamma_S = 0.9\angle 14.5°$).

Table 4.7: The load-pull measurement results for the maximum P_{out} and PAE for the two different input matching conditions.

Γ_{Sf0}	I_{DQ} [mA]	V_{DQ} [V]	$\Gamma_{Poutf0,\ max.}$	$\Gamma_{PAEf0,\ max.}$
0.9∠14.5°	163	28	0.65∠-35.0°	0.72∠64°
0.9∠12.5°	163	28	0.74∠-34.6°	0.74∠-59°

The results are showing that taking into account the measurement tolerance, the output impedance change within the observed input matching impedance range (the phase of the Γ_S between *12.5°* and *14.5°*) is not significant and it can be neglected.

4.3.2 Power Amplifier for Dynamic Gate Bias Operation

In the previous section, the comprehensive load-pull measurement of the 10 W HEMT device has been performed to find the optimal load matching impedance for the maximum output power and the maximum PAE under the dynamic gate bias operation. Furthermore, the input matching impedances of the different gate bias conditions for the maximum small-signal gain have been tested in order to find the convenient gain versus output power spread for the gain flattening (Figure 4.7). It has been shown that the optimum load impedance does not change significantly for the tested input matching impedances (Table 4.7). The selected matching conditions at the input and the output of the DUT are shown in Table 4.8. Note that these reflection coefficients are referred to the reference planes shown in Figure 4.1 and Figure 4.2.

Table 4.8: Selected matching conditions at the input and the output of the DUT for the PA design.

Γ_{Sf0}	Γ_{Lf0}	Γ_{L2f0}	Γ_{L3f0}
0.9∠13.5°	0.67∠50.8°	0.95∠-30°	0.95∠-60°

The matching networks for the design of the PA are found in the Agilent ADS CAD tool [45]. The measured matching reflection coefficients from Table 4.8 are embedded to the new reference planes i.e. to the stabilisation circuit at the input (gate) and to the transistor package at the output (drain) side of the DUT in Figure 4.1 (the fixture for the load-pull measurements). Higher harmonics (2nd and 3rd) are not considered at the input side of the DUT. The layout of the PA is shown in the photo in Appendix B.

4.4 The measurement of the Power Amplifier for the Simulation Model

To make the model of the manufactured PA, the PA is subjected to the time-domain waveform measurement (see Section 2.10.2). The measurement system is shown in Figure 4.8, and it is a simplified version of the time-domain waveform measurement system with the load-pull entity developed at Cardiff University [46]. In the measurement system in Figure 4.8 the

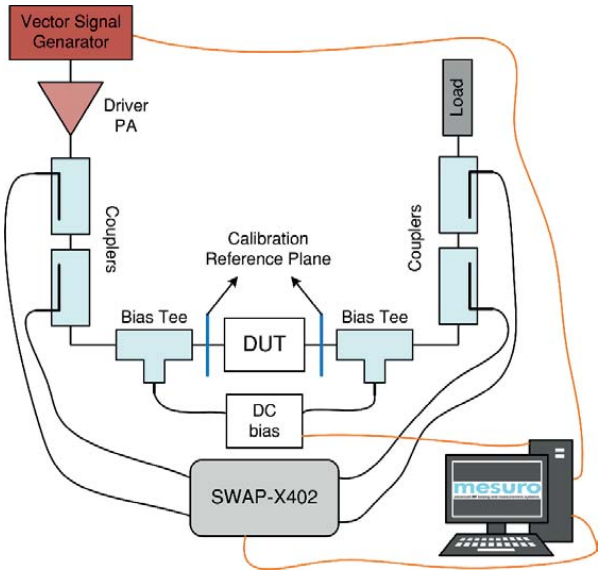

Figure 4.8: Time-domain waveform measurement system for the PA model measurement.

load-pull entities (the multiplexer and the RF generators for the active load-load pull measurement) are replaced with the *50 Ω* load since the measured PA is already matched to the *50 Ω*. The measurement system is calibrated at the calibration reference plane (3.5 mm connectors). The signal generator provides the source signal at the fundamental frequency of f_0 *= 2 GHz* and the DC power supply is used to supply the PA with the supply voltage. The sampler receiver SWAP-X402 [43] measures the incident and reflected waveforms (the *a* and *b* waves at the calibration reference planes). The measurement system is controlled with Mesuro Ltd. measurement suite [41].

The time-domain measurement is done with the gate bias voltages V_{GQ} *= (-2.85:0.05:-1.8) V* covering the bias range from the deep class AB to the class A (I_{DQ} *= 15-500 mA*). The drain bias voltage is set to the nominal value of V_{DQ} *= 28 V* [10]. The input power P_{in} is ranging from

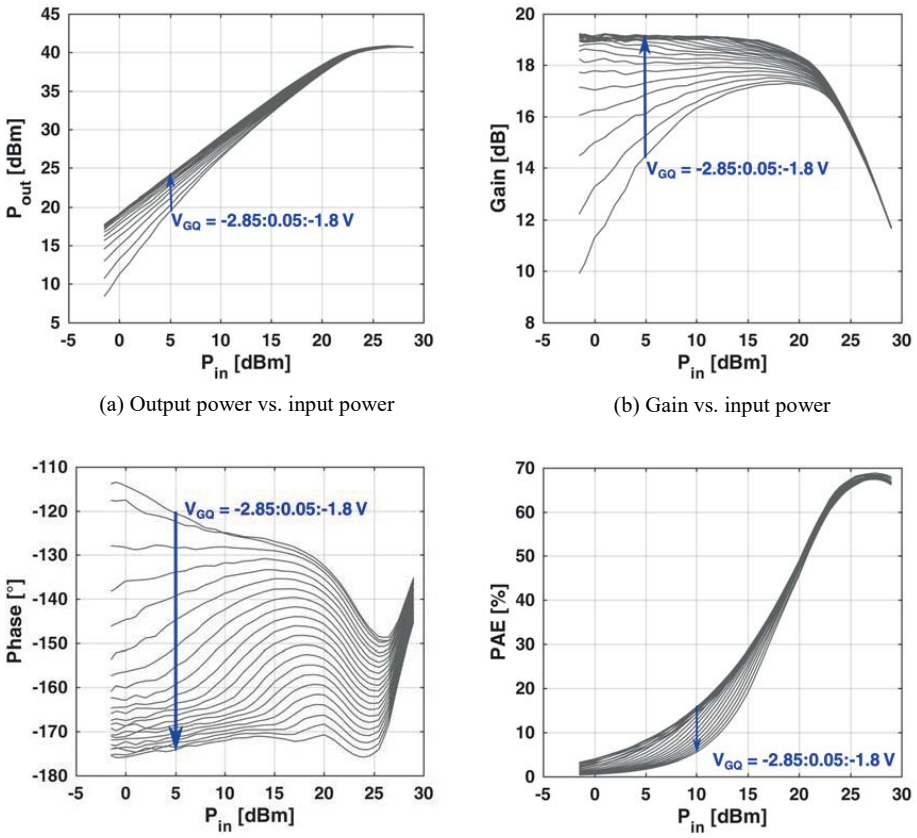

(a) Output power vs. input power

(b) Gain vs. input power

(c) Transfer phase vs. input power

(d) PAE vs. input power

Figure 4.9: Measured results of the time-domain waveform measurement for the PA model.

-1.5 dBm to *28.5 dBm* with the *1 dB* step. The measured results of the output power, power added efficiency, gain and transfer phase are shown in Figure 4.9. These results are then extrapolated down to the input power level of $P_{in} = 0\ W$ in order to cover the full input power dynamic range required for the Matlab simulation. Extrapolation is done in a way that the $P_{out} = 0\ W$ and the $PAE = 0\ \%$ when the $P_{in} = 0\ W$, while the gain and phase values are kept at the constant level of the lowest measured power level to the input power level of $P_{in} = 0\ W$.

4.5 Summary

This chapter describes the design procedure of the power amplifier for the dynamic gate bias (gate tracking) operation. Since the optimal output load impedance for the maximum output power and the maximum efficiency varies with the gate bias voltage, it is important to find the optimal output matching impedance (the optimal load impedance) for the dynamic gate bias operation. In this work, the 10 W GaN HEMT [10] is subjected to such operating conditions and the characterization of its optimum load impedances (reflection coefficients) for the fundamental, second and third harmonics is done using the load-pull measurement technique. The fixture designed for the stabilisation of the transistor for the load-pull measurement and the measurement setup are described in Section 4.1.1 and Section 4.1.2. Section 4.1.3 describes the conditions applied to the DUT for the load-pull measurement of each harmonic. The results of the measurement are shown in Section 4.2 showing that the output load impedance of the DUT does not change much when it achieves the maximum output power or the maximum PAE under the tested gate bias conditions. Furthermore, the overlapping impedance area for the 2nd and 3rd harmonics is detected, where the *PAE* does not drop for more than *3* percentage points from the maximum PAE value. The selection of the optimal matching impedance up to 3rd harmonic for the designed PA is done according to these results. The design of the PA for the dynamic gate bias operation is described in Section 4.3. This section also points out the importance of the input matching impedance for the small-signal gain. The different input matching impedances result in the different spread of the gain curves between the different gate bias conditions.

Section 4.4 explains the time-domain waveform measurement of the PA designed as it is explained in Section 4.3. The measurement is done for the set of the gate bias voltage values covering an area for the dynamic gate bias operation. The measured data is used as the model

of the PA in the Matlab simulation and for the gate tracking functions estimation in following chapters.

Chapter 5

Gate Tracking (Dynamic Gate Biasing)

Nowadays, the requirement on the data rate and the number of different services in the modern wireless communication systems is increasing, the modulation schemes are getting more complicated and more sensitive to the nonlinear distortion, while the frequency spectrum becomes densely occupied and the guard between the channels is getting narrower. The nonlinear distortion produces spurious components within and outside the occupied signal bandwidth. The former can lead to the loss of information contained in the signal and the later causes the degradation of the signal in the adjacent channels. This means that the signal amplification should be linear in order to keep the information carried by the signal intact and not to degrade the signal quality in the adjacent channels. Some of the linearization techniques that have been developed over the years are presented in Section 2.9.

This chapter discusses the linearization capabilities of the Gate Tracking (GT) technique also called the dynamic gate bias variation or the dynamic gate biasing. The chapter presents the simulation and measured results of the Power Gate Tracking (PGT) used for flattening the gain or the phase of the PA. Furthermore, it shows the measured results of the PGT PA with the gate tracking functions optimised for the *STDR* presented in Chapter 3.

5.1 Perspective of the Gate Tracking

There are two types of nonlinear distortion in memoryless PAs, the amplitude distortion or the AM-AM conversion and the phase distortion or the AM-PM conversion (Figure 5.1). The AM-AM and AM-PM conversions are defined in Section 2.6.1. The amplitude distortion is

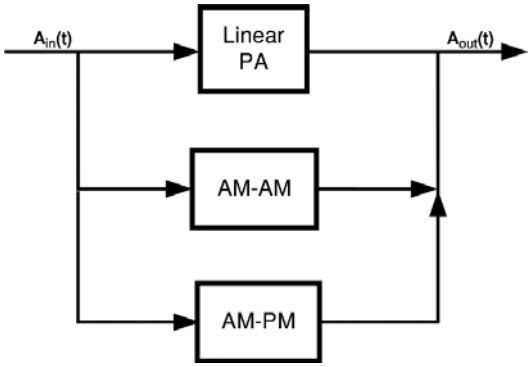

Figure 5.1: Nonlinear distortion in the memoryless power amplifiers [24].

related to the gain of the PA, and the phase distortion is related to the transfer phase between the input and the output of the PA. In this work, the gain and the phase are flattened with the PGT technique in order to reduce the amplitude or the phase distortion. Figure 5.2 shows the power gain and the transfer phase curves of the PA for different static gate bias values spanning from the class A to the deep class AB, and an example of the constant gain and phase located within the "area" of the static bias gain and the static bias phase curves.

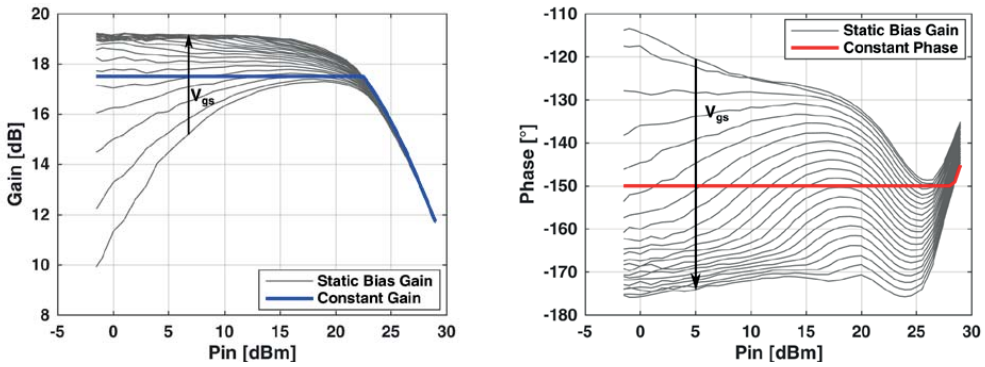

(a) Gain (b) Phase

Figure 5.2: Static gate bias gain (a) and the transfer phase (b) for the set of the gate bias values form the class A to the deep class AB and the constant gain (a) and the phase (b) with the dynamic gate bias variation.

From Figure 5.2 it can be seen that an adequate gate bias voltage V_{gs} can be selected for the certain instantaneous input power levels in such a way that the gain or the phase of the PA is flattened. The linearization of the gain results in lower amplitude distortion and the linearization

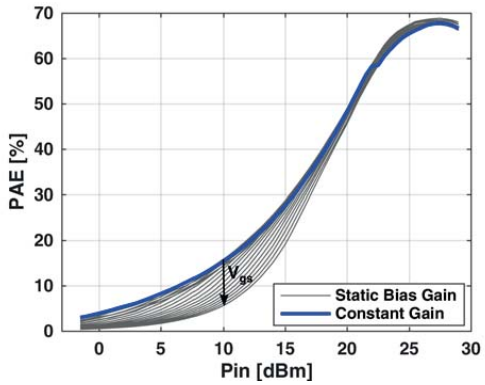

Figure 5.3: Static gate bias PAE for the set of the gate bias values form the Class A to the deep Class AB and for the constant gain with the dynamic gate bias variation.

of the phase results in lower phase distortion. It can be noticed that the gate tracking cannot linearize the gain or the phase when the PA operates in deep compression, but that part may be partly linearized in combination with other linearization techniques. For example, if it is combined with the auxiliary envelope tracking (AET) technique [3] (which expands the gain by increasing the drain bias voltage for the peak levels of the signal), the compression region may also be partly linearized. Figure 5.3 shows corresponding *PAE* for the same static gate bias values and the same constant gain value as in Figure 5.2. Note that by choosing the appropriate dynamic gate bias for either the flat gain or the flat phase so that the RF PA operates with the reduced conduction angle (in the class AB area) during the back-off operation, the efficiency would be higher compared to the linear class-A operation.

The supply modulator (voltage amplifier/tracker) at the gate of the PA can be realised by a rather simple circuit due to the negligible gate current. This means that the power requirement of the voltage tracker is minimal, making the design much simpler compared, for example, to the drain tracker in the envelope tracking (ET) technique.

So far, the possibility of the gate tracking (GT) technique for the linearity improvement is not investigated thoroughly in literature. One similar work has been reported by A. M. Conway et al. [47] where the gate bias was used to flatten the gain and minimise the third order intermodulation product of the GaN HFET device for the two tone test. A different approach has been presented by P. Medrel et al. in [48] where the 10 W GaN class B PA was linearized by increasing the gate bias voltage above the pinch-off voltage for the RF signal levels below the threshold. That way the nonlinearity caused around the pinch-off voltage in the class B PA is avoided.

5.2 Gate Tracking Functions

In this work, the gate tracking functions are chosen to be the polynomial functions used to approximate the gate bias voltage for the gain or the phase flattening according to the modulated input signal. As the variable of the tracking functions, one can use the envelope or the power of the modulated signal. The gate bias voltage, in this work, is changed according to the power of the input signal (5.1), where *n* is the order of the polynomial function. The reason for using the power of the modulated signal instead of its envelope is the narrow bandwidth of the power of the modulated signal compared to the bandwidth of its envelope (see Section 2.5).

$$v_{gs}(t) = a_n p_{in}(t)^n + a_{n-1} p_{in}(t)^{n-1} + \cdots + a_1 p_{in}(t) + a_0 \tag{5.1}$$

Figure 5.4 shows measured gain and phase for the set of the static gate bias voltages (V_{GQ} = *-1.8:0.05:-2.85 V*). The area of interest is marked with the green colour in Figure 5.4, and it is the area where the gain or the transfer phase can be flattened for the most of the dynamic input power range. The tracking functions for the flat gain or the phase are estimated from the $V_{GQ} - P_{in}$ (quiescent gate voltage versus input power) relation, where the input power is in watts. An example of the $V_{GQ} - P_{in}$ relation is shown in Figure 5.4. In other words, the gate bias voltage is the function of the input power (the power gate tracking - PGT). The coefficients of the *n-th*

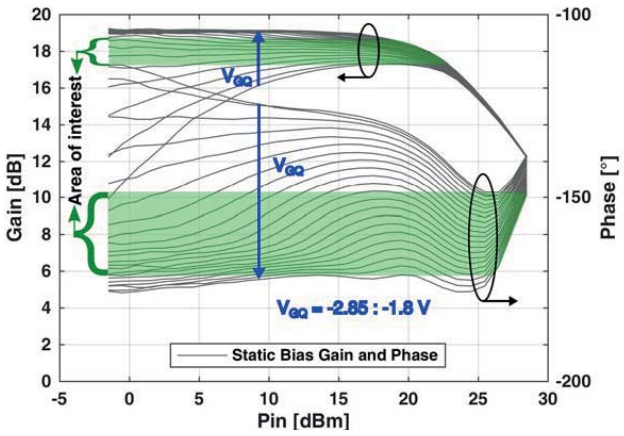

Figure 5.4: Static gate bias gain and phase with the area of interest for the gain or the phase flattening (green).

order polynomial functions are optimised to fit the ideal tracking function that results in the constant gain or phase for the given input power range. The optimisation is done with the polynomial fitting function in the Matlab, and each point is weighted with the corresponding value of the normalised input power level during the polynomial fitting procedure.

5.3 Investigation of the Linearity Improvements of the PA with Flattened Gain or Phase

Section 5.1 introduced the perspective of how the gate tracking technique used for flattening the gain or the phase of the PA can reduce the amplitude or the phase distortion and improve its linearity. In this section, those linearization capabilities are verified with the ACPR and the EVM by simulating the performance of the PA model amplifying the 16-QAM signal. The performance is verified with the Matlab simulations based on the premeasured data of the PA as it is explained in Section 4.4.

Tracking Functions

Flattening the gain is done with the polynomial function of the 2nd order, flattening the phase is done with the polynomial function of the 4th order. If the biasing gate voltage V_{gs} value reaches the level higher than for the class-A operation (I_{DQ} = *500 mA*) or lower than for the very deep class-AB operation (I_{DQ} = *15 mA*) the tracking curves are clipped at these values.

Simulation

The 16-QAM signal with the symbol rate of *1 MHz* is used in the simulation. The signal is generated in Matlab as a sequence of *1000* symbols. The signal is filtered by the raised-cosine filter with the roll-off factor α = *0.22* and oversampled with the factor of *80* which is the maximum sampling rate of the signal generator used for the laboratory measurements. The *PAPR* of the signal is *7.2 dB* and the complementary cumulative distribution function (CCDF) of the signal is shown in Figure 5.5. The same 16-QAM signal (the same symbol sequence) is used for all the simulations and the measurements in this thesis. The PGT tracking functions for the flat gain or phase that are investigated in this work are designed to have low V_{gs} keeping the PA in the deep Class-AB in the back-off. If the PGT PA operates in deep class-AB in the back-off, the average efficiency can be improved compared to the static bias class-A PA.

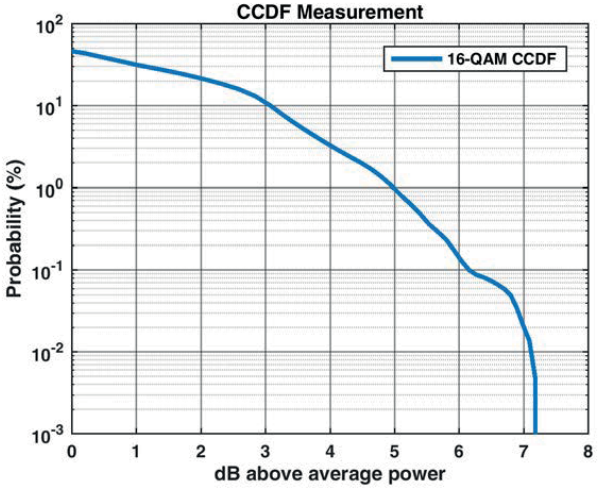

Figure 5.5: CCDF function of the 16-QAM signal used in this thesis.

5.3.1 Flattened Gain

The simulation results of the RF PA with the flattened gain using the 2nd order tracking function for the target gain values of *G = 17.6 dB* and *G = 17.3 dB*, the reference static bias class AB (I_{DQ} *= 200 mA*) and the class A (I_{DQ} *= 500 mA*) are shown in Table 5.1. The presented results are simulated so that the average output power is the same ($P_{out,avg}$*= 35.6 dBm*) for all the cases. The results of the flattening gain tracking function, the corresponding phase and the *PAE* for the target gain of *G = 17.6 dB* are shown in Figure 5.6. The tracking function is fitted with the 2nd order polynomial function that is clipped at the voltage resulting in I_{DQ} *= 500 mA* as explained earlier. The results are showing the significant degradation in the linearity for the both gain targets compared to the reference static bias class AB PA (I_{DQ} *= 200 mA*) and the

Table 5.1: Results of the dynamic gate bias PA for the flat gain with the 2nd order tracking function.

PA	$P_{out,avg}$ [dBm]	PAE_{avg} [%]	ACPR [dB]	EVM [%]
Static Bias				
I_{DQ}=500 mA	35.57	26.5	-39.92	3.09
I_{DQ}=200 mA	35.59	33	-34.58	4.87
Flattened gain Gate supply voltage bandwidth BW_{Vgs}= *2 MHz*				
G= 17.3 dB	35.56	35.72	-27.90	7.89
G= 17.6 dB	35.59	35.12	-25.97	12.76

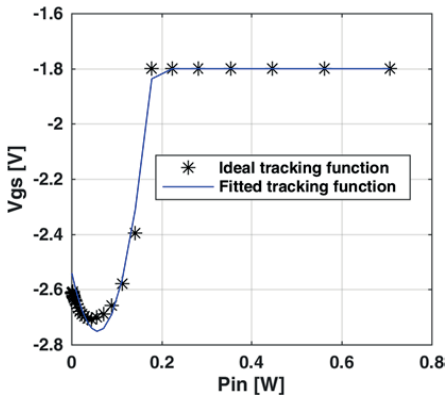

(a) Ideal and fitted tracking function for the flattened gain.

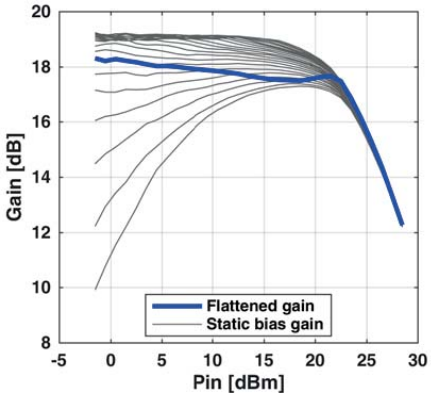

(b) Flattened gain.

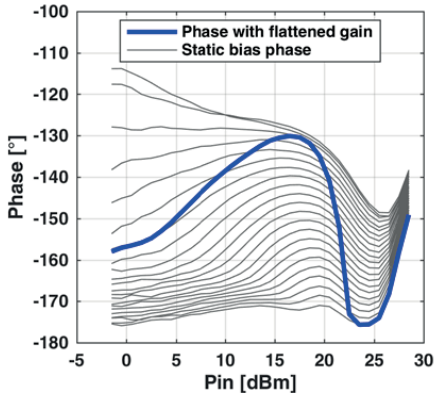

(c) Corresponding phase for the flattened gain.

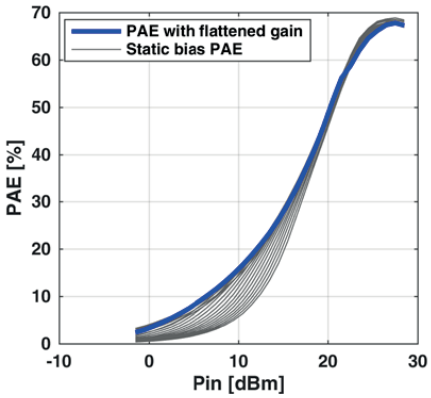

(d) Corresponding PAE for the flattened gain.

Figure 5.6: Second order tracking function for the flattened gain ($G = 17.6\ dB$), flattened gain, corresponding phase when the gain is flattened and the corresponding *PAE* when the gain is flattened.

class A PA ($I_{DQ} = 500\ mA$). The reason for this can be found in Figure 5.6. It can be seen that the phase of the PA, when the gain is flattened, changes dramatically through the input power dynamic range. This increases the phase distortion (AM-PM), and consequently, overall distortion is increased, regardless of the flattened gain (AM-AM). The *PAE* is high for the whole dynamic range as expected, due to the deep class AB operation for the low signal levels.

It is important to note that usage of a different device (transistor) could result in the narrower spread of the static gate bias phase curves and the gain flattening may lead to the linearity improvement. Changing the input matching impedance may also result in the narrower spread of the static bias transfer phase curves, but the gain would also be reduced due to the mismatch.

However, the spread of the static gate bias phase curves could be beneficial for flattening the phase with an acceptable order of the tracking function. Namely, lower order of tracking functions leads to the lower bandwidth of the gate voltage waveform.

5.3.2 Flattened Phase

This section investigates the linearization capabilities of the PGT technique for the phase flattening. The phase is flattened using the 4th order polynomial function as the tracking function for the target phase values of $\varphi = -149°$ and $\varphi = -155°$. The results with the constant average output power of $P_{out,avg} = 35.6\ dBm$ for the flattened phase, static bias class A PA and the

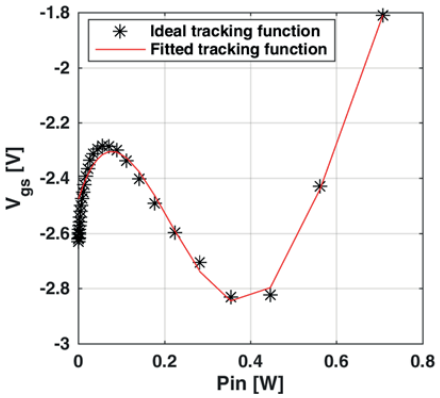

(a) Ideal and fitted tracking function for flattened phase.

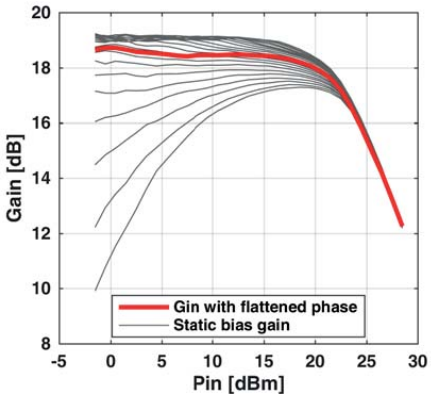

(b) Corresponding gain for flattened phase.

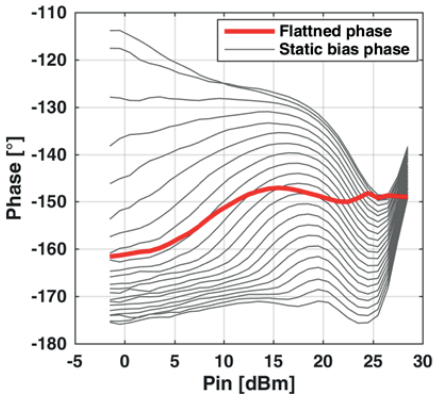

(c) Flattened phase.

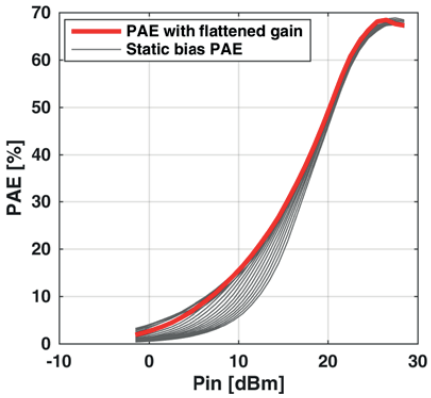

(d) Corresponding PAE for flattened phase.

Figure 5.7: Fourth order tracking function for the flattened phase ($\varphi = -149°$), corresponding gain when phase is flattened, flattened phase and the corresponding PAE when phase is flattened.

Table 5.2: Results of the dynamic gate bias PA for the flat phase with the 4th order tracking function.

PA	$P_{out,avg}$ [dBm]	PAE_{avg} [%]	ACPR [dB]	EVM [%]	φ_{error}
Static bias					
I_{DQ}=500 mA	35.57	26.5	-39.92	3.09	2.14
I_{DQ}=200 mA	35.59	33	-34.58	4.87	3.1
Flattened phase Gate supply voltage bandwidth BW_{Vgs}= *4 MHz*					
φ=-155°	35.58	32.6	-39.38	2.83	1.95
φ=-149°	35.58	33.7	-39.57	2.73	2.02

reference class AB PA are shown in Table 5.2. The results are showing significant improvement in the linearity with the preserved efficiency compared to the reference class AB PA. Compared to the most linear static bias class A PA the linearity is comparable while the efficiency is higher. Compared to the reference class AB PA, the *ACPR* is improved for *4.99 dB* and the *EVM* is improved by *2.14* percentage points with the phase target value of $\varphi = -149$ ° while the *PAE* is *0.7* percentage points higher. The plots of the tracking function, flattened phase, corresponding gain and the *PAE* for the target phase of $\varphi = -149$° are shown in Figure 5.7. It can be noticed that the corresponding gain, when the phase is flattened, varies insignificantly assuring the overall linearity improvement. It can also be noticed that for the low signal levels the RF PA operates in deep class AB which assures the preserved *PAE* compared to the reference class AB operation. A comprehensive investigation on the phase flattening is presented in the next section.

5.3.3 Comprehensive Investigation of the Phase Flattening Capabilities for the Linearity Improvement

The bandwidth of the PGT voltage waveform increases with the higher order of the tracking function. The narrower bandwidth of the gate voltage waveform, on the other hand, makes the design of the gate tracker (the gate voltage amplifier) simpler. However, the higher order of the tracking function results in the tracking function that is much better approximation of the ideal tracking function i.e. in the flatter phase and potentially in the better overall linearity performance. In order to find the trade-off between the bandwidth of the gate voltage waveform and the linearity improvement, the tracking functions of the 3rd, 4th and 6th order (5.1) are tested in the Matlab simulation. The tracking function of the 5th order is not tested because the polynomial fitting of the 5th and 4th order polynomials results in almost identical tracking functions and the preliminary results have shown no significant difference between them. The

tracking functions are shown in Figure 5.8. It can be seen that the 3rd order tracking function does not fit very well to the ideal tracking function for the flat (constant) phase, the 4th order tracking function differs from the ideal for the low signal levels, while the 6th order function fits quite well for the complete input power dynamic range. These tracking functions are used for the phase flattening for the several transfer phase levels within the area of interest (Figure 5.4) with the step of *5°* in two simulation cases. The Case I has the constant average output power of $P_{out,avg}$*= 35.6 dBm* and in the Case II the *ACPR* is set to be at least *-40 dBc*. The results with the constant average output power of $P_{out,avg}$ *= 35.6 dBm* with the flattened phase, static bias class A and the reference class AB are shown in Table 5.3. It shows the simulated results of the $P_{out,avg}$, *PAE*, *ACPR*, *EVM* and the phase error φ_{error}. The phase error is calculated as shown in the equation (5.2), where the φ_i is the phase corresponding to the instantaneous input power P_{in}, and the $\varphi_{reference}$ is the phase value corresponding to the minimum instantaneous input power level P_{in}.

$$\varphi_{error} = \sqrt{\frac{1}{N}\sum_{i=1}^{N}\left(\varphi_i - \varphi_{reference}\right)^2} \tag{5.2}$$

It can be noticed that the 3rd order function does not result in the significant linearity improvement while the *PAE* is preserved compared to the reference Class AB PA. The best linearity performance is achieved for the target phase value of φ = *-170°* which is comparable

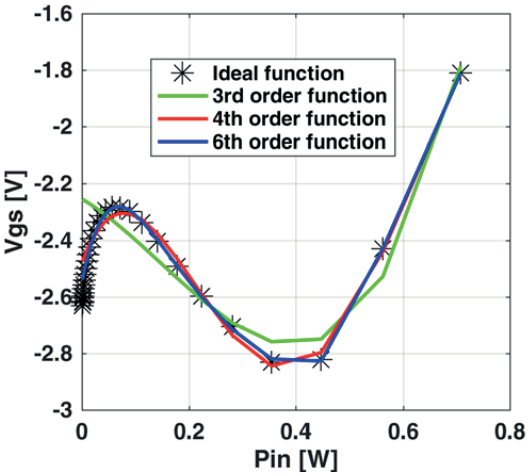

Figure 5.8: Ideal tracking function for the flat phase and the estimated 3rd, 4th and 6th order polynomial tracking functions.

Table 5.3: Case I simulation results for the flattened phase PA with the 3rd, 4th, and 6th order tracking functions within the area of interest, and the static bias class AB and class A PAs. The average output power is $P_{out,avg} = 35.6\ dBm$.

PA	$P_{out,avg}$ [dBm]	PAE_{avg} [%]	ACPR [dB]	EVM [%]	φ_{error}
Static bias					
I_D=500 mA	35.6	26.5	-39.9	3.1	2.14
I_D=200 mA	35.6	33	-34.6	4.9	3.1
Flattened phase with 3rd order tracking function Gate supply voltage bandwidth $BW_{Vgs} = 3BW_{RF} = 3\ MHz$					
φ=-170°	35.6	27.0	-40.3	3.0	1.7
φ=-165°	35.6	29.4	-36.2	3.9	2.0
φ=-160°	35.6	31.2	-36.4	4.3	2.2
φ=-155°	35.6	31.7	-31.6	7.2	2.9
φ=-149°	35.6	33.3	-33.2	6.5	2.9
Flattened phase with 4th order tracking function Gate supply voltage bandwidth $BW_{Vgs} = 4BW_{RF} = 4\ MHz$					
φ=-170°	35.6	26.8	-40.8	2.9	1.4
φ=-165°	35.6	29.7	-41.2	2.7	1.4
φ=-163°	35.6	30.6	-40.6	2.7	1.9
φ=-160°	35.6	31.4	-39.7	2.9	1.7
φ=-155°	35.6	32.6	-39.4	2.8	1.9
φ=-152°	35.6	33.1	-39.1	2.9	2.7
φ=-149°	35.6	33.7	-39.6	2.7	2.0
Flattened phase with 6th order tracking curve Gate supply voltage bandwidth $BW_{Vgs} = 6BW_{RF} = 6\ MHz$					
φ=-170°	35.6	26.7	-40.6	2.9	1.5
φ=-165°	35.6	29.7	-41.5	2.6	1.1
φ=-160°	35.6	31.3	-41.5	2.3	1.2
φ=-155°	35.6	32.6	-41.1	2.3	1.3
φ=-149°	35.6	33.7	-41.0	2.5	1.5

to the static bias class A PA in the linearity and the efficiency performance. The best efficiency performance is achieved for the target phase value of $\varphi = -149°$ and in this case, the *PAE* is comparable to the reference class AB PA, while the linearity is slightly worse. As the compromise between the linearity and efficiency, the target phase value of $\varphi = -160°$ can be selected. However, the cost of the complexity of the dynamic gate biasing would be too high for such poor performance increase.

The simulation results with the 4th order tracking function are showing significant improvement in the linearity compared to the reference static bias class AB PA. The highest efficiency is achieved for the target phase $\varphi = -149$, which results in the *0.7* percentage points higher *PAE*, *5 dB* better *ACPR* and the *2.7* percentage points better *EVM* compared to the reference class AB operation. The phase error is also smaller as it is expected since the phase is flattened.

Furthermore, it provides the comparable linearity with the most linear static bias class A PA with the *7.2* percentage points higher *PAE*. The target phase value of φ = *-165°* results in the best linearity performance but with the cost of the lower *PAE*. Still, it has better linearity and the efficiency performance compared to the class A PA.

When the phase is flattened with the 6th order tracking function, the linearity is further improved with no loss in the efficiency. As with the 4th order tracking function, the target phase value of φ = *-149°* provides the highest *PAE = 33.7 %*. Regarding linearity, the *ACPR* is improved by *1.4 dB*, and the *EVM* is insignificant *0.2* percentage points smaller. One can see that the improvement in the linearity is not significant compared to the 4th order tracking function, but the bandwidth of the gate bias voltage is *1.5* times wider. As it has been mentioned earlier, the wider bandwidth of the gate bias voltage complicates the design of the gate tracker, and because of that, the 4th order tracking function is selected as the optimum between the linearity improvement and the gate bias voltage bandwidth.

It can be seen that with the 4th and 6th order tracking function linearity of the PA with the flattened phase is improved for all the tested phase target values. Furthermore, the efficiency is preserved compared to the reference class AB PA only when the dynamic gate bias voltage keeps the PA in deep class AB operation for the low input signal levels i.e. in the back-off (that is achieved only for the certain target phase values).

Another interesting consideration of the PA performance is to look at the output power that is delivered to the load with the certain constant level of the linearity. Therefore, in another simulation case (the Case II), the *ACPR* is kept at approximately constant level of at least *-40*

Table 5.4: Case II simulation results for the flattened phase PA with the 4th order tracking function within the area of interest, and the static bias class AB and class A PAs. ACPR ≥ -40 dBc.

PA	$P_{out,avg}$ [dBm]	PAE_{avg} [%]	ACPR [dB]	EVM [%]	φ_{error}
Static bias					
I_D=500 mA	35.4	25.8	-40.2	3.0	2.1
I_D=200 mA	25.6	7.1	-40.2	3.3	3.1
Flattened phase with 4th order tracking curve Gate supply voltage bandwidth = $4BW_{RF}$ = *4 MHz*					
φ=-170°	35.8	28.0	-40.2	3.0	1.4
φ=-165°	36.0	31.5	-40.0	3.0	1.4
φ=-160°	35.3	30.3	-40.1	2.8	1.7
φ=-155°	34.8	29.4	-40.3	2.6	1.9
φ=-149°	35.2	32.2	-40.1	2.5	2.0

dBc. The simulation is done for the 4th order tracking function within the area of interest (Figure 5.4) with the *5°* step between the phase target values as in the Case I. The 4th order tracking function is selected as the trade-off between the gate voltage bandwidth and the linearity improvement capability as mentioned earlier. The results are shown in Table 5.4, which shows some pretty exciting results. The target phase value of φ = *-165°* is selected as the optimum between the $P_{out,avg}$, *PAE*, and the *EVM*. It can be seen that the average output power $P_{out,avg}$ that can be delivered to the load is *10.4 dB* higher with *24.4* percentage point higher *PAE* compared

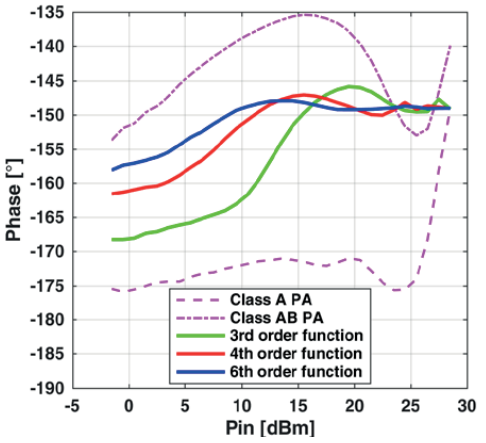

(a) Static bias and flattened phase.

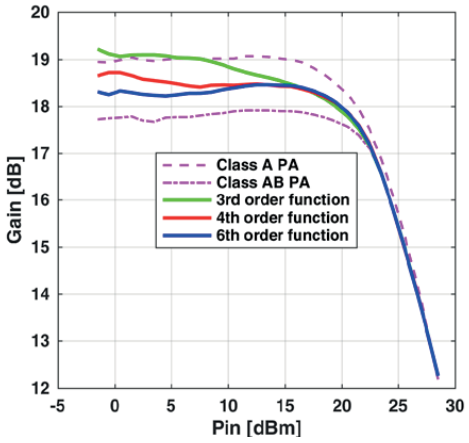

(a) Static bias gain and gain with flattened phase.

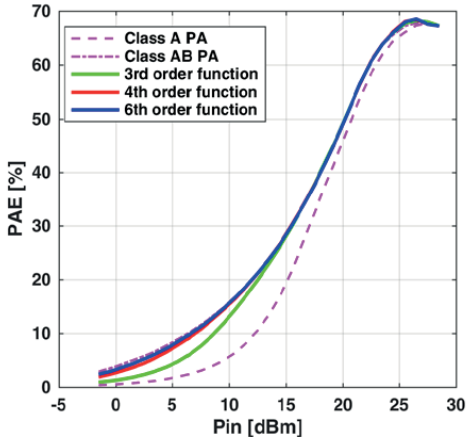

(a) Static bias PAE and PAE with flattened phase.

Figure 5.9: Static bias class A phase, static bias Class AB and flattened phase with the 3rd, 4th and 6th order tracking function with the corresponding gain andthe PAE. For the target phase value of φ = -149°.

to the reference class AB PA. Compared to the class A PA the $P_{out,avg}$ is *0.6 dB* and the *PAE* is *6.7* percentage points higher.

Figure 5.9 shows the phase, corresponding gain and the *PAE* curves for the static bias class A PA, the reference static bias class AB PA and the PA with flattened phase for the target values of φ = *-149°* with the 3rd, 4th and 6th order tracking functions (Figure 5.8). It is clear that the phase is flatter when it is flattened with the higher order tracking function. It can also be noticed that the flattened phase is more flat than the reference class AB PA, especially for the higher input power levels. Moreover, the corresponding gain is also flatter for the higher order tracking functions. The *PAE* when the phase is flattened is higher than for the class A PA for the low power levels due to the selected target phase values which keep the PA in the deep class AB during the dynamic gate bias operation. Consequently, the average *PAE* is preserved compared to the reference class AB PA.

5.4 Measurement of the PA with the Flattened Phase

In the previous section, the simulation has shown the linearity improvement with the preserved efficiency of the PA with the flattened phase using the PGT technique. This section shows measured results of the PA subjected to the PGT operation for the flattened phase under laboratory conditions. The RF PA is designed as it is described in Chapter 4. Since the behaviour model of the PA used for the simulation is based on the measured data of the RF PA used in this chapter, the tracking functions in the measurement are chosen to be the same as in the simulation. It is necessary to apply the DC offset to the generated gate voltage waveform due to the device temperature difference between the static measurement used for modelling and the dynamic operation with the modulated 16-QAM signal in the laboratory measurement. Another reason for the adjustment is the different measurement equipment used for these two measurements. The adjustment is done by changing the constant term (coefficient) of the tracking functions. However, the shape (other coefficients) of the tracking functions are intact. Besides the verification of the linearity improvement with the PGT technique, the model based on the one-tone static measurement is also verified.

5.4.1 Measurement Setup and Tracking Functions

The measurement is done using the 16-QAM signal with the symbol rate of *1 MHz* as the input signal. The modulated signal is oversampled with the factor of *80* (which is the maximum

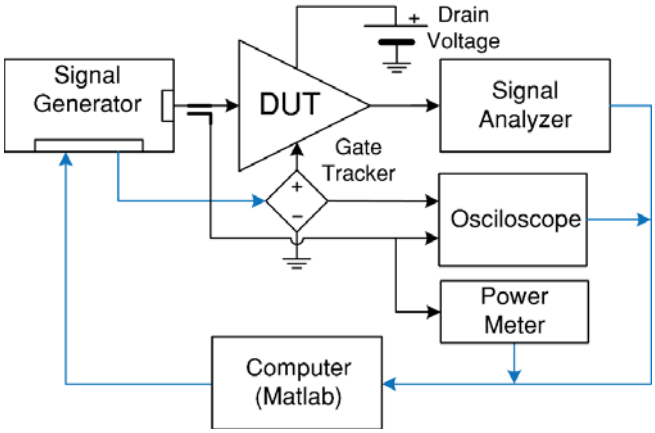

Figure 5.10: Dynamic gate biasing measurement setup.

sampling rate of the used measurement equipment) and filtered with the raised-cosine filter with the roll-off factor of $\alpha = 0.22$. It is the same signal sequence as in the simulation. The measurement setup used for the PGT operation is shown in Figure 5.10. The modulated signal and the dynamic gate voltage waveform V_{gs} are generated in Matlab and uploaded to the signal generator (SG) Rhode & Schwarz SMU 200. One baseband AWG (arbitrary waveform generator) of the SG is used for the upconversion of the modulated signal to the RF frequency of *2 GHz* feeding the input of the DUT. The other baseband AWG is used for feeding the gate tracker with the dynamic V_{gs} voltage waveform. The gate tracker then supplies the DUT with the gate bias voltage. The alignment between the input RF signal and the V_{gs} at the gate of the DUT is verified with the Agilent Infiniium MSO9254A oscilloscope and by assuring the symmetry between the lower and higher adjacent powers of the output signal. Although the signal envelope and the bias voltage are not measured intrinsically, the parasitic components do not delay the envelope frequencies significantly and the time alignment between them is a good indicator in combination with the adjacent power symmetry. The average P_{in} is measured with the Anritsu ML2438A power meter, and the output signal is measured and captured with the Rhode & Schwarz FSQ40 signal analyser for the further analysis. The gate tracker (the gate voltage amplifier) has been designed with an operational amplifier, its bandwidth is about 10 MHz, and its efficiency is not taken into account. The schematic of the gate tracker can be found in [49]. All the losses in the measurement system have been premeasured with the VNA with the accuracy of *0.1 dB*. The accuracy of the measurement instruments is about *0.1 dB*.

The phase is flattened with the PGT technique using the 4th order tracking function shown in the equation (5.1). The coefficients a_n of the 4th order gate tracking function for the phase flattening of the PA are calculated based on the same data (see Section 4.4) as for the simulation in Section 5.3 i.e. the same tracking functions are used. The gate tracking functions are estimated according to the input power. In order to calculate the V_{gs} (dynamic gate voltage waveform) that corresponds to the instantaneous power at the input of the DUT, the envelope power of the generated modulated signal is scaled to fit the measurement test-bench. Since the device temperature under static one-tone operation (which has been used for the measurement of the model data) is different from the temperature of the device under the dynamic signal operation, the I-V curves (V_{gs}-I_D relation) are changed. In order to compensate for that change, the DC voltage offset has to be applied to the calculated dynamic gate voltage waveform. The DC offset is determined by comparing the shape of the gain and the transfer phase curves of the PA from the Matlab simulation results and from the measured results for the same phase target value. The average output power is constant at $P_{out,avg.} = 35.6\ dBm$. The DC offset is tuned until the shapes of the corresponding curves are not as close as possible. It is also important to note that slightly different DC offset has to be applied to the dynamic gate voltage waveforms for the different phase target values. The modulated signal and the adopted gate voltage waveform are then uploaded to the SG.

5.4.2 Measurement Results

The PGT PA with the flattened transfer phase for several transfer phase levels within the area of interest (Figure 5.4) is measured for two cases. The Case I has the constant average

Table 5.5: Case I measured results for the flattened phase PA with the 4th order tracking function within the area of interest, and the static bias the class AB and class A PAs. $P_{out,avg}$ = 35.6 dBm

PA	$P_{out,avg}$ [dBm]	PAE_{avg} [%]	ACPR [dB]	EVM [%]
Static bias				
I_D=500 mA	35.6	29.9	-36.9	4.9
I_D=200 mA	35.6	38.0	-32.4	7.6
Flattened phase with 4th order tracking curve Gate supply voltage bandwidth $BW_{Vgs} = 4BW_{RF} = 4\ MHz$				
φ=-165°	35.6	33.5	-38.0	3.4
φ=-160°	35.6	33.8	-38.3	3.1
φ=-155°	35.6	35	-38.5	3.15
φ=-150°	35.6	35.5	-39.6	2.7

output power of $P_{out,avg}$= *35.6 dBm* and in the Case II the *ACPR* is set to be at least *-40 dBc*. The same has been done in the simulation shown in Section 5.3.3. The results of the PGT PA operation are compared to the reference static bias class AB and the class A PA. The quiescent gate bias voltage V_{DQ} that results in the quiescent drain current I_{DQ} of *200 mA* with the quiescent drain voltage V_{DQ} of *28 V* and P_{in} = *0 W* is chosen as the reference (the class-AB operation). The class A PA is biased so that the quiescent drain current is I_{DQ} = *500 mA* with the V_{DQ}= *28 V* and P_{in} = *0 W* according to the derating curve [10].

The results for the Case I presented in Table 5.5 are showing *5.6-7.7 dB* better *ACPR* and *4.2-4.9* percentage points better *EVM*, while the *PAE* is reduced for *2.5-4.5* percentage points compared to the reference static bias operation. The best result is achieved for the flat transfer phase of φ= *-150°*. Furthermore, the results for the Case II presented in Table 5.6 show *1.7-2.7 dB* higher average output power with the *1.3-8.5* percentage points higher *PAE*. The best result is achieved for the flat transfer phase of φ= *-150°*.

The measured results with the 4th order tracking function for the Case I show a good match to the simulation results with the same tracking curve in the *ACPR* and *EVM*, while the *PAE* is slightly decreased. The results for the Case II show higher average output power delivered to the load and higher *PAE*. The measured results show smaller improvement compared to the simulation results in Section 5.3.3. The reason for that may be much better results of the reference class AB PA achieved in the laboratory measurement than in the simulation.

Table 5.6: Case II measured results for the flattened phase PA with the 4th order tracking function within the area of interest, and the static bias class AB and class A PAs. ACPR ≤ -40 dBc

PA	$P_{out,avg}$ [dBm]	PAE_{avg} [%]	ACPR [dB]	EVM [%]
Static bias				
I_D=500 mA	34.5	24.4	-40.2	3.0
I_D=200 mA	32.7	26.5	-40.1	3.0
Flattened phase with 4th order tracking curve Gate supply voltage bandwidth = $4BW_{RF}$ = *4 MHz*				
φ=-165°	34.4	27.8	-40.0	3.9
φ=-160°	35.0	30.8	-40.1	3.7
φ=-155°	35.0	32.5	-40.2	2.54
φ=-150°	35.4	35	-40.1	3.28

Figure 5.11 shows the measured phase and gain of the PGT PA with the 4th order tracking function used for the phase flattening for the target phase value of φ = *-150°* and for the

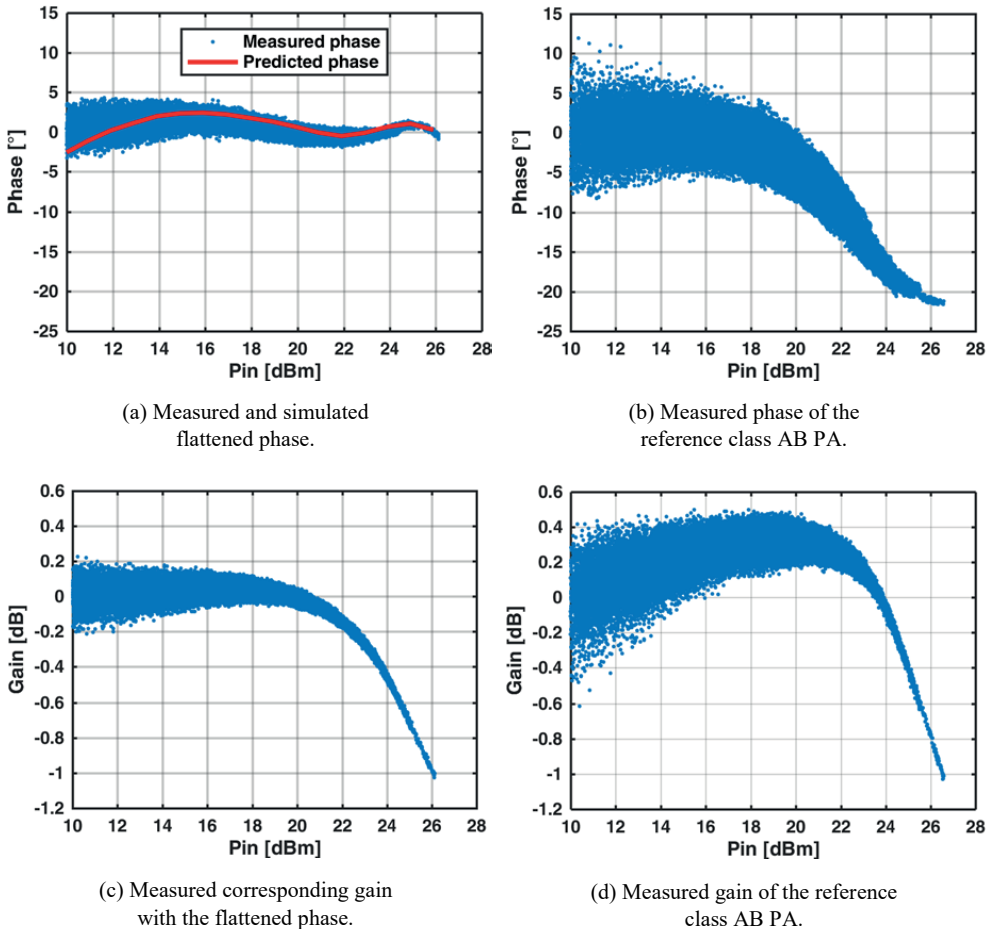

(a) Measured and simulated flattened phase.

(b) Measured phase of the reference class AB PA.

(c) Measured corresponding gain with the flattened phase.

(d) Measured gain of the reference class AB PA.

Figure 5.11: Measured and simulated phase and measured gain of the dynamic gate bias PA with the 4th order tracking function for the flattened target phase of φ = -150°, the measured phase and gain of the reference static bias class AB PA. All measurements and simulations have the same average output power $P_{out,avg}$ = 35.6 dBm.

reference static bias class AB PA. It can be clearly seen that the phase is flatter compared to the reference PA and that gain is also flatter for the PGT PA. These results are confirming that the PGT technique can be used for the phase flattening of the 10 W GaN PA reducing the phase distortion and consequently, the amplified digitally modulated signal suffers less distortion (improved *ACPR* and *EVM*). Moreover, Figure 5.11 (a) also shows the simulated (predicted) flattened phase for the PGT PA with the same tracking function and phase target value. It can be noticed that these two results match very well. Both results (simulated and measured transfer phase) have maximum peaks around the P_{in}= *15 dBm* and the P_{in}= *25 dBm* with a minimum

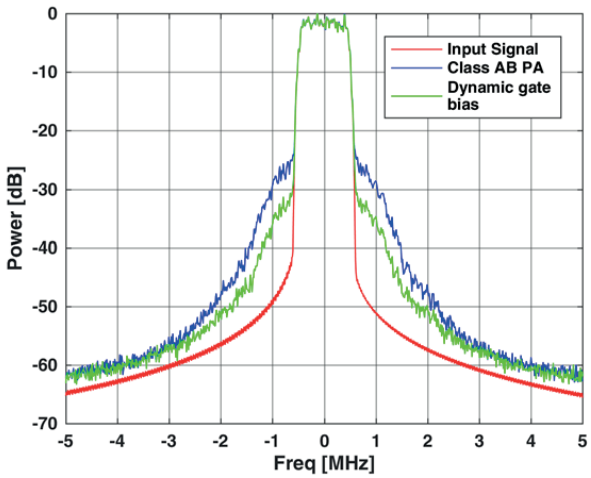

Figure 5.12: Power spectral density of the input 16-QAM signal and the measured output signal for the static bias class AB PA and the dynamic gate biasing PA for the flat phase of φ= -150° with the constant average P_{out} = 35.6 dBm.

peak around the P_{in}= *22 dBm*. This leads to the conclusion that the static one-tone measurement data can be used as the model of the 10 W GaN HEMT [10] PA operating with digitally modulated signals with the varying envelope. Furthermore, it is shown that the same data can be used for the tracking function estimation and simulation of the PGT PA. However, a small adjustment of the gate voltage waveform has to be applied as mentioned earlier. It is important to note that the one-tone static measurement does not account for the memory effects. This means that this amplifier does not suffer from significant memory effects while amplifying the 16-QAM signal used in the presented simulation and measurement. The power spectral density of the input (not distorted) 16-QAM signal, amplified signal with the reference static bias class AB PA and the dynamic gate biasing PA with the flattened phase (the 4th order tracking function for target phase of φ = *-150°*) is shown in Figure 5.12. It clearly shows improvement in the spectral regrowth i.e. the *ACPR*.

Intuitively, the best linearity performance of the PGT PA is not the flat phase or the flat gain. There is, for sure, a trade-off between the transfer phase and gain functions which means that the coefficients of the tracking function should be optimised for the overall best linearity. This can be done by optimising the coefficients for the *ACPR* and *EVM* simultaneously in order to minimise the nonlinear distortion outside and inside the signal bandwidth. Optimisation for the

ACPR and *EVM* requires sort of a cost function, which may be complicated to set up. In the next section, the optimisation is done using the *STDR* as FOM which evaluates the nonlinear distortion inside and outside of the signal bandwidth. Development of the *STDR* is described in Chapter 3.

5.5 Optimisation of a Gate Tracking Function for STDR

The optimal gate tracking function for the linearity improvement of the PA is probably not the tracking function that provides the flat phase or the flat gain. Thus, the optimisation of the gate tracking function coefficients for the linearity is necessary to find an optimal function and to achieve the best linearity performance of the dynamic gate biasing or the PGT PA.

5.5.1 Optimization process

In order to optimise the tracking functions of the PGT PA for the linearity, the coefficients of the gate tracking functions are optimised for the maximum *STDR*. The STDR is the novel linearity measure described in Chapter 3. During the optimisation process described below, some boundary requirements have to be satisfied.

The optimisation is done for the polynomial functions (5.1) of the 1st, 2nd, 3rd and 4th order. For the optimisation purpose, a simple search algorithm that searches for the optimal coefficients of the optimised polynomial (tracking) functions is developed. The initial (starting) coefficients are alternately changed for the positive and the negative value of the step *S* in the optimisation loop. Adding and subtracting the initial coefficients value for the step *S*, the set of

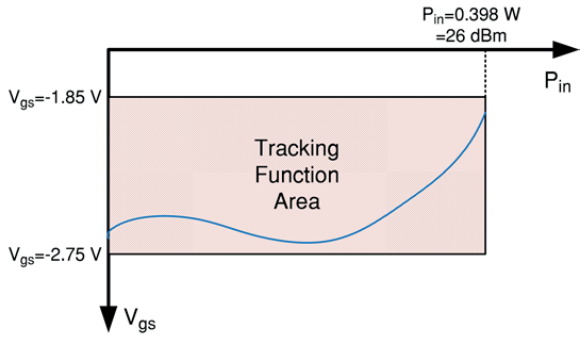

Figure 5.13: Gate tracking function boundary area for the optimization.

the new tracking function coefficients is created. Generated gate voltage waveforms that are generated by the tracking functions with the new coefficients (found by the search algorithm) have to be within the minimum and the maximum allowed gate voltage values for the defined input power range. The minimum allowed gate voltage is $V_{gs,min} = -2.75\ V$ which results in the quiescent drain current of $I_{DQ} = 15\ mA$ (deep class AB), and the maximum allowed voltage is $V_{gs,max} = -1.85\ V$ which results in the quiescent drain current of $I_{DQ} = 500\ mA$ (the class A). These conditions have to be satisfied for the input power range from the $P_{in} = 0\ W$ to the $P_{in} = 0.398\ W = 26\ dBm$ which drives the PA up to the *3 dB* compression when the PA is biased with the $I_{DQ} = 163\ mA$ and $V_{DQ} = 28\ V$. This boundary condition is graphically presented as the tracking function area in Figure 5.13. The tracking functions that do not satisfy this boundary condition are disregarded and are not considered further in the process. If the tracking function exceeds the voltage limitation outside of the defined input power range, it is clipped at the $V_{gs,min}$ or the $V_{gs,max}$ value. Next, the tracking functions with the coefficients that satisfy the boundary requirements are used in the PGT PA measurement and evaluated for the *PAE* and the *STDR*. The coefficients of the tracking function that result in the best *STDR* and in the best *PAE* which is higher than *35 %* are selected for the further optimisation. The defined *PAE* requirement is *90 %* of the *PAE* for the reference static bias PA operation (I_{DQ}*=163 mA*, V_{DQ} *= 28 V)* when it delivers the output power of P_{out}*= 35.6 dBm* i.e. *35 %*. Selected coefficients are the further optimised in the same manner. I would like to note that this simple search algorithm is not ideal and it may not lead to the global optimum solution. However, it optimises the tracking functions and it verifies the STDR as the linearity optimisation FOM. The optimisation is done using the same 16-QAM signal as in all previous measurements and simulations.

The initial (starting) coefficients of the tracking functions for each optimisation, for each optimised tracking function order, are found by performing the same optimisation process in Matlab. For the optimisation in Matlab, the same data (model) of the 10 W GaN HEMT PA has been used as for the Matlab simulations in the previous sections. In the Matlab optimisation, the starting coefficients are the coefficients of the tracking functions for the flattened phase for the target phase values of $\varphi = -150°$, $\varphi = -155°$ and $\varphi = -160°$ i.e. the target phase values that result in the higher *PAE* (see Section 5.3). The coefficients that result in the best *STDR* are used as initial coefficients in the laboratory optimisation.

5.5.2 Optimization results

The measured results of the PGT PA using the optimised tracking functions, the PGT PA with flattened phase for $\varphi = -150°$ and the static bias class AB and class A are presented in Table 5.7. The results are showing that if the polynomial function is optimised for the maximum *STDR*, even the low order polynomial function (order one) shows the improvement of *4.86 dB* in *STDR*, *4.82 dB* in *ACPR* and *3.61* percentage points in *EVM* compared to the reference static bias class AB PA (I_{DQ}= *163 mA*). The 4th order function results in the *7.39 dB* better *STDR*, *7.66 dB* improvement in *ACPR* and the *5.29* percentage points in *EVM* compared to the reference class AB PA. It is also shown that the optimised 3rd order tracking function gives better results than the 4th order flattened phase tracking function. The *PAE* is slightly higher for all the PGT operation cases compared to the reference static bias class AB PA. It is important to notice that both the *ACPR* and the *EVM* are improved. This suggests that maximising the *STDR* reduces the nonlinear distortion outside and inside of the output signal bandwidth which has been predicted in Chapter 3. It can be seen from the results that increasing the polynomial function order from two to three results in the significant improvement regarding linearity, while the improvement between order one and two as well as between three and four is not so big. This result also shows the bandwidth of the gate voltage waveform (the tracking function order) vs. linearity improvement relation, and it can be used to find the trade-off between the tracking function order (the gate voltage bandwidth) and the linearity. It is also shown that the coefficients of the gate tracking functions for the PGT PA operation can be optimised using the *STDR* measure to give lower distortion inside and outside of the output signal bandwidth (EVM

Table 5.7: Measured results of the dynamic gate biasing PA with the optimised gate tracking functions for the STDR, the dynamic gate biasing PA for the flat phase, and the static bias class AB and class A PAs.

PA	BW_{Vg} [MHz]	STDR [dB]	$P_{out,avg.}$ [dBm]	PAE_{avg} [%]	ACPR L [dBc]	ACPR R [dBc]	EVM [%]
Static gate bias operation							
I_{DQ}= 500 mA	-	24.43	35.58	30.57	-38.80	-38.17	4.10
I_{DQ}= 163 mA	-	19.57	35.59	38.9	32.68	-32.36	7.85
Dynamic gate bias operation for flat phase							
φ= -150° Order 4	4	26.37	35.59	35.5	-40.12	-39.60	2.76
Dynamic gate bias operation with optimised coefficients							
Order 1	1	24.43	35.60	36.4	-37.50	-37.03	4.24
Order 2	2	25.2	35.59	37.7	-37.63	-37.16	3.67
Order 3	3	26.63	35.58	37.2	-39.87	-39.20	2.71
Order 4	4	26.96	35.57	37.25	-40.6	-40.02	2.56

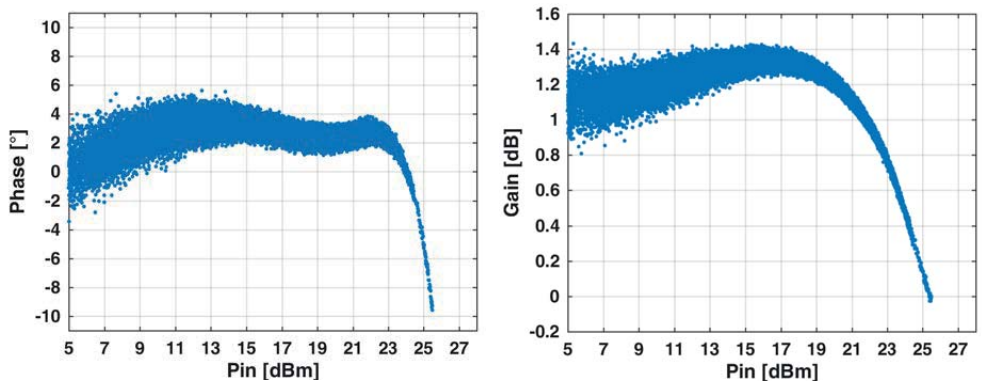

(a) Measured phase. (b) Measured gain.

Figure 5.14: Measured phase and gain of the dynamic gate bias PA with the optimized 4th order tracking function for the maximum STDR with the average output power $P_{out,avg}$ = 35.6 dBm.

and ACPR). This makes this approach convenient for the PA linearity evaluation and optimisation. Moreover, it is also verified that the presented FOM ensures the high output power level i.e. the gain of the PA during optimisation of the PA or the linearization technique.

Figure 5.14 shows the phase and gain of the PGT PA with the 4th order tracking function with the optimised coefficients. It clearly shows that this result is not the ideal flat phase or gain. Namely, it can be noticed that the phase drops in the compression area which is not the case for the result with the flattened phase with the 4th order tracking function (see Figure 5.11). One of the reasons for that may be the probability density function (PDF) of the 16-QAM signal used in the optimisation process (see Figure 2.5). The probability that the 16-QAM signal reaches peak values driving the PA in the deep compression is not high. This means that the linearity of the PA for these drive levels is not as important as for the drive levels with the higher probability. Another one may be that the best linearity of the PA is achieved with the trade-off between the gain and the phase flatness.

The example of the time domain waveform of the input 16-QAM signal and the gate bias voltage waveform is shown in Appendix C.

5.6 Summary

This chapter presents the comprehensive investigation of the linearization capability of the PGT technique. Section 5.1 shows the perspective of flattening the gain or the phase of the PA with dynamic gate bias in order to reduce the nonlinear distortion in the amplified signal. It is

shown that by the "smart" selection of the gate bias voltage for each instantaneous input power level, the gain or the phase can be flattened reducing the amplitude or the phase distortion of the PA. In order to calculate the dynamic gate bias voltage for the gain or phase flattening, the tracking functions are required. Those functions are chosen to be the polynomial functions of the power of the input signal as the variable as explained in Section 5.2.

In Section 5.3 it is shown that flattening the gain does not improve the linearity of the PA. Actually, it makes it even worse. The reason for that is found to be the corresponding phase of the flattened gain of the PA, which changes dramatically over the observed input power dynamic range. This increases the phase distortion, and consequently, the overall distortion is larger regardless to the reduced amplitude distortion. However, flattening the phase of the PA shows great potential for the PA linearization. This is confirmed by comprehensive investigation based on the Matlab simulation using the model of the PA (see Section 4.4) presented in Section 5.3.3.

The laboratory measurement results and the measurement setup for the PGT PA for the flattened phase are shown in Section 5.4. The measurements have been done with the 4^{th} order (polynomial) tracking function for the several target phase values within the area of interest. The selection of the tracking function order has been done based on the optimal simulation results in Section 5.3.3. The results show a significant linearity improvement with the preserved efficiency if the PA operates in deep class AB area during the PGT operation i.e. for the certain phase target values. Moreover, it is shown that measured flattened phase with 16-QAM signal matches with flattened phase predicted by the Matlab simulation with the model based on the one-tone measurement results of the PA. This suggests that the behaviour model of the 10 W GaN PA based on the one-tone measurement can be used for the simulation with the modulated signals with varying envelope and for the gate tracking function estimation.

Intuitively, the best linearity of the PA is not achieved with the flattened phase or the flattened gain but with the trade-off between these two. This means that the optimisation of the gate tracking function is required. In order to reduce the overall distortion in the amplified output signal i.e. outside and inside of the signal bandwidth, the *ACPR* and the *EVM* must be improved. Since it can be complicated to optimise the coefficients of the gate tracking function for the *ACPR* and the *EVM* simultaneously and it would possibly require a cost function between these two linearity measures, the novel linearity metric as the signal to total distortion ration (*STDR*) hase been developed. The STDR is the metric that evaluates nonlinear distortion outside and inside of the signal bandwidth presented in Chapter 3. It also includes all the sources

of the nonlinear distortion in the chain. Since it is the ratio of the linear over nonlinear power, the optimisation for the maximum *STDR* leads to maximising linear and minimising nonlinear power. That way, the linearity of the PA is improved, and the output power i.e. the gain of the PA is preserved.

Section 5.5 shows results from the laboratory optimisation of the coefficients for the gate tracking functions using the *STDR*. Results are showing better linearity of the PGT PA with the optimised gate tracking function for the *STDR* compared to the operation with the gate tracking function for the flat phase with the same order. This result also verifies the *STDR* as linearity measure and as the figure of merit for the PA optimisation for the linearity or for evaluation of different linearization techniques.

Chapter 6

Drain Power Envelope Tracking

One of the commonly used efficiency enhancement technique is the envelope tracking or simply the ET [2], [50]. The basic principle of the ET technique is described in Section 2.8.3. High efficiency of the ET system is achieved when both the RF PA and the supply voltage amplifier (the envelope tracker) are highly efficient. In order to achieve high efficiency of the ET PA (the RF power amplifier subjected to the dynamic drain bias operation), the supply voltage waveform must be the accurate replica of the signal envelope. In theory, the bandwidth of the signal envelope is infinite, and the process of shaping or filtering the voltage waveform must be applied to reduce its bandwidth to the acceptable level. Luckily, most of the envelope power is stored in the approximately 4x-10x bandwidth of the signal [30] which allows the bandwidth reduction, but with the low loss in the ET PA efficiency. Furthermore, the distortion introduced to the supply voltage waveform may lead to the distortion of the output signal. This means that the supply voltage amplifier should be as linear as possible. These requirements lead to huge challenges in the supply voltage amplifier design. Namely, it is hard to design highly efficient, highly linear amplifier with the wide bandwidth. There are different supply voltage amplifiers (modulators/trackers) architectures [51], [52] developed to achieve the wanted performance. Since it is not easy to design the linear supply voltage amplifier with the wide bandwidth and high efficiency, it is common to reduce the supply voltage bandwidth as mentioned above. A common technique for the reduction of the supply voltage bandwidth is usage of the envelope shaping functions or by filtering the signal envelope [34], [53]. Reduction of the voltage supply bandwidth leads to the higher efficiency performance of the supply

voltage amplifier, and although the shaped supply voltage waveform may lead to the lower efficiency of the RF PA, the efficiency of the ET system may be maintained or even increased.

This chapter presents the power envelope tracking (PET) technique (see Section 6.2) applied to the 10 W GaN RF PA where the drain supply voltage is modulated according to the power of the input signal instead of its envelope. The advantage of tracking the power of the signal is in its limited and analytically well-defined bandwidth equal to the RF bandwidth of the modulated signal[23]. Section 6.4 presents the 2nd order PET where the 2nd order PET tracking function, with the reduced supply voltage bandwidth, approximates the conventional ET tracking function. The measured results of the PET and the 2nd order PET techniques are presented and compared with the conventional ET and the class AB PAs. Furthermore, the measured results of the PET and the 2nd order PET in combination with the PGT (power gate tracking) technique for the improved linearity are also presented. Theoretical analysis of the PET and 2nd order PET is presented in Sections 2.5.1and Section 2.5.2.

6.1 Influence of the Gate Bias Voltage on Linearity of the Envelope Tracking PA

Since the envelope tracked RF PA operates in compression, the linearity of the envelope tracked RF PA is poor, and the linearization is required. A common linearization technique used with the ET PAs is a digital predistortion DPD [2], [54], [55]. A common approach in designing the ET PAs is to bias them in the class B or deep class AB. Although the ET PA is commonly linearized with the DPD, it is beneficial to get the best linearity performance from the ET PA itself with no loss in the efficiency.

With different constant gate bias conditions, the AM-AM and AM-PM transfer functions (gain and transfer phase) are varying. With the smart selection of the gate bias voltage of the ET RF PA providing the optimal AM-AM and AM-PM characteristics, the ET PA may result in the better linearity compared to the conventional design approach (bias the PA in the class B or deep class AB). Designing the ET PA with the optimal gate bias that results in better linearity, the DPD may be simplified i.e. its order and power requirement may be lower.

6.1.1 Measurement Setup and Tracking Function

Since the 2nd and the 3rd harmonics of the 10 W GaN PA are tuned for the maximum *PAE* when the PA operates *3 dB* in compression (see Chapter 4), the ET PA is envelope tracked at

the same compression level to achieve high *PAE*. The drain voltage of the ET PA spans from *6 V* to *28 V*. The 16-QAM signal with the symbol rate of *1 MHz*, filtered with the raised-cosine filter (α=0.22) is used in the measurements (the same signal as in the previous measurements). The measurement system is the same as shown in Figure 3.1. The 16-QAM signal, static gate and dynamic drain (ET) voltage waveforms, are generated in Matlab and uploaded to the signal generator. The modulated signal is then upconverted to the RF frequency of *2 GHz* and sent to the RF input of the DUT. The gate and drain voltage waveforms are sent to the drain tracker, which supplies the PA with the gate and drain bias voltages. Note that in this measurement, the gate voltage is constant, but the PA is supplied with the gate tracker due to the measurement setup structure. The alignment between the output RF signal and the drain bias voltage is verified with the oscilloscope and by assuring the symmetry between the lower and higher adjacent channel powers of the output signal. Although the signal envelope and the supply voltage are not measured intrinsically, the parasitic components do not delay the envelope frequencies significantly and the time alignment between them is a good indicator in combination with the adjacent channel power symmetry. The input power is measured with the power meter and the output signal is captured and measured with the signal analyser. The captured data of the output signal is then further processed in Matlab. The drain tracking function is shown in Figure 6.1. The drain voltage spans from *6 V* to *28 V,* and it is clipped at the low end to prevent the gain collapse below the knee voltage and at the high end in order not to exceed the nominal drain voltage of *28 V* of the device [10]. Usually, in the ET PAs the drain

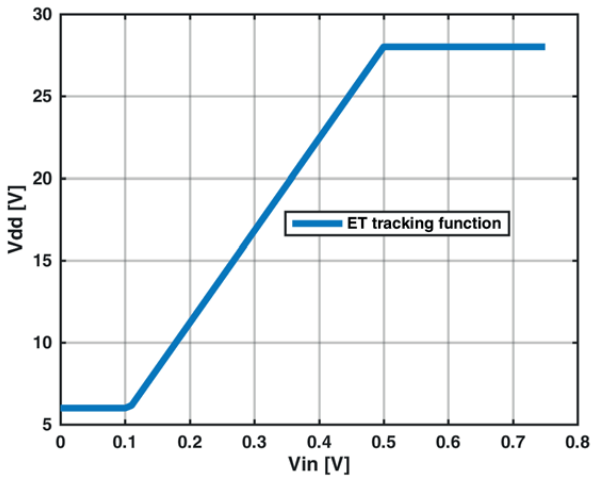

Figure 6.1: Drain supply voltage tracking function.

voltage reaches its maximum value with the maximum drive level (at the PEP of the signal). In this work, the drain voltage reaches the nominal value of *28* V with the input power level that drives the RF PA *3 dB* in compression since the RF PA is designed to have the maximum *PAE* at that compression level. Due to that clipping (decresting) of the drain voltage is required. Since driving the RF PA into compression changes its behaviour and the envelope of the output signal, it is not "pure" envelope tracking. Although the term envelope tracking is used for that kind of operation more correct term would perhaps be a PA with dynamic supply. This statement applies to all the dynamic supply techniques under the same operating conditions.

The gain and phase of the ET PA are measured for the set of the static quiescent gate voltage values V_{GQ}= *-2.7:0.1:-1.9 V*, which corresponds to the quiescent drain currents I_{DQ}= *15-500 mA* (from deep class-AB to class-A) with the nominal quiescent drain voltage. For each gate bias voltage, the input signal power is adjusted so that the level of the average output power is $P_{out,\,avg.}$ = *35.6 dBm*.

6.1.2 Measurement Results

The measured results of the ET PA are presented in Table 6.1. Linearity of the PA for each gate bias voltage is evaluated with the adjacent channel power ratio (ACPR), error vector magnitude (EVM) and the signal to total distortion ratio (STDR) (see Section 5.5). The efficiency is evaluated with the power added efficiency (PAE). The best linearity performance is achieved with the V_{GQ} = *-2.5 V* and the best efficiency performance with the V_{GQ} = *-2.3 V*. More precisely, the former has *1.8 dB* better *ACPR* and *0.86* percentage points better *EVM* with *1* percentage point better *PAE,* while the latter has *1.1* percentage points better *PAE* compared to the V_{GQ}=*-2.7 V* (deep Class-AB) which is the bias that could commonly be chosen for the

Table 6.1: Measured results of the ET PA for the set of static gate bias values.

V_{GQ} [V]	P_{in} [dBm]	PAE [%]	$ACPR_L$ [dBc]	$ACPR_R$ [dBc]	EVM [%]	STDR [dB]
-2.7	20.27	65.62	-28.36	-28.74	10.13	18.77
-2.6	20.12	66.40	-29.45	-29.80	9.30	19.51
-2.5	20.01	66.64	-30.12	-30.35	9.27	19.60
-2.4	19.84	66.68	-30.11	-30.12	10.13	18.93
-2.3	19.83	66.70	-29.60	-29.52	11.20	18.04
-2.2	19.78	66.39	-28.70	-28.56	12.6	17.00
-2.1	19.69	66.28	-27.66	-27.60	14.13	15.96
-2.0	19.74	64.75	-26.71	-26.56	15.52	15.09
-1.9	19.69	63.07	-25.87	-25.74	16.95	14.27

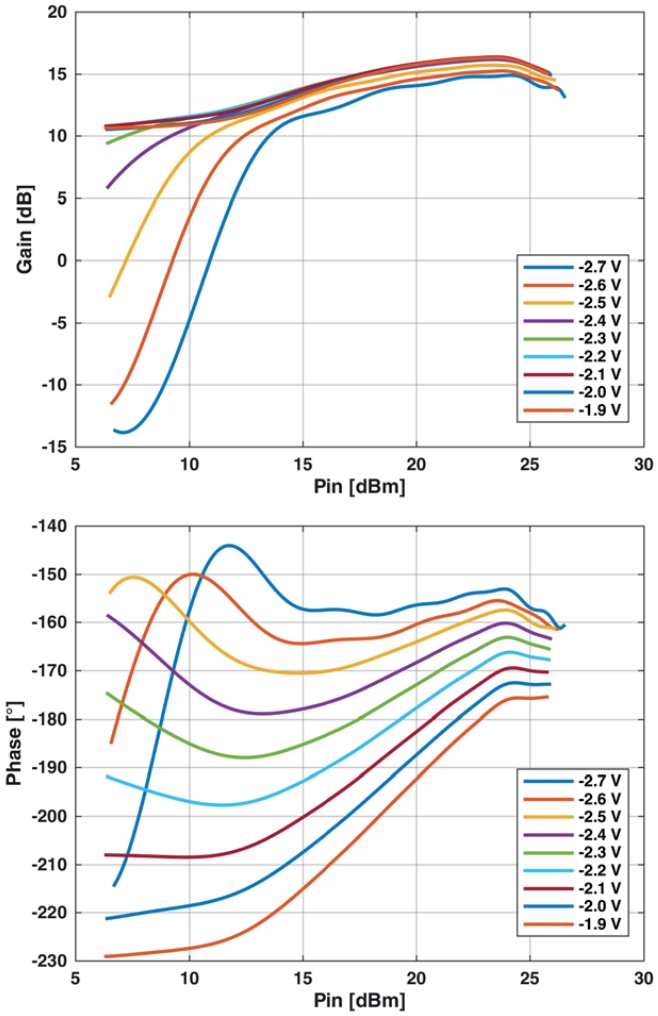

Figure 6.2: Gain (top) and Phase (bottom) of the ET PA for the set of the static gate bias voltage values.

ET PA. This result suggests that the gate bias voltage of V_{GQ} = *-2.5 V* would be the better choice than V_{GQ} = *-2.3 V* for both the linearity and the efficiency performance.

However, the ET PAs produce the significant amount of the nonlinear distortion, and they are usually combined with the DPD in order to achieve the acceptable level of linearity. It may be beneficial to analyse the gain and the transfer phase curves (the AM-AM and the AM-PM transfer functions) for the measured set of the gate bias voltages in Figure 6.2. The measured scattered gain and the phase of the signal are approximated with the fitted function in order to get smooth gain and transfer phase curves. It can be seen that for the low gate bias voltage

values, the gain and the transfer phase of the ET PA drop significantly in the back-off region (for the low input signal levels). Such significant change of the gain and transfer phase requires a higher order digital predistorter. Selection of the gate bias voltage for which the gain and the transfer phase acts more constant within the given power dynamic range may lead to the simplification of the DPD design in terms of the required order. Moreover, since the loss of the gain must be compensated with the DPD to reduce the amplitude distortion, choosing the bias voltage with more constant gain may simplify the design of the DPD in terms of the power requirement. Looking at the gain and phase curves on Figure 6.2 one can notice that the gain and phase are rather flat for the static gate bias of V_{GQ} = *-2.3 V* and V_{GQ} = *-2.4 V*. These bias points may simplify the DPD system more than the bias that results in the best *ACPR* and *EVM*. Nevertheless, the efficiency performance must be checked before selecting the gate bias. It would be a drawback losing the efficiency with the efficiency enhancement technique as the ET. In Table 6.1 can be seen that the gate bias values of the V_{GQ} = *-2.3 V* and V_{GQ} = *-2.4 V* are providing the high *PAE*.

Observations in this section should be analysed by the realisation of the DPD for each case, which is a scope for future work.

The same principle can be applied to the PET, which is also presented in this chapter.

6.2 Power Envelope Tracking

In Section 2.5.1 it is shown that the power of the modulated signal has significantly narrower and analytically defined bandwidth compared to the bandwidth of its envelope which is infinite in theory. Using the signal power instead of the signal (voltage) envelope simplifies the design of the supply voltage amplifier in the envelope tracking systems especially for the wideband systems. It is easier to design the linear and highly efficient voltage amplifier with the narrower bandwidth.

This section presents the PET (see Section 2.5.1) technique, which simultaneously improves the efficiency and the linearity of the 10 W GaN RF PA, where the drain supply voltage is modulated according to the power of the input signal. The measured results of the PET and the 2nd order PET are presented and compared with the conventional ET PA operation and the reference class AB PA. Furthermore, the measured results of the PET in the combination with the PGT, presented in Chapter 5, for further improvement in linearity are also shown.

6.2.1 Measurement System

The 10 W GaN PA used in this work has been designed as explained in Chapter 4. The measurement system is shown in Figure 3.1. The 16-QAM signal with the *1 MHz* bandwidth filtered with the raised cosine filter with the roll-off factor $\alpha = 0.22$, the drain and gate supply voltage waveforms are calculated in Matlab using the preselected tracking functions. The 16-QAM signal and the voltage waveforms are uploaded to the signal generator. The modulated signal is then upconverted to the RF frequency of *2 GHz* and sent to the input of the DUT. The gate and drain voltage waveforms are sent to the gate and drain supply voltage amplifiers (the gate and drain tracker) which supply the PA with the gate and drain bias voltages. Alignment between the envelope of the RF signal and the gate supply voltage at the input as well as the drain supply voltage at the output of the RF PA is verified with the oscilloscope and by assuring the symmetry between the lower and higher adjacent powers of the output signal. Although the signal envelope, the bias and the supply voltages are not measured intrinsically, the parasitic components do not delay the envelope frequencies significantly and the time alignment between them is a good indicator in combination with the adjacent power symmetry. The input power is measured with the power meter and the output signal is captured and measured with the signal analyser. The measurement accuracy is about 0.1 dB. The supply voltage amplifiers have been designed with an operational amplifier, and their efficiency performance is not the scope of this work. The bandwidth of the gate tracker is about *10 MHz* and the bandwidth of the drain tracker is about *5-6 MHz*. The schematic of the gate and the drain trackers can be found in [49].

6.2.2 Tracking Functions

The tracking functions for the ET, PET and 2nd order PET heve been analysed in Section 2.5.1 and examples of the ideal tracking functions are shown in Figure 2.8.

Usually, in the ET systems the maximum drain supply voltage $V_{dd,max}(t)$ of the RF PA is achieved for the maximum envelope voltage $v_{e,max}$ and the detroughing has to be applied to the ET tracking function at the low drain voltages to avoid the gain collapse close to the knee voltage. The same can be applied to the ideal PET tracking function with no need for detroughing because it is detroughed naturally due to the requirements as it is shown in Section 2.5.1 and in Figure 2.8. In this work, the PET tracking function is shaped so that $V_{dd,max}(t) = 28\ V$ is achieved when the level of the input power p drives the RF PA *3 dB* into compression. The reason for such tracking function, and not the ideal one, lies in the RF PA design (see Chapter 4). The RF PA is harmonically tuned to achieve the maximum *PAE* when it is driven *3 dB* in

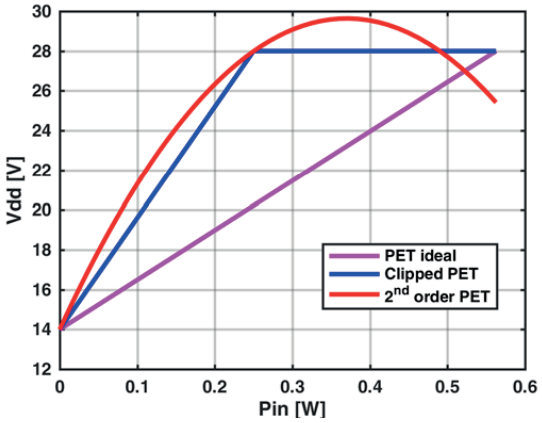

Figure 6.3: Drain tracking functions as the function of the signal power.

the compression. Consequently, the conventional (ideal) PET tracking function would cause significantly deeper compression, which would result in the efficiency and gain collapse. To avoid that, the PET tracking function reaches the $V_{dd,max}(t) = 28\ V$ for the $v_e(t) < v_{e,max}$. As a consequence, the drain supply voltage $V_{dd}(t)$ would exceed the maximum value for the high drive levels. Therefore, the supply voltage that exceeds $V_{dd,max}$ is clipped (decresting is applied) at the same voltage level. Clipping of the tracking function increases the bandwidth of the supply voltage waveform significantly. The bandwidth is in theory increased to the infinity. In the measurement system used in this work the drain voltage waveform is filtered by the supply voltage amplifier which has approximately *5 MHz* bandwidth. It is important to note that such filtering may add the distortion to the supply voltage. In order to avoid the clipping, the PET tracking function is approximated with the 2nd order polynomial function i.e. the 2nd order PET tracking function is used and fitted to the clipping PET tracking function (see Section 2.5.1). The requirement during the fitting procedure is to have the same minimum voltage point, the same point where the clipped PET function reaches the $V_{dd,max}$ and that the $V_{dd}(t)$ never exceeds the value of *30 V*. The ideal PET tracking function (2.8), clipped PET tracking function and the 2nd order PET tracking function (2.11) used in the measurement with the power as the variable are shown in Figure 6.3. The corresponding bandwidths of the drain supply voltages of the PET, clipped PET, 2nd order PET and the signal envelope bandwidth with the DC component included for the *1 MHz* 16-QAM signal used in this measurement are shown in Figure 6.4. It is clear that the bandwidth of the PET voltage is well defined and it is the same as the RF

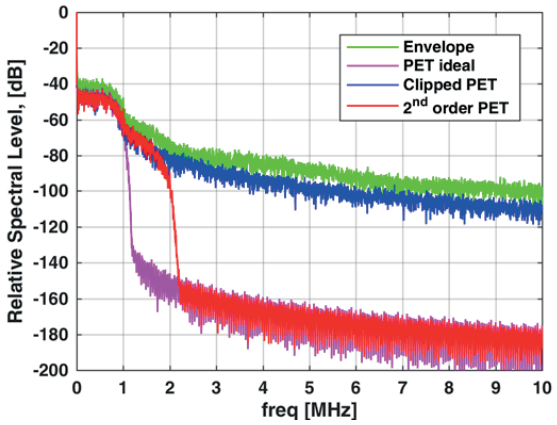

Figure 6.4: Spectral bandwidth of the signal envelope and the drain supply voltage with different tracking curves of the 1 MHz 16-QAM signal.

bandwidth. The bandwidth of the clipped PET drain supply voltage is increased to the infinity, and it is *2* times the RF bandwidth wide for the 2nd order PET.

6.2.3 Measurement Results

The PET and 2nd order PET PAs are evaluated for the *PAE, ACPR, EVM* and the *STDR*. The *STDR* is the novel linearity metric that evaluates nonlinear distortion outside and inside the signal bandwidth (see Chapter 3). First, the evaluation is done for several gate bias voltage values in order to find the optimal gate bias for the linearity and the efficiency performance. The motivation to check the linearity-efficiency performance for different gate bias conditions is explained in Section 6.1. The gate bias voltage that results in I_{DQ}*=250 mA* with the quiescent drain bias V_{DQ}*= 28 V* is selected as optimal. The measured results of the PET and the 2nd order PET for all the static gate bias voltage values are shown in Appendix A. The measurements are done for the two cases. The Case I has the constant average output power of $P_{out,avg}$ *= 35.6 dBm* and for the Case II the *ACPR* is set to be at least *-40 dBc*.

The measured results for the Case I and the Case II with the optimal gate bias (I_{DQ}*=250 mA*) for the linearity and the efficiency are shown in Table 6.2. In addition, the measured results of the conventional ET PA with the optimal static gate bias (I_{DQ} *= 165 mA*) and the reference static bias class AB PA (V_{DD}*=28 V* and I_{DQ}*=160 mA*) are presented. The detroughing and decreasting (clipping above the knee voltage and above the maximum drain voltage i.e. 6 and 28 V respectively) of the voltage supply waveform is applied due to the RF PA design.

The Case I results for the PET and the 2nd order PET PA are showing *16.8* and *14.4* percentage points higher *PAE*, *9.1*, *10.5 dB* better *ACPR*, *5.95* and *6.39* percentage points better *EVM* respectively compared to the reference class AB PA. Compared to the ET PA, the *PAE* is *7.1* and *9.5* percentage points lower, the *ACPR* is improved for *11* and *12.2 dB*, and the *EVM* is improved for *6.56* and *7* percentage points respectively. This result is expected since the drain supply voltage in the PET technique does not follow the envelope of the signal as close as in the ET technique, especially in the power back-off region. Because of this, the PET RF PA is less compressed in the power back-off region, which results in less efficiency and better linearity. However, the compared to the conventional static bias class AB PA, the significant simultaneous linearity and efficiency improvements are achieved with the PET and 2nd order PET techniques. Compared to the ET PA the efficiency is reduced but the linearity is significantly improved. The Case II measurement shows that the PET and 2nd order PET techniques can deliver *3.8* and *4.4 dB* more output power than the class AB PA respectively, while the *ACPR* is the same. The ET PA is not measured for the Case II because by its nature it operates in the compression and it distorts too much.

Table 6.2: Measured results of the Case I ($P_{out,avg}$ = 35.6 dBm) and the Case II (ACPR ≤ -40 dBc) for the PET and the 2nd order PET techniques with the measured results of the class AB PA and the ET PA for comparison.

PA	BW_{Vds} [MHz]	P_{out} [dBm]	PAE [%]	η_D [%]	$ACPR_L$ [dBc]	$ACPR_R$ [dBc]	EVM [%]	STDR [dB]
Case I $P_{out,avg}$ = 35.6 dBm								
Class AB PA		35.6	38.2		-31.8	-31.5	8.63	
ET PA	BW_{Vds}*	35.6	62.1	64.0	-30.1	-30.3	9.24	19.73
PET PA	1	35.6	55.0	56.3	-41.1	-41.1	2.68	28.69
2nd order PET PA	2	35.6	52.6	53.9	-42.3	-42.4	2.24	30.69
Case II ACPR ≤ -40 dBc								
Class AB PA		32.2	25.65		-40.2	-40.2	3.33	
PET PA	1	36.0	56.1	57.5	-40.0	-40.0	2.77	28.37
2nd order PET PA	2	36.6	54.7	56.0	-40.0	-40.2	1.73	28.71

* Drain voltage bandwidth of the ET PA is theoretically infinite and in this work it is filtered by the drain tracker to approximately 5-6 MHz

6.3 Power Envelope Tracking with Gate Power Tracking

To improve the linearity of the PA even more, the PET and 2nd order PET techniques are combined with the power gate tracking PGT (dynamic gate biasing) operation (see Chapter 5). This means that the RF PA is under dual dynamic biasing operation. The coefficients for the gate tracking functions up to 3rd order are optimised for the STDR to improve the linearity and to maintain the output power. The optimisation process is explained in Section 5.5.

6.3.1 Tracking functions

The tracking functions at the drain side of the RF PA (the PET and 2nd order PET tracking functions) are identical tracking function as the ones used in the previous section i.e. the 2nd order PET tracking function is fitted to approximate ideal PET tracking function. The tracking functions for the gate tracking are polynomial functions (6.1) with the power of the signal as

$$v_{gs}(t) = a_n p_{in}(t)^n + a_{n-1} p_{in}(t)^{n-1} + \cdots + a_1 p_{in}(t) + a_0 \tag{6.1}$$

the variable. The bandwidth requirement of the gate voltage amplifier is also narrower than it would be if the signal envelope is used as the variable.

6.3.2 Measurement and Results

The measurement system is the same system used in the previous section. The PET and the 2nd order PET PAs in the combination with the PGT technique are evaluated for the *PAE, ACPR, EVM* and the *STDR*. The measurements are performed for the two cases as in the previous section. The Case I has the constant average output power of $P_{out,avg}$ = *35.6 dBm* and in the Case II, the *ACPR* is set to be at least *-40 dBc*.

The measured results with the gate tracking functions that result in the linearity improvement are presented in Table 6.3. It shows additional improvement of *3.4 dB* in the *ACPR* and one percentage point in the *EVM* when the PET PA is combined with the 3rd order PGT in the Case I. measurement. The lower order gate tracking functions do not result in the significant improvement. The 2nd order PET PA in combination with PGT results in the significant linearity improvement with the 1st order polynomial function and does not improve further with the higher order tracking functions. There is no significant loss in the efficiency of the PET and the 2nd order PET PA in the combination with the PGT. The PET PA with the PGT shows slightly better linearity and efficiency performance compared to the 2nd order PET PA but with the 2

Table 6.3: Measured results of the Case I ($P_{out,avg}$ = 35.6 dBm) and the Case II (ACPR ≤ -40 dBc) for the PET and the 2nd order PET techniques in the combination with the power gate tracking PGT technique.

PA	BW_{Vds} [MHz]	BW_{Vg} [MHz]	P_{out} [dBm]	PAE [%]	η_D [%]	$ACPR_L$ [dBc]	$ACPR_R$ [dBc]	EVM [%]	STDR [dB]
Case I $P_{out,avg}$ = 35.6 dBm									
Class AB PA			35.6	38.2		-31.8	-31.5	8.63	
ET PA	BW_{Vds} *		35.6	62.1	64.0	-30.1	-30.3	9.24	19.73
PET, 3rd order PGT	1	3	35.6	54.4	55.8	-44.8	-44.5	1.61	32.85
2nd order PET, 1st order PGT	2	1	35.6	51.6	52.7	-43.9	-44.0	1.80	32.54
2nd order PET, 2nd order PGT	2	2	35.6	51.5	52.6	-44.0	-44.0	1.94	32.17
Case II ACPR ≤ -40 dBc									
Class AB PA			32.2	25.6		-40.2	-40.2	3.33	
PET 3rd order PGT	1	3	36.6	58.0	59.4	-40.4	-40.3	1.61	28.23
2nd order PET, 1st order PGT	2	1	36.7	54.2	55.4	-40.5	-40.4	1.56	28.63
2nd order PET, 2nd order PGT	2	2	36.7	54.1	55.3	-40.3	-40.2	1.61	28.47

orders higher gate tracking function which increases the bandwidth of the gate voltage waveform from the RF bandwidth to the 3 times the RF bandwidth. It is also worth noting that the realisation of the gate tracker for the PGT may be rather simple due to the negligible power requirement (the negligible gate current) and the limited bandwidth of the voltage waveform.

6.4 Second Order Power Envelope Tracking for limited Supply Voltage Bandwidth

Section 2.5.1 introduces the 2nd order PET tracking function with three degrees of freedom, and these can be arbitrarily selected. This means that it can fit the ET tracking function closer than the PET tracking function and result with the efficiency of the RF PA that is much closer to the ET case [23]. The narrower bandwidth requirement on the supply voltage amplifier (modulator/tracker) with the 2nd order PET makes easier to achieve the higher efficiency (of the voltage amplifier) than with the ET technique. This may lead to the compensation of the efficiency loss in the RF PA in the overall 2nd order PET system.

* Drain voltage bandwidth of the ET PA is theoretically infinite and in this work it is filtered by the drain tracker to approximately 5-6 MHz

This section shows results of the 2nd order PET with the tracking function shaped so that it closely follows the ET tracking function. These results are compared with the results of the ET tracking function with the hard clipping (the detroughing and decresting) tracking function and the tracking function with the smoothened clipping areas.

6.4.1 Tracking Functions

In the conventional ET PA, the drain supply voltage $V_{dd}(t)$ is the amplified version of the signal envelope. The ideal ET tracking function would reach the maximum drain supply voltage $V_{dd,max}(t)$ for the largest level of the signal envelope $v_{e,max}(t)$, and it is $V_{dd}(t) = 0\ V$ when the envelope is $v_e(t) = 0\ V$ (see Figure 2.8). In general, the conventional ET tracking function can be expressed as

$$V_{dd}(t) = k_1 v_e(t), \tag{6.2}$$

where the $V_{dd}(t)$ is the drain supply voltage and the $v_e(t)$ is the envelope of the input signal. Due to the gain collapse below the knee voltage of the transistor, the drain tracking function is commonly detroughed (clipped at the low end) above the knee voltage. Hard clipping increases the bandwidth of the supply voltage significantly (to infinity) and such abrupt change may cause the "ringing" of the supply voltage around those values. That effect can cause the unwanted distortion, so the detroughing (clipping) is usually smoothened, or the tracking function is shaped in the manner to avoid the hard clipping [34].

As it is mentioned earlier, in this work it is necessary to apply decresting (clipping at the high end) of the ET tracking function. The reason for that is in the RF PA design (see Chapter 4). Namely, the RF PA is harmonically tuned in order to achieve the maximum *PAE* when it operates approximately *3 dB* in compression. If the tracking function result in $V_{dd}(t) = V_{dd,max}(t) = 28\ V$ when the $v_e(t) = v_{e,max}(t)$ the RF PA is compressed to much resulting with the poor *PAE*, low output power and significant nonlinear distortion.

Although smoothening of the abrupt detroughing and decresting can reduce the bandwidth of the supply voltage for the ET operation, there is still the requirement for some sort of the supply voltage bandwidth reduction due to the infinite bandwidth of the signal envelope. In order to smoothen the detroughing and decresting and achieve the narrower bandwidth, which is well defined, the 2nd order PET function can be used instead of the ET tracking function as it is suggested in Section 2.5.1.

Tracking functions for the ET with the abrupt detroughing and decresting, the ET with the smoothened detroughing and decresting and the 2nd order PET are shown in Figure 6.5. The coefficient k_1 in the equation (6.2) for the ET tracking function is selected so that the ET PA operates *3 dB* in compression with the nominal drain voltage $V_{DD}(t)=28\ V$. In this work, the minimum allowed drain voltage is $V_{dd,min}(t)=\ 6\ V$ and the ET function is detroughed at this value. The maximum allowed voltage is $V_{dd,max}(t)=\ 28\ V$ and the ET function is decrested at this value. The abrupt detroughing and decresting areas are smoothened using the 2nd order polynomial function in case of the smoothened ET function. The coefficients of these 2nd order polynomial functions are adjusted so that the derivative of the polynomial function matches with the derivative of the ET function with the abrupt detroughing and decresting at intersection points. The 2nd order PET tracking function is of the form shown by the equation (2.11). The coefficients k_n are selected so that the maximum drain supply voltage $V_{dd,max}(t)$ value is not much higher than $V_{dd}=28\ V$ (higher than *30 V* in this case) and it is allowed for the $V_{dd}(t)$ voltage to decrease for the highest values of the signal envelope, which occurs rarely in the 16-QAM signal. The further requirement is that the 2nd order PET tracking function does not cross the ET tracking function because it would lead to the deeper compression than desired for the certain envelope levels. Another possibility is to keep the $V_{dd}(t)$ at the constant level when it reaches its maximum $V_{dd,max}(t)$ (when the derivative of the tracking function $dV_{dd}(t)/dt=0$), but

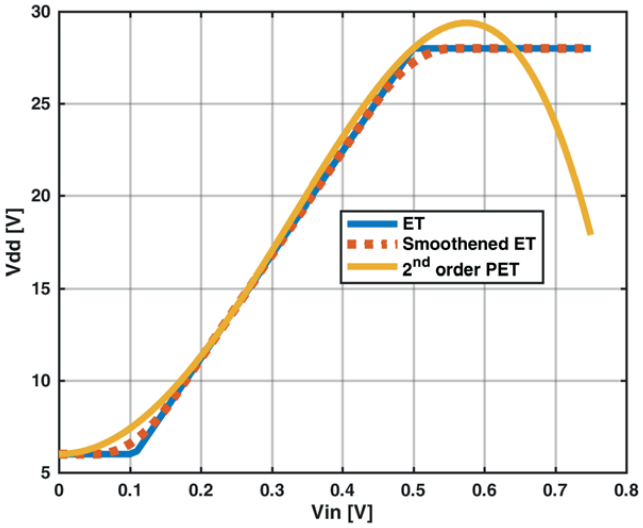

Figure 6.5: Tracking functions for the ET with the abrupt detroughing, the ET with smoothened detroughing and the 2nd order PET tracking function.

it would increase the bandwidth of the supply voltage waveform to more than $2B_{RF}$. It is important to note that the coefficients k_n can be arbitrarily selected to get the best fit to the desired conventional tracking curve.

The spectral content of the envelope and the drain supply voltage calculated for these tracking functions with the DC component for the 16-QAM signal with the *1 MHz* RF bandwidth are shown in Figure 6.6. The width of the envelope bandwidth is the same as it would be for the drain supply voltage calculated with the ideal ET tracking function (6.2) with no clipping.

It can be seen that the ET tracking function has somewhat wider bandwidth than the envelope of the signal. This is due to the clipping at the low and high end of the function (the detroughing and decresting). The smoothened ET tracking function, with the smoothened clipping edges, results in somewhat narrower bandwidth. The 2nd order PET tracking function results in a significant reduction in the bandwidth of the $V_{dd}(t)$ voltage waveform. As it is expected, it has a well defined bandwidth of *2* times the RF bandwidth, which for the 1 *MHz* 16-QAM signal results in the bandwidth of *2 MHz*. This is significantly narrower bandwidth compared to the waveforms generated with the ET and the smoothened ET tracking functions. The reason for that lies in the fact that waveforms calculated with the ET and the smoothened ET tracking functions are directly dependent on the envelope of the signal, which have the infinite bandwidth in theory. The waveform calculated with the 2nd order PET tracking function is related to the power of the signal, which has the limited bandwidth to the RF bandwidth (see

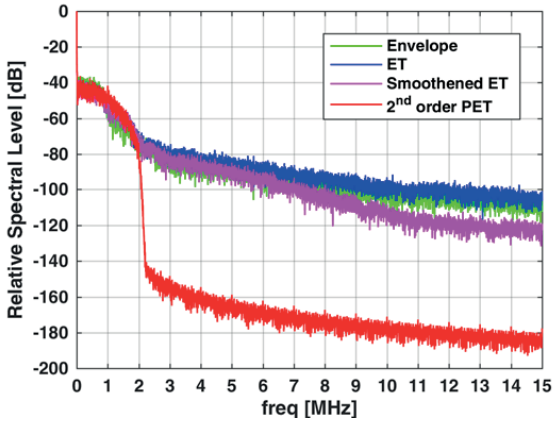

Figure 6.6: Measured spectral bandwidth of the signal envelope and the drain supply voltage for different tracking functions for the 1 MHz 16-QAM signal.

Section 2.5.1). This significantly narrower and defined bandwidth of the 2nd order PET supply voltage gives it the advantage for designing more efficient supply amplifiers especially for the modulated signals with the wide bandwidth.

6.4.2 Measurement Results

The measurement setup that is used is shown in Figure 3.1 and described in Section 6.2.1. The measurement is done for the ET, smoothened ET and the 2nd order PET with the tracking functions presented in the previous section. The measurement system evaluates each technique for the average output power $P_{out,avg}$, Power Added Efficiency *PAE*, drain efficiency η_D, *ACPR*, *EVM* and the *STDR* of the RF PA. The efficiency of the drain supply voltage amplifier is not the scope of this research, and it is not taken into account.

In Section 6.1 it is shown that it is possible to find the gate bias voltage that results in the optimal efficiency and linearity performance of the ET PA. The same can be applied to the 2nd order PET technique. Because of that result, the ET, smoothened ET and the 2nd order PET systems are measured for the several gate bias voltage values with the constant average output power of $P_{out,avg} = 35.6\ dBm$. The optimal gate bias voltage is found to be the one resulting in the quiescent drain current of $I_{DQ} = 160\ mA$ while the quiescent drain voltage is $V_{DQ} = 28\ V$. The measured results for the optimal gate bias with the same average output power $P_{out,avg} = 35.6\ dBm$ are presented in Table 6.4. The static bias class AB PA ($I_{DQ} = 160\ mA$ and $V_{DQ} = 28\ V$) is presented as the reference. The measured results for the complete set of the static gate bias voltages for all the tested tracking curves are shown in Appendix A.

Table 6.4: Measured results of the ET, Smoothened ET and the 2nd order PET PAs with the same $P_{out,avg}$ = 36.6 dBm.

PA	BW_{Vds} [MHz]	$P_{out,avg}$ [dBm]	PAE [%]	η_D [%]	$ACPR_L$ [dBc]	$ACPR_R$ [dBc]	EVM [%]	STDR [dB]
Static Bias PA (Reference)								
V_{DQ}=28 V I_{DQ} = 160 mA		35.6	38.2		-31.8	-31.5	8.63	
Dynamic Drain Bias PA								
ET	BW_{Vds}*	35.6	62.1	64.0	-30.1	-30.3	9.24	19.73
Smoothened ET	BW_{Vds}*	35.6	63.1	65.1	-30.4	-30.8	8.47	20.36
2nd order PET	2	35.6	61.8	63.8	-30.0	-30.3	8.64	19.68

* Drain voltage bandwidth of the ET PA is theoretically infinite and in this work it is filtered by the drain tracker to approximately 5-6 MHz

The results are showing that the efficiency and the linearity performance is comparable for all three tracking functions. The smooth ET tracking function with the smoothened clipping areas has a slightly higher efficiency (one percentage point) and linearity performance, but it is not significant. This result shows that the presented 2nd order PET tracking function results in the similar performance as the conventional ET tracking function. This characteristic gives a great advantage to the 2nd order PET compared to the traditional ET shaping functions due to the narrower and well defined drain voltage waveform bandwidth. It is especially beneficial for the signals with the wide bandwidth.

As it is shown in the previous section in Figure 6.6, the bandwidth of the 2nd order PET drain supply voltage is significantly narrower compared to the conventional ET or smoothened ET drain supply voltage. Narrower bandwidth of the supply voltage waveform simplifies the design of the supply voltage amplifier with the higher efficiency and better linearity. The efficiency of the supply voltage amplifier is important since it defines the efficiency of the overall tracking system, and the linearity is important since the distortion in the supply voltage waveform may cause the distortion and the memory effects in the tracked RF PA. With the maintained efficiency of the RF PA under such conditions, the overall efficiency of the 2nd order PET PA may be even higher compared to the conventional ET PA.

The combination of the above techniques with the dynamic gate biasing optimised for the linearity is also considered. However, there is no achieved linearity improvement. That can be explained if one looks at the gain and phase curves on Figure 6.2. It can be noticed that the gain as well as the phase curves are rather linear in the saturation area, and in the back-off the spread between the curves for different gate bias voltages is such that there is not possible to do much. At least not with the reasonable gate tracking function order.

The example of the approximated intrinsic output envelope of the 16-QAM signal and the supply voltage waveforms of the detroughed ET, PET and 2nd order PET are presented in Appendix C.

6.5 Summary

This chapter points out the advantage of tracking the power of the modulated signals instead of its envelope in the dynamic bias variation PA systems. In the ET systems, it is very important that the drain supply voltage amplifier (the voltage modulator/tracker) has high efficiency and high linearity. The efficiency of the supply voltage amplifier is important if one wants to

achieve high overall efficiency of the dynamically biased system, and the linearity is important because the nonlinear distortion of the supply voltage waveform may cause the distortion and the memory effects in the RF PA subjected to the ET operation. The challenge in designing the supply voltage amplifiers with the high efficiency and linearity becomes more complicated for the signals with wide bandwidth. It is shown in Section 2.5.1 that the envelope of the signal has the infinite bandwidth in theory. This leads to the infinite bandwidth of the supply voltage in the ET systems. Since it is not necessary that the supply voltage is the exact replica of the envelope, the bandwidth of the supply voltage is usually reduced to 4-10 times the RF bandwidth of the signal. The bandwidth reduction can be done by using the supply voltage shaping functions or by filtering. Analysing the power of the modulated signal, it is shown that bandwidth of the power of the signal has analytically well defined bandwidth of only the RF bandwidth. In Section 2.5.2 it is shown that the ideal Power Envelope Tracking (PET) tracking curve does not follow the conventional ET tracking curve closely which as the consequence result in the lower efficiency as shown in Section 6.2. As the answer to that problem, the 2^{nd} order PET is defined with the tracking function as the 2^{nd} order polynomial function with the power as the variable or the 4^{th} order polynomial function with only the even order degrees with the envelope as the variable. This way the ET tracking function can be approximated more closely with the increased bandwidth of the supply voltage by the factor of *2* compared to the ideal PET i.e. the bandwidth of *2* times the RF bandwidth.

Section 6.1 shows the dependence of the efficiency and the linearity performance of the RF PA subjected to the ET operation to the static gate bias. From the results, it is evident that it may be of the great value to choose the optimal gate bias condition for the linearity and the efficiency and possibly simplify the DPD system which is commonly used for the ET PA linearization.

Section 6.2 shows the measured results of the PET technique applied to the RF PA. In this work, the PET tracking function has to be shaped so that the RF PA operates 3 dB in the compression during the dynamic drain bias operation due to the RF PA design. This requires the hard clipping (decresting) of the PET tracking function at the drain supply voltage of *28 V*. That hard clipping, which increases the bandwidth of the PET supply voltage significantly, is avoided by using the 2^{nd} order PET tracking function. Results are showing significant simultaneous improvement in the linearity and the efficiency compared to the reference static bias class AB PA. Compared to the conventional ET PA the efficiency is lower, but the linearity is much better as it is expected. Furthermore, it is shown that the PET and the 2^{nd} order PET in

the combination with the Power Gate Tracking PGT (the dynamic gate bias operation) with the coefficients of the gate tracking functions optimised for the Signal to Total Distortion Ratio (STDR) results in the additional improvement in the linearity of the RF PA with the maintained efficiency.

Section 6.4 shows the measured results of the 2nd order PET tracking function shaped to fit the conventional ET tracking function. Results are presented for the ET tracking function, ET tracking function with the smoothened clipping areas (detroughed and decrested areas) and the 2nd order PET tracking function. It is shown that the *PAE,* the drain efficiency and the linearity for all three tracking functions are comparable. This makes the 2nd order PET technique a good candidate for the ET tracking function estimation and the supply voltage bandwidth reduction. That way the bandwidth of the supply voltage is well defined and limited to only *2* times the RF bandwidth of the modulated signal, and there is no need for the additional filtering and processing as in the ET technique.

Chapter 7

Auxiliary Power Tracking

Dynamic biasing on the drain or the collector side of the device does not necessary need to be used for the efficiency improvement as it is done in the previous chapter. Z. Yusoff et.al. presented the Auxiliary Envelope Tracking AET technique [3] which is the linearization technique. This chapter presents the Auxiliary Power Tracking (APT) technique where the power of the modulated signal is used as the tracking variable instead of its envelope. This way, as it has been mentioned in earlier chapters, the bandwidth of the supply voltage is reduced which makes the design of the supply voltage amplifier (tracker) simpler and possibly more efficient and linear. It is important to note that in architectures with the dynamic bias operation, the efficiency of the supply voltage tracker has a significant impact on the overall efficiency of the system.

This chapter presents the APT technique and compares performance with the AET technique. Both techniques are applied to the 10 W GaN HEMT PA. Furthermore, the linearity dependence of the AET PA and the APT PA on the static gate bias voltage value is tested. In addition, the APT PA is combined with the dynamic gate bias voltage operation (the power gate tracking PGT). The gate tracking functions up to 3rd order are optimised for the linearity. It is important to note that in this scenario, the PGT technique linearizes the RF PA in the back-off while the APT technique linearizes the RF PA in the saturation (compression). It is not possible to linearize the RF PA in a deep compression using the dynamic gate bias variation.

7.1 Influence of the Gate Bias Voltage on Linearity of the Auxiliary Envelope Tracking PA

Since the AET technique [3] is the linearity enhancement technique, it is important to exploit the maximum linearization capability out of it. As it has been already discussed in Section 6.1, the AM-AM and AM-PM transfer functions (the gain and transfer phase) are different for various gate bias conditions (voltage values). With the smart selection of the gate bias voltage of the AET RF PA with the optimal AM-AM and AM-PM characteristic, it is possible to achieve the maximum linearity performance of the observed PA subjected to the AET operation. It is also important to pay attention to the efficiency performance during the optimal gate bias selection. Although the AET is the linearization technique, it is not desirable to lose a significant amount of the efficiency. The same idea can be applied to the APT technique.

7.1.1 Measurement Setup and Tracking Function

The measurement system used is the same as the one explained in Section 6.1.1 and shown in Figure 3.1. The original AET signal in [3], where the modulated signal was generated form the two single tones (making one two tone-signal), was generated by the third single tone generator since the envelope of the two-tone signal is the sinewave. The sinusoidal signal was then combined with the DC voltage making the AET signal which supplies the RF PA. The dynamic AET supply voltage spans several volts (approximately +/- 3 volts) around the DC component at the safe distance from the signal envelope. Baring the original work in mind, in this work, the AET drain tracking function (7.1) is shaped in such a way that the drain voltage

$$V_{ddAET}(t) = k_1 v_e(t) + k_0 \tag{7.1}$$

spans from *24* to *32 V* i.e. *4* volts above and below the nominal quiescent drain voltage V_{DQ} = *28 V*. This assures the slight expansion of the supply voltage for the high peak levels of the signal envelope and the slight reduction of the supply voltage for the lower level of the signal envelope. Note that the AET supply voltage is function of the signal envelope (the 16-QAM in this case). The RF PA is operated at the *1 dB* in compression for the nominal drain quiescent voltage of V_{DQ} = *28 V* and the gate quiescent voltage that corresponds to the I_{DQ} = *160 mA*. If the drain voltage tends to exceed the maximum value of *32 V* for the highest drive levels, it is hard clipped. The AET tracking function is shown in Figure 7.1.

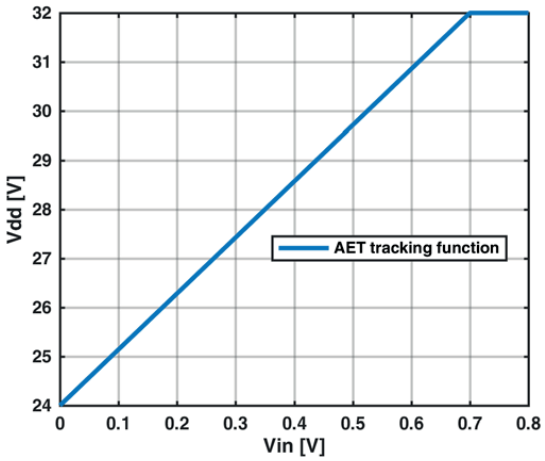

Figure 7.1: Drain supply voltage tracking function for the AET technique

7.1.2 Measurement and Results

The gain and the phase of the AET PA are measured with the static quiescent gate voltage V_{GQ}= *-2.7:0.1:-1.9 V*, which corresponds to the quiescent drain current I_{DQ}= *15-500 mA* (from deep Class-AB to Class-A). For each gate bias voltage, the input signal level is adjusted so that the level of the average output power is $P_{out,\,avg.}$ = *35.6 dBm*. The AET PA is also evaluated for the *PAE, ACPR, EVM* and *STDR* during the measurements for each gate bias voltage. The results of the measurement are presented in Table 7.1, the gain and phase curves are shown in Figure 7.2.

Table 7.1: Measured results of the AET PA for the set of the static gate bias voltage values.

V_{GQ} [V]	P_{in} [dBm]	PAE [%]	$ACPR_L$ [dBc]	$ACPR_R$ [dBc]	EVM [%]	STDR [dB]
-2.7	19.57	37.32	-28.74	-28.68	10.53	17.72
-2.6	19.3	37.00	-30.84	-30.78	8.40	19.44
-2.5	18.96	36.75	-33.46	-33.46	6.31	21.44
-2.4	18.68	36.68	-36.65	-36.54	4.47	23.84
-2.3	18.50	36.19	-39.44	-39.27	2.98	26.26
-2.2	18.29	35.14	-39.97	-39.82	2.59	27.59
-2.1	18.21	33.72	-39.12	-38.99	3.10	27.62
-2.0	18.04	32.41	-38.92	-38.77	3.28	27.79
-1.9	17.97	30.11	-39.70	-39.78	2.90	28.06

From the results in Table 7.1, it is clear that the linearity (*ACPR* and *EVM*) varies with the gate bias as well as the *PAE* as it is the case for the ET PA (see Section 6.1). The optimal gate bias voltages for the linearity and the efficiency could easily be V_{GQ} = *-2.2 V* or V_{GQ} = *-2.3 V*. The gate bias voltage of V_{GQ} = *-2.2 V* results in the best *ACPR* = *-39.82 dBc* and the *EVM* = *2.59 %* with the *PAE* = *35.14 %*. The gate bias voltage of V_{GQ} = *-2.3 V* results in slightly worse linearity (*ACPR* = *-39.27 dBc* and *EVM* = *2.98 %)* but one percentage point better *PAE* = *36.19 %*. That opens the possibility to make the trade-off between the linearity and the efficiency.

This result suggests that it is of the great importance to select the optimal gate bias voltage value in the AET or the APT systems in order to achieve the best linearity performance out of

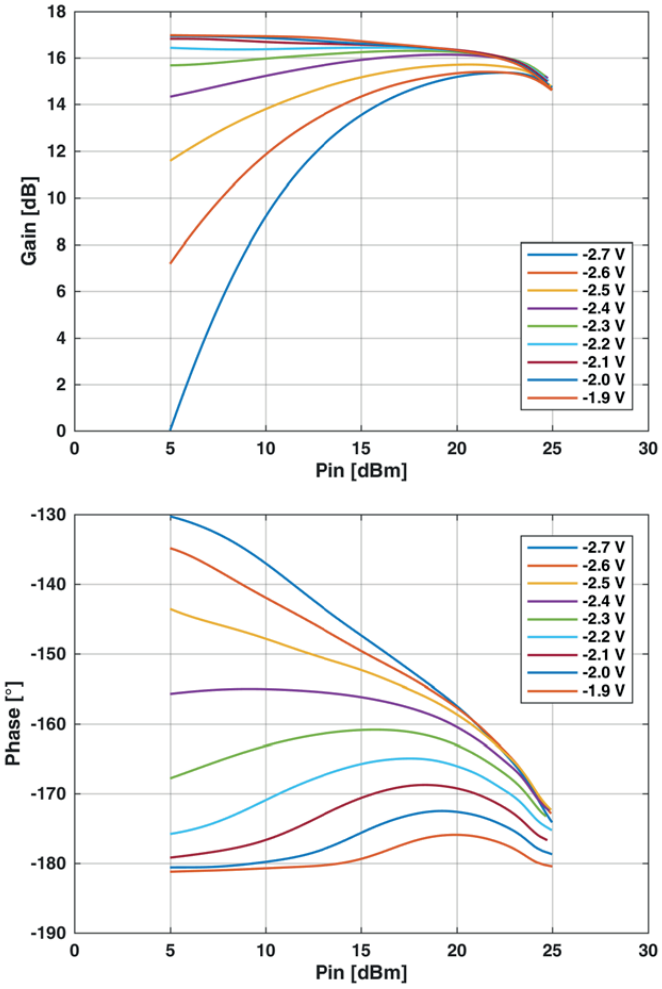

Figure 7.2: Gain (top) and Phase (bottom) of the AET PA for the set of the static gate bias voltage values.

these techniques. It is even more important to do so for the AET PA than for the ET PA since the AET is linearization technique, while the ET PA is commonly linearized with the DPD.

7.2 Auxiliary Power Tracking – APT

7.2.1 Tracking Functions

As it has been discussed, the benefit of tracking the power of the modulated signal instead of its envelope lies in the limited bandwidth of the supply voltage waveform (see Section 2.5.1). While in the AET technique the dynamic drain supply voltage $V_{dd}(t)$ is related to the signal envelope, in the APT technique it is related to the signal power. It is much simpler to design the efficient and linear supply voltage tracker (amplifier) for the waveforms with the narrow bandwidth, and its efficiency is of the great importance in order to achieve high overall efficiency of any kind of dynamic bias architectures (APT, AET, PET or ET). The limited supply voltage bandwidth of the power tracking technique may be especially beneficial for tracking the modulated signals with the wide bandwidth.

In this work, the drain voltage of the AET and APT PAs spans from the *24 V* to the *32 V*. The AET tracking function is already presented in Section 7.1. The APT tracking function (7.2)

$$V_{ddAPT}(t) = k_1 {v_e}^2(t) + k_0 = k_1 p(t) + k_0 \tag{7.2}$$

calculates the drain supply voltage $V_{ddAPT}(t)$ according to the power of the input signal. It is shaped so that the RF PA operates *1 dB* in the compression with the nominal quiescent drain voltage V_{DQ} = *28 V* and the gate quiescent voltage that results in I_{DQ} = *160 mA*, which is the same condition as for the AET tracking function. In case the drain voltage tends to exceed the maximum value of *32 V* for the highest drive levels, the AET and APT drain supply voltages $V_{dd}(t)$ are hard clipped. Hard clipping significantly increases the bandwidth of the voltage waveform, which is, in this work, filtered with the supply voltage tracker with the bandwidth of approximately *5-6 MHz*. This filtering may produce some distortion in the voltage waveform and consequently distortion in the RF PA. In the AET PA clipping occurs at the high drive levels that are not reached in this measurement. For the APT PA, clipping occurs only for the highest drive levels, which do not occur often in the modulated signal used in this work (16-QAM), so the influence of the distortion caused by the drain voltage clipping is minimised. The tracking functions for the AET and APT systems are shown in Figure 7.3.

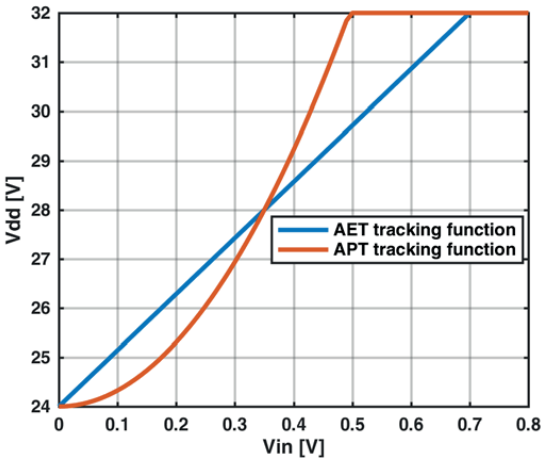

Figure 7.3: Drain supply voltage tracking function for the AET and the APT technique.

7.2.2 Measurement and Results

The measurement setup that is used is the same as one used for the PET PA measurements, and it is described in Section 7.1.1. The AET and APT PAs are evaluated for the *PAE, ACPR, EVM* and the *STDR*. The evaluation is done for the several gate bias voltage values in order to find the optimal performance in terms of the linearity and the efficiency (see Section 7.1). The measurements are done for the two cases. The Case I has the constant average output power of $P_{out,avg} = 35.6\ dBm$ and in the Case II, the *ACPR* is set to be at least *-40 dBc*.

The results of the AET and APT PAs for the set of the static gate bias voltages that deliver certain quiescent drain current I_{DQ} of the PA operating between the class B and the class A, the static bias class A ($I_{DQ} = 500\ mA$) and the reference static bias class AB ($I_{DQ} = 163\ mA$) PAs are shown in Table 7.2 (results for the whole set of the static gate bias voltages can be found in Appendix A). The results are showing that by changing the gate bias, linearity changes significantly and the optimal bias can be found. The best linearity performance is achieved for the I_{DQ} which results in the optimal combination of the AM-AM and AM-PM characteristics. It is important to note that the efficiency must be taken into account as well. From the presented results, it can be seen that the $I_{DQ} = 345\ mA$ provides slightly better linearity compared to the $I_{DQ} = 280\ mA$, but the latter has one percentage point better *PAE* for both, the AET and the APT cases. The selected optimum result is the $I_{DQ} = 280\ mA$. Compared to the reference class AB PA the improvement of *7.8 dB* in *ACPR* and *5.6* percentage points in the *EVM* is achieved

with the *2* percentage points lower *PAE* for the AET PA. Improvement of *8.8 dB* in the *ACPR* and *6.5* percentage points in the *EVM* is achieved with only one percentage point lower *PAE* for the APT PA. This result highlights the importance of the gate bias voltage selection in order to achieve the best performance from the AET or the APT linearization techniques regardless for which gate bias voltage the RF PA is designed for. Furthermore, it can be seen from the results that the linearity performance of the APT is somewhat better than for the AET (*1 dB* in *ACPR* and *0.8* percentage points in *EVM*) with the one percentage point higher *PAE*. Moreover, the drain supply voltage $V_{dd}(t)$ has significantly narrower bandwidth for the APT than for the AET technique.

Table 7.2: Measured results of the Case I ($P_{out,avg}$ = 35.6 dBm) for the AET and APT PAs for the set of the static gate bias conditions and the reference static bias PAs.

I_{DQ} [mA]	PAE [%]	$ACPR_L$ [dBc]	$ACPR_R$ [dBc]	EVM [%]	STDR [dB]
Static Drain Voltage V_{DQ}= 28 V (for reference)					
163	38.2	-31.79	-31.49	8.63	
500	29.9	-37.45	-36.87	4.93	
Auxiliary Envelope Tracking AET Drain voltage bandwidth BW_{Vds}[*]					
120	37.00	-30.84	-30.78	8.40	19.44
163	36.71	-34.54	-34.49	5.62	22,30
280	**36.19**	**-39.44**	**-39.27**	**2.98**	**26.26**
345	35.15	-39.97	-39.82	2.59	27.59
Auxiliary Power Tracking APT Drain voltage bandwidth BW_{Vds}= BW_{RF} = 1 MHz					
120	38.05	-30.94	-30.99	7.59	19.80
163	37.42	-34.81	-34.92	4.74	23.08
280	**37.10**	**-40.34**	**-40.32**	**2.17**	**27.45**
345	36.22	-40.91	-40.90	1.85	29.08

7.3 Auxiliary Power Tracking with Gate Power Tracking

In order to additionally improve the linearity of the PA, the APT technique is combined with the PGT (dynamic gate biasing technique) (see Chapter 5), subjecting the RF PA to the dual dynamic bias operation.

[*] Drain voltage bandwidth of the ET PA is theoretically infinite and in this work it is filtered by the drain tracker to approximately 5-6 MHz

7.3.1 Tracking Functions

The tracking function at the drain side of the PA (APT tracking function) is identical tracking function as one used in the previous section. Tracking functions for the gate tracking (the PGT tracking functions) are polynomial functions (7.3) with the power of the signal as the variable. This means that the bandwidth requirement on the gate voltage amplifier is also narrower than it would be if the signal envelope is used as the variable.

$$v_{gs}(t) = a_n p_{in}(t)^n + a_{n-1} p_{in}(t)^{n-1} + \cdots + a_1 p_{in}(t) + a_0 \tag{7.3}$$

7.3.2 Measurement and Results

The measurement system is the same system used in the previous section. The APT PA in combination with the PGT technique is evaluated for the *PAE, ACPR, EVM* and the *STDR*. The measurements are done for the two cases as in the previous section. The Case I has the constant average output power of $P_{out,avg} = 35.6\ dBm$ and in the Case II, the *ACPR* is set to be at least *-40 dBc*.

The coefficients of the polynomial tracking functions (7.3) up to the 3rd order ($n = 3$) are optimised for the *STDR* (see Chapter 3) in order to achieve the better linearity performance compared to the static gate bias operation. The results for the Case I are presented in Table 7.3.

Table 7.3: Measured results of the Case I ($P_{out,avg}$ = 35.6 dBm) for the APT PA in the combination with the PGT technique. (Drain voltage bandwidth BW_{Vds}=BW_{RF}=1 MHz)

Tracking curve order	BW_{Vgs} [MHz]	P_{in} [dBm]	PAE [%]	$ACPR_L$ [dBc]	$ACPR_R$ [dBc]	EVM [%]	STDR [dB]
1st order	1	18.75	36.90	-42.80	-42.95	1.35	30.49
2nd order	2	18.72	37.43	-42.80	-43.00	1.32	30.53
3rd order	3	18.69	37.36	-43.15	-43.42	1.49	31.08

The results are showing that the PGT technique in the combination with the APT PA using the 1st order polynomial tracking function improves the linearity for the additional *2.5 dB* in the *ACPR* and *0.8* percentage points in the *EVM* compared to the APT PA with the selected optimal static gate bias, while the *PAE* is preserved. The PGT using the 2nd order function results in almost the same performance and with the 3rd order function it performs slightly better compared to the 1st order function. That means that the low order gate tracking function is sufficient to linearize the PA in the back-off region, and in the compression it is linearized with

the APT technique by increasing the drain voltage for the high drive levels as mentioned earlier. In general, it is not possible to linearize the RF PA with the dynamically changing the gate bias when it operates in deep compression.

The results for the Case II (*ACPR ≤ -40 dBc*) of the conventional static gate bias PAs (the class A and the class AB), the APT PA with the selected optimal static gate bias voltage (quiescent drain current I_{DQ} = *280 mA*) and the APT technique in the combination with the PGT technique are shown in Table 7.4. The results are showing that if the *ACPR* is at the same level of at least *-40 dBc*, the PGT with the 1st order tracking function in the combination with the APT technique delivers *0.5 dB* more output power compared to the APT with the optimal static gate bias. The *PAE* is higher for *1.8* percentage points compared to the selected optimal APT result.

It is important to note that in the scenario with the 1st order PGT tracking function the bandwidth of both voltage waveforms, on the gate and drain side, is limited to the RF bandwidth (1 MHz in this work). This is due to the linear change of the gate and drain voltages according to the instantaneous power of the input signal. Moreover, the realisation of the gate tracker can be even simpler than the realisation of the drain tracker due to the minimal power requirement since the gate current is negligible. To realise this kind of the system, only the additional hardware is required i.e. there is no need for the additional digital processing of the supply voltage waveforms. This is not the case for the tracking functions of the higher orders. Tracking the gate with the higher order tracking functions gives some more linearity improvement, but also it increases the bandwidth of the voltage waveform.

Table 7.4: Measured results of the Case II (ACPR ≤ -40 dBc) for the conventional static bias PAs, the APT PA and the APT PA in combination with the PGT technique. (APT drain voltage bandwidth: BW_{Vds}= BW_{RF} = 1 MHz)

I_{GQ} [mA]	BW_{Vgs} [MHz]	P_{in} [dBm]	$P_{out,avg.}$ [dBm]	PAE [%]	EVM [%]	STDR [dB]
Static Drain Voltage V_{DQ}= 28 V (for reference)						
163		14.78	32.24	25.65	3.33	
500		16.62	34.5	24.40	3.00	
Auxiliary Power Tracking APT						
280		18.59	35.72	37.42	2.16	27.15
APT in combination with PGT						
1st order	1	19.57	36.25	39.23	1.83	27.02
2nd order	2	19.57	36.23	39.85	1.63	27.28
3rd order	3	19.71	36.42	40.36	2.00	27.26

The example of the approximated intrinsic output envelope of the 16-QAM signal and the supply voltage waveforms of the AET and the APT are presented in Appendix C.

7.4 Summary

It has been shown by Z. Yusoff et.al. [3] that the dynamic variation of the drain supply voltage can be used to improve the linearity of the PA with a little or no efficiency loss. They proposed the Auxiliary Envelope Tracking (AET) technique, where the drain supply voltage is increased for the high drive levels and reduced for the low drive levels.

It is shown in Section 7.1 that the linearity and the efficiency performance of the AET PA significantly depends on the static gate bias, and that the optimal gate bias for the linearity and the efficiency performance can be found. The optimal bias then assures that the maximum linearization capabilities are achieved from the AET PA. This optimal bias is not necessarily the bias the RF PA is designed for. The reason for the gate bias dependence is the fact that the AM-AM and AM-PM characteristics of the RF PA vary for different gate bias conditions, and the best linearity performance is achieved with the optimal combination of these two characteristics.

As it has been discussed in previous chapters, tracking the envelope of the signal leads to the very wide bandwidths of the drain supply voltage (infinite in theory). As a consequence, designing the voltage amplifiers (modulators) with the high efficiency and linearity is very difficult. As the answer to that problem, the Auxiliary Power Tracking (APT) technique is presented in Section 7.2. In this technique, the drain supply voltage is calculated according to the power of the signal. Since the power of the signal has the analytically defined bandwidth of only the RF bandwidth of the signal, the bandwidth of the supply voltage in the APT technique is significantly narrower and well defined compared to the AET technique. The measured results show the APT technique has somewhat better linearity performance than the AET technique with somewhat better efficiency.

The APT technique, by its nature, linearizes the RF PA for the high drive levels (in the compression area). In order to improve the linearity for the low drive levels (back off area) the Power Gate Tracking (PGT) technique is combined with the APT technique. The results of this dual dynamic bias variation concept additionally improves linearity with the maintained efficiency.

Chapter 8

Conclusions and Future Work

In this thesis, the most attention is dedicated to the two methods or techniques. The first is the gate tracking (GT) or dynamic gate biasing for the linearity improvement of the RF power amplifier. The second is the power tracking (PT) technique where the power of the modulated signal with the varying envelope is used as the variable in the dynamic biasing technique (whether on the gate or the drain side of the transistor) instead of its envelope as in the envelope tracking (ET) technique. The power tracking is applied to the gate side making the power gate tracking (PGT) technique, and the drain side making the power envelope tracking (PET) technique and the auxiliary power envelope tracking (APT) technique. The PGT is tested with the static bias at the drain side of the device and in the combination with the dynamic bias (PET, 2^{nd} order PET and APT) at the drain side in the dual dynamic bias operation. Different combinations of these techniques improve either the linearity or the efficiency of the RF PA or simultaneously both the linearity and the efficiency. These techniques are applied directly to the RF PA, which may simplify the extrinsic linearization techniques like the DPD, or lead to the better overall performance of the RF PA if the extrinsic technique is applied.

8.1 Conclusions

The basic theory is covered in Chapter 2, wich first presents different transistor types and materials used in the active device design and some of the signal properties and RF PA parameters. Closer attention is dedicated to the GaN HEMT devices since it is the technology that has been used in this work due to high power density and high breakdown voltage of GaN

devices, which makes it convenient for the dynamic bias operation. Furthermore, Chapter 2 describes the basic operation principles of the linear power amplifier classes and the common efficiency enhancement and the linearization techniques.

It is important to highlight Section 2.5, which covers the theoretical analysis of the power tracking technique. The power of the modulated signal has significantly narrower and analytically well defined bandwidth compared to the envelope of the modulated signal. This advantage is used for calculation of the bias voltage waveforms for the dynamic biasing at the gate and the drain of the transistor. Namely, the result is the narrower bandwidth of the supply voltage waveform, so the required bandwidth of the supply voltage amplifier is lower. Two types of the tracking functions are proposed; the first one is the PET where the supply voltage is the linear function of the power resulting in the bandwidth equal to the RF bandwidth of the signal, the second one is the 2^{nd} order PET where the supply voltage is the 2^{nd} order polynomial function of the power with the bandwidth of twice the RF bandwidth of the signal.

Chapter 3 presents development of the novel linearity measure as the total nonlinear power contained in the distorted signal. It describes the nonlinear distortion located inside of the signal bandwidth as well as outside of the signal bandwidth. Based on the presented total nonlinear power, the novel figure of merit as the signal to total distortion ratio or simply *STDR* has been developed as the ratio of the linear over the nonlinear power of the observed signal. Maximising the *STDR* minimises the total nonlinear power while simultaneously maximising the linear power. Optimising the RF PA or the linearization technique (the dynamic gate bias tracking curve, DPD, etc.) for the *STDR* simultaneously reduces the distortion outside and inside of the signal bandwidth (*ACPR* and *EVM*).

Chapter 4 deals with the behaviour of the output impedance of the transistor under the dynamic gate bias operation and consequently the question about the optimal matching network. In Chapter 4 the output impedance of the 10 W GaN HEMT from Wolfspeed/Cree is tested by performing the load-pull measurements. The result show that the load impedance for the maximum output power and the maximum *PAE* at the fundamental frequency does not change significantly when the device operates between deep class AB and class A. That makes this device suitable for the dynamic gate bias operation. Furthermore, it is shown that there is the overlapping area of the matching impedances for the 2^{nd} and 3^{rd} harmonics tuned for the maximum *PAE,* where the *PAE* does not drop for more than 3 percentage points from its maximum value when the device operates inside the same gate bias ranege. The large-signal measurements in Section 4.3.1 show that choosing the input matching network which results in

the optimal spread of the gain and/or transfer phase may reduce the required order of the tracking function required for the PA linearization.

Chapter 5 analyses the dynamic gate biasing technique for the linearization of the RF power amplifier. The dynamic gate bias voltage variation is done using the power gate tracking (PGT) due to the advantages explained in Section 2.5. The Matlab simulations based on the measured data of the 10 W GaN RF PA (sort of a behaviour model) showed that the flattening the gain of the RF PA does not improve linearity while flattening the transfer phase provides the significant improvement in the linearity of the RF PA. This result is also confirmed by the laboratory measurements. The measured results using the 4th order gate tracking function are showing *7.2 dB* better *ACPR* and *4.9* percentage points better *EVM* with the *2.5* percentage points lower *PAE* compared to the reference static bias class AB PA. The optimisation of the gate tracking functions for the maximum *STDR* showed that even the low order (1st order i.e. linear function) improves the linearity for *4.6 dB* in *ACPR* and *3.6* percentage points in *EVM* with the *2.5* percentage points lower *PAE*. The gate tracking function of the 3rd order with the optimised coefficients for the maximum *STDR* achieves approximately the same result as the 4th order tracking function for the flat phase.

Section 6.1 in Chapter 6 and Section 7.1 in Chapter 7 are showing how the linearity of the ET and the AET PAs depends on the quiescent gate bias. The measured results show that it is possible to bias these PAs to be more linear with no significant loss in the efficiency. This observation can be applied to any kind of dynamic drain bias PA (ET, PET, AET or APT).

Chapter 6 is mostly dedicated to the power envelope tracking or (PET) and the 2nd order PET techniques presented in Section 2.5. Here, the PET drain voltage tracking curve is strictly defined, while the 2nd order PET drain voltage tracking curve with more degrees of freedom is used for the estimation of the hard-clipped PET and the ET tracking functions in order to reduce the bandwidth of the supply voltage. Compared to the reference static bias class AB PA the PET PA has *9.6 dB* better *ACPR* and *6* percentage points better *EVM* with the *16.8* percentage points higher *PAE*, while the 2nd order PET PA (approximating hard clipped PET) has *10.8 dB* better *ACPR* and *6.4* percentage points better *EVM* with the *14.4* percentage points higher *PAE*. It is clear that both, the PET and the 2nd order PET techniques, are simultaneously improving the linearity and the efficiency of at the RF PA. This is a very exciting result, but it should be noted that it is only tested on the 10 W GaN HEMT and it may not be that effective on other technologies. Compared to the ET PA, the PET PA has *11 dB* better *ACPR* and *6.56* percentage points better *EVM* with *7.1* the percentage points lower *PAE*, while the 2nd order PET PA has

12.2 dB better *ACPR* and *7* percentage points better *EVM* with *9.5* the percentage points lower *PAE*. The significant linearity improvement with the cost of the efficiency is clear from these measured results. The combination of the PET technique with the PGT technique (dual dynamic bias) additionally improves the linearity for *3.7 dB* in the *ACPR* and one percentage point in the *EVM* with the 3rd order PGT tracking function. The combination of the 2nd order PET technique with the PGT technique additionally improves the linearity for *1.7 dB* in *ACPR* and *0.45* percentage point in *EVM* with the 1st order (linear) PGT tracking function.

In Section 6.4 the 2nd order the PET tracking function is used to approximate the conventional ET tracking function with the smoothened clipping areas. The results are showing comparable linearity performance with *1.3* percentage point lower *PAE*. It is clear that both, the 2nd order PET PA and the ET PA have comparable performance, but the former technique assures the significantly narrower bandwidth of the drain supply voltage waveform which is the great advantage of the 2nd order PET over the ET technique. Reduced demand on the bandwidth of the drain supply voltage amplifier simplifies its design. This may lead to the design of the drain supply voltage amplifier with the higher efficiency and possibly better overall efficiency of the 2nd order PET system.

Chapter 7 presents the APT technique based on the power instead of the envelope tracking that is used in the manner of the linearization AET technique. The laboratory measurement of the APT PA shows slightly better linearity and efficiency performance compared to the AET PA. Compared to the reference static bias class AB PA the *ACP*R is improved for *8.8 dB*, *EVM* is *6.4* percentage points lower, and only one percentage point is lost in the *PAE*. The combination of the APT with the PGT technique (combination of two linearization techniques in dual dynamic bias operation) resulted with the additional improvement of *2.5 dB* in the *ACPR* and *0.8* percentage points in the *EVM* with the first order (linear) gate tracking function. Higher orders of the gate tracking functions do not result in significantly better performance.

All measurement in this thesis have been done on the same 10 W GaN PA with the same *1 MHz* 16-QAM signal filtered with the raised cosine filter with the roll-off factor $\alpha=0.22$.

8.2 Future Work

After all the work that has been done, there are still unanswered questions that should be answered in the future work. These questions are summarised below.

Other Materials and Technologies

All techniques in this dissertation have been applied to the 10 W GaN HEMT device, but it would be valuable to test some of these techniques on the other GaN or GaAs based devices. First, it would be worth to check the optimal output impedance sensitivity on the dynamic gate bias operation of other devices.

Due to the suitable gain and transfer phase spread with different gate bias voltages the GaN device can be linearized by flattening the transfer phase with the dynamic gate bias operation using the reasonably high order of the tracking function. It would be valuable to check the gain and transfer phase spread of the other devices and see if dynamic gate biasing can improve their linearity performance and in which way (flattening the phase, flattening the gain or simply optimising for linearity).

Digital Predistortion – DPD

It would also be interesting to see the performance of the PGT PA in combination with the DPD. The question is if DPD system can be simplified if the AM-PM distortion is reduced with the PGT technique and the AM-AM distortion with the DPD or vice versa. The other question here is if the dynamic gate bias of the PA should be generated from the original input signal or the predistorted signal.

Section 6.1indicates that the ET PA can be more linear if one carefully selects the gate bias voltage (not necessarily common class B or deep class AB) with no significant loss in the efficiency. It should be investigated how that influences on the DPD complexity and the performance. The flatter AM-AM and AM-PM characteristics should reduce the DPD order and the power requirements.

Supply Voltage Amplifier (Modulator)

In this dissertation, the efficiency results of the dynamic bias PAs do not include the efficiency of the supply voltage amplifier (tracker). A lot of attention has been dedicated to the power tracking due to reduced and well defined bandwidth of the supply voltage. Future work should include the development of the efficient supply amplifiers for the envelope and the power tracking in order to evaluate and compare these two techniques. Furthermore, techniques should be tested with the signals with much wider bandwidth than *1 MHz*, which requires the wideband supply voltage amplifiers.

References

[1] F. H. Raab, P. Asbeck, S. Cripps, P. B. Kenington, Z. B. Popovich, N. Pothecary, J. F. Sevic, and N. O. Sokal, "RF and Microwave Power Amplifier and Transmitter Technologies-Part 4," *High Freq. Electron.*, pp. 22–36, 2003.

[2] P. B. Kenington, *High-Linearity RF Amplifier Design*. Boston: Artech House, 2000.

[3] Z. Yusoff, J. Lees, J. Benedikt, P. J. Tasker, and S. C. Cripps, "Linearity improvement in RF power amplifier system using integrated Auxiliary Envelope Tracking system," in *2011 IEEE MTT-S International Microwave Symposium*, 2011, pp. 1–4.

[4] M. Juan, O. Morten, and K. M. Gjertsen, "Dual Dynamic Biasing with Input Power Pre compensation for Class-A/AB enhancement," in *TELFOR*, 2009.

[5] J. F. Miranda, K. M. Gjertsen, and M. Olavsbraten, "Optimization theory applied to dynamic biasing for power amplifier performance enhancement," in *2012 IEEE Topical Conference on Power Amplifiers for Wireless and Radio Applications*, 2012, pp. 17–20.

[6] J. F. M. Medina, M. Olavsbraaten, and K. M. Gjertsen, "Biasing an HBT MMIC transistor for efficiency and output power enhancement," in *2012 Workshop on Integrated Nonlinear Microwave and Millimetre-wave Circuits*, 2012, pp. 1–3.

[7] J. F. Miranda, M. Olavsbraten, K. M. Gjertsen, and W. Caharija, "First and second order polynomial functions for bandwidth reduction of dynamic biasing signals," in *2010 IEEE International Conference on Wireless Information Technology and Systems*, 2010, pp. 1–4.

[8] W. Charija, "A Cost-Based Path-Search Algorithm for Enhanced Design With Dynamic Bias," in *TELFOR*, 2009.

[9] P. Lavrador, T. Cunha, P. Cabral, and J. Pedro, “The Linearity-Efficiency Compromise,” *IEEE Microw. Mag.*, vol. 11, no. 5, pp. 44–58, Aug. 2010.

[10] “CGH40010 10-W RF Power GaN HEMT | Wolfspeed.” [Online]. Available: http://www.wolfspeed.com/cgh40010.

[11] J. J. Komiak, “GaN HEMT: Dominant Force in High-Frequency Solid-State Power Amplifiers,” *IEEE Microw. Mag.*, vol. 16, no. 3, pp. 97–105, Apr. 2015.

[12] D. W. Runton, B. Trabert, J. B. Shealy, and R. Vetury, “History of GaN: High-Power RF Gallium Nitride (GaN) from Infancy to Manufacturable Process and Beyond,” *IEEE Microw. Mag.*, vol. 14, no. 3, pp. 82–93, 2013.

[13] R. S. Pengelly, S. M. Wood, J. W. Milligan, S. T. Sheppard, and W. L. Pribble, “A Review of GaN on SiC High Electron-Mobility Power Transistors and MMICs,” *IEEE Trans. Microw. Theory Tech.*, vol. 60, no. 6, pp. 1764–1783, Jun. 2012.

[14] R. Dwilinski, R. Doradzinski, L. Sierzputowski, R. Kucharski, M. Zajac, and J. Krupka, “Highly resistive GaN substrates for high frequency electronics,” in *2013 European Microwave Conference*, 2013, pp. 523–525.

[15] I. D. Robertson and S. Lucyszyn, *RFIC and MMIC Design and Technology*. The Institution of Engineering and Technology, Michael Faraday House, Six Hills Way, Stevenage SG1 2AY, UK: IET, 2001.

[16] F. H. Raab, P. Asbeck, S. Cripps, P. B. Kenington, Z. B. Popovich, N. Pothecary, J. F. Sevic, and N. O. Sokal, “RF and Microwave Power Amplifier and Transmitter Technologies — Part 3,” *High Freq. Electron.*, vol. 2003, pp. 22–36, 2003.

[17] S. A. Maas, *Nonlinear Mivrowave and RF Circuits*, 2nd ed. Artech House, 2003.

[18] R. J. Trew, G. L. Bilbro, W. Kuang, Y. Liu, and H. Yin, “Microwave AlGaN/GaN HFETs,” *IEEE Microw. Mag.*, vol. 6, no. 1, pp. 56–66, Mar. 2005.

[19] J. Schellenberg, A. Tran, Lani Bui, A. Cuevas, and E. Watkins, “37 W, 75–100 GHz GaN power amplifier,” in *2016 IEEE MTT-S International Microwave Symposium (IMS)*, 2016, pp. 1–4.

[20] S. Marsh, *Practical MMIC design*. Artech House, 2006.

[21] E. McCune, *Practical Digital Wireless Signals*, vol. 40700. Cambridge University Press, 2010.

[22] G. Josephson, “On the Definition and Measurement of Occupied Bandwidth,” *IEEE Trans. Electromagn. Compat.*, vol. EMC-12, no. 2, pp. 33–37, May 1970.

[23] M. Olavsbraaten and D. Gecan, “Bandwidth Reduction Technique for Supply Modulated RF PAs using Power Envelope,” *IEEE Microw. Wirel. Components Lett.*

[24] S. C. Cripps, *Advanced Techniques in RF Power Amplifier Design*. 2002.

[25] J. Vuolevi and T. Rahkonen, *Distortion in RF power amplifiers*. Artech House, 2003.

[26] D. Schreurs, M. ODroma, A. A. Goacher, and M. Gadringer, Eds., *RF Power Amplifier Behavioral Modeling*. Cambridge: Cambridge University Press, 2008.

[27] “MathWorks – Makers of MATLAB and Simulink.” [Online]. Available: http://www.mathworks.com/.

[28] D. Gecan, K. M. Gjertsen, and M. Olavsbråten, “Novel Metric Describing Total Nonlinearity of Power Amplifier With a Corresponding Figure of Merit for Linearity Evaluation and Optimization,” *IEEE Microw. Wirel. Components Lett.*, vol. 27, no. 1, pp. 85–87, Jan. 2017.

[29] Mi. Albulet, *RF power amplifiers*. Atlanta, GA: Noble Publishing Corp., 2001.

[30] S. C. Cripps, *RF Power Amplifiers for Wireless Communications, 2nd Edition*. Narwood, MA: Artech House, 2006.

[31] W. H. Doherty, “A New High-Efficiency Power Amplifier for Modulated Waves*,” *Bell Syst. Tech. J.*, vol. 15, no. 3, pp. 469–475, Jul. 1936.

[32] H. Chireix, “High Power Outphasing Modulation,” *Proc. IRE*, vol. 23, no. 11, pp. 1370–1392, Nov. 1935.

[33] T. Barton, “Not Just a Phase: Outphasing Power Amplifiers,” *IEEE Microw. Mag.*, vol. 17, no. 2, pp. 18–31, Feb. 2016.

[34] B. Kim, J. Kim, D. Kim, J. Son, Y. Cho, J. Kim, and B. Park, “Push the Envelope: Design Concepts for Envelope-Tracking Power Amplifiers,” *IEEE Microwave Magazine*, vol. 14, no. 3, pp. 68–81, May-2013.

[35] J. Kim and K. Konstantinou, “Digital predistortion of wideband signals based on power amplifier model with memory,” *Electron. Lett.*, vol. 37, no. 23, p. 1417, 2001.

[36] D. R. Morgan, Z. Ma, J. Kim, M. G. Zierdt, and J. Pastalan, “A Generalized Memory Polynomial Model for Digital Predistortion of RF Power Amplifiers,” *IEEE Trans. Signal Process.*, vol. 54, no. 10, pp. 3852–3860, Oct. 2006.

[37] A. Zhu, J. C. Pedro, and T. J. Brazil, “Dynamic Deviation Reduction-Based Volterra Behavioral Modeling of RF Power Amplifiers,” *IEEE Trans. Microw. Theory Tech.*, vol. 54, no. 12, pp. 4323–4332, Dec. 2006.

[38] A. Katz, J. Wood, and D. Chokola, “The Evolution of PA Linearization: From Classic Feedforward and Feedback Through Analog and Digital Predistortion,” *IEEE Microw. Mag.*, vol. 17, no. 2, pp. 32–40, Feb. 2016.

[39] “Maury Microwave.” [Online]. Available: https://www.maurymw.com/.

[40] “Focus Microwaves.” [Online]. Available: http://www.focus-microwaves.com/.

[41] “Mesuro - advanced RF testing and measurment systems.” [Online]. Available: http://www.mesuro.com/.

[42] P. J. Tasker, “Practical waveform engineering,” *IEEE Microw. Mag.*, vol. 10, no. 7, pp. 65–76, Dec. 2009.

[43] Verspecht-Teyssier-DeGroote SAS, “SWAP-X402 The simple and affordable way to add time domain waveform capability to your load-pull setup.”

[44] Maury Microwave, “Device characterization with harmonic source and load pull,” *Appliction Note 5C-044*, 2000.

[45] “Advanced Design System (ADS) | Keysight (formerly Agilent’s Electronic Measurement).” [Online]. Available: http://www.keysight.com/en/pc-1297113/advanced-design-system-ads?cc=US&lc=eng.

[46] J. Benedikt, R. Gaddi, P. J. Tasker, M. Goss, and M. Zadeh, “High power time domain measurement system with active harmonic load-pull for high efficiency base station amplifier design,” in *2000 IEEE MTT-S International Microwave Symposium Digest (Cat. No.00CH37017)*, vol. 3, pp. 1459–1462.

[47] A. Conway, Yu Zhao, P. Asbeck, M. Micovic, and Jeong Moon, “Dynamic Gate Bias Technique for Improved Linearity of GaN HFET Power Amplifiers,” in *IEEE MTT-S International Microwave Symposium Digest, 2005.*, pp. 499–502.

[48] J. F. Villemazet, A. Ramadan, L. Lapierre, P. Medrel, J. M. Nebus, and P. Bouysse, “High efficiency class B GaN power amplifier with dynamic gate biasing for improved linearity,” *Electron. Lett.*, vol. 48, no. 18, pp. 1136–1137, Aug. 2012.

[49] J. F. Medina, “Dynamic biasing for linear power amplifier efficiency enhancement (Doctoral disertation),” Norwegian University of Science and Technology, 2012.

[50] E. McCune, *Dynamic power supply transmitters : envelope tracking, direct polar, and hybrid combinations*. Cambridge: Cambridge University Press.

[51] L. Larson, D. Kimball, and P. Asbeck, “Wideband envelope tracking power amplifiers for wireless communications,” in *2014 IEEE 14th Topical Meeting on Silicon Monolithic Integrated Circuits in Rf Systems*, 2014, pp. 32–37.

[52] M. Hassan, L. E. Larson, V. W. Leung, D. F. Kimball, and P. M. Asbeck, “A Wideband CMOS/GaAs HBT Envelope Tracking Power Amplifier for 4G LTE Mobile Terminal Applications,” *IEEE Trans. Microw. Theory Tech.*, vol. 60, no. 5, pp. 1321–1330, May 2012.

[53] J. Jeong, D. F. Kimball, M. Kwak, C. Hsia, P. Draxler, and P. M. Asbeck, “Wideband envelope tracking power amplifier with reduced bandwidth power supply waveform,” in *2009 IEEE MTT-S International Microwave Symposium Digest*, 2009, pp. 1381–1384.

[54] Jinseong Jeong, D. F. Kimball, Myoungbo Kwak, Chin Hsia, P. Draxler, and P. M. Asbeck, “Wideband Envelope Tracking Power Amplifiers With Reduced Bandwidth Power Supply Waveforms and Adaptive Digital Predistortion Techniques,” *IEEE Trans. Microw. Theory Tech.*, vol. 57, no. 12, pp. 3307–3314, Dec. 2009.

[55] P. J. Draxler, D. F. Kimball, and P. M. Asbeck, “Nonlinearity consideration of GaN based envelope tracking power amplifiers,” in *2012 IEEE/MTT-S International Microwave Symposium Digest*, 2012, pp. 1–3.

Appendices

Appendix A

Tables containing Measured Results of Linearity Dependence on Gate Bias Voltage

This appendix contains measured data of the PAs that have been dynamically biased at the drain side for a set of the static gate bias voltages between the deep class AB to the class A. It shows only the measured data that has not presented earlier.

A.1 Linearity Dependence of the PET PA on Gate Bias Voltage

Table A.1: Measured results of the PET PA for the set of the static gate bias voltage values.

V_{GQ} [V]	P_{in} [dBm]	PAE [%]	$ACPR_L$ [dBc]	$ACPR_R$ [dBc]	EVM [%]	STDR [dB]
-2.7	20.0	55.5	-28.6	-28.4	10.11	19.17
-2.6	19.7	55.7	-30.5	-30.8	7.62	21.53
-2.5	19.6	55.7	-33.2	-33.6	5.04	24.74
-2.4	19.5	55.0	-36.7	-37.4	3.12	28.17
-2.3	19.3	55.0	-41.1	-41.1	2.68	28.68
-2.2	19.2	54.4	-41.0	-40.2	3.52	26.36
-2.1	19.2	53.4	-37.4	-36.8	5.26	23.40
-2.0	19.2	52.3	-34.7	-34.3	7.01	21.25
-1.9	19.1	50.8	-33.1	-32.8	8.12	19.86

A.2 Linearity Dependence of the 2nd order PET PA Approximating Tracking Curve of the PET PA on Gate Bias Voltage

Table A.2: Measured results of the 2nd order PET approximation of the PET PA for the set of the static gate bias voltage values.

V_{GQ} [V]	P_{in} [dBm]	PAE [%]	$ACPR_L$ [dBc]	$ACPR_R$ [dBc]	EVM [%]	STDR [dB]
-2.7	19.9	52.0	-28.9	-28.8	9.5	19.4
-2.6	19.6	52.3	-30.7	-31.2	7.2	21.54
-2.5	19.3	53.3	-34.0	-33.9	4.78	24.91
-2.4	19.2	52.7	-37.6	-38.7	2.63	29.22
-2.3	19.1	52.6	-42.3	-42.4	2.24	30.69
-2.2	18.9	53.2	-40.1	-40.4	3.56	27.18
-2.1	18.9	51.7	-36.4	-36.2	5.41	23.82
-2.0	18.9	49.1	-34.0	-33.8	7.01	21.72
-1.9	18.8	47.6	-32.5	-32.3	8.23	20.21

A.3 Linearity Dependence of the ET PA with Smoothened Clipping Edges on Gate Bias Voltage

Table A.3: Measured results of the ET PA with the smoothened clipping edges for the set of the static gate bias voltage values.

V_{GQ} [V]	P_{in} [dBm]	PAE [%]	$ACPR_L$ [dBc]	$ACPR_R$ [dBc]	EVM [%]	STDR [dB]
-2.7	20.8	62.0	-28.9	-28.5	-	19.22
-2.6	20.6	62.4	-29.6	-30.1	8.32	20.23
-2.5	20.6	63.1	-30.4	-30.8	8.5	20.36
-2.4	20.5	62.3	-30.6	-30.3	9.48	19.70
-2.3	20.4	62.0	-29.9	-29.7	10.87	18.60
-2.2	20.4	61.6	-28.9	-28.7	12.39	17.47
-2.1	20.4	61.7	-27.8	-27.7	13.97	16.39
-2.0	20.3	60.2	-26.8	-26.6	15.61	15.40
-1.9	20.3	59.4	-25.9	-25.9	17.07	14.60

A.4 Linearity Dependence of the 2nd order PET PA Approximating Tracking Curve of the ET PA on Gate Bias Voltage

Table A.4: Measured results of the 2nd order PET approximation of the PET PA for the set of the static gate bias voltage values.

V_{GQ} [V]	P_{in} [dBm]	PAE [%]	$ACPR_L$ [dBc]	$ACPR_R$ [dBc]	EVM [%]	STDR [dB]
-2.7	20.8	60.1	-28.0	-28.6	9.09	17.76
-2.6	20.6	61.6	-29.6	-29.3	8.34	19.66
-2.5	20.4	61.6	-30.3	-29.9	8.54	19.77
-2.4	20.4	61.1	-29.9	-30.1	9.45	19.16
-2.3	20.3	61.7	-29.5	-29.3	10.85	18.17
-2.2	20.3	60.8	-28.5	-28.4	12.37	17.10
-2.1	20.2	61.0	-27.4	-27.4	14.18	15.99
-2.0	20.2	60.2	-26.5	-26.4	18.81	15.04
-1.9	20.2	57.5	-25.8	-25.6	17.16	14.35

A.5 Linearity Dependence of the APT PA on Gate Bias Voltage

Table A.4: Measured results of the APT PA for the set of the static gate bias voltage values.

V_{GQ} [V]	P_{in} [dBm]	PAE [%]	$ACPR_L$ [dBc]	$ACPR_R$ [dBc]	EVM [%]	STDR [dB]
-2.7	19.5	38.1	-28.8	-28.9	9.82	18.01
-2.6	19.2	38.0	-30.9	-31.0	7.59	19.80
-2.5	19.0	37.6	-33.7	-33.7	5.55	22.04
-2.4	18.7	37.1	-37.0	-37.0	3.61	24.67
-2.3	18.5	37.1	-40.3	-40.3	2.17	27.45
-2.2	18.3	36.2	-40.1	-40.9	1.85	29.09
-2.1	18.3	34.6	-39.6	-39.4	2.83	28.31
-2.0	18.1	33.2	-38.8	-38.9	3.47	27.56
-1.9	17.9	31.1	-39.1	-39.1	3.19	27.54

Appendix B

Layouts of measured devices and measurement setup

B.1 Fixture for load-pull measurements

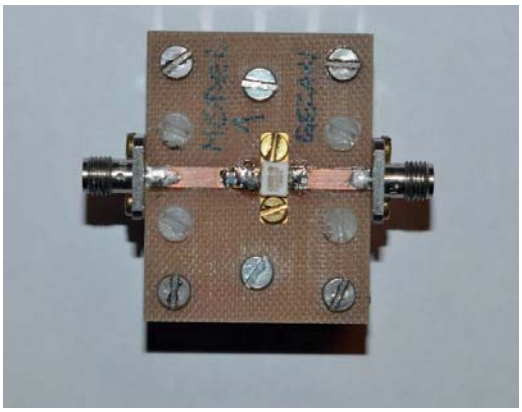

Figure B.1: Fixture for the load-pull measurements.

B.2 Photo of the 10 W GaN HEMT PA measured in this dissertation

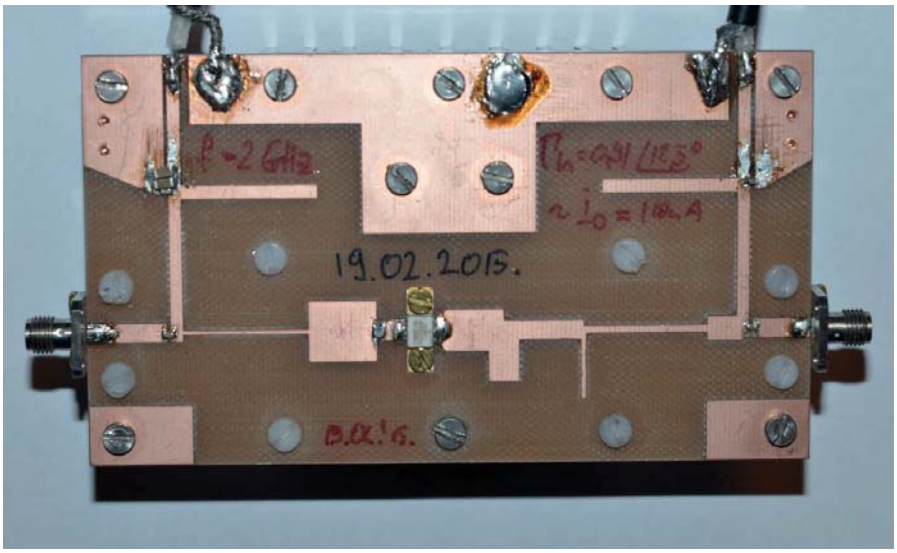

Figure B.2: Photo of the 10 W GaN HEMT PA measured in this dissertation.

B.3 Large signal measurement setup

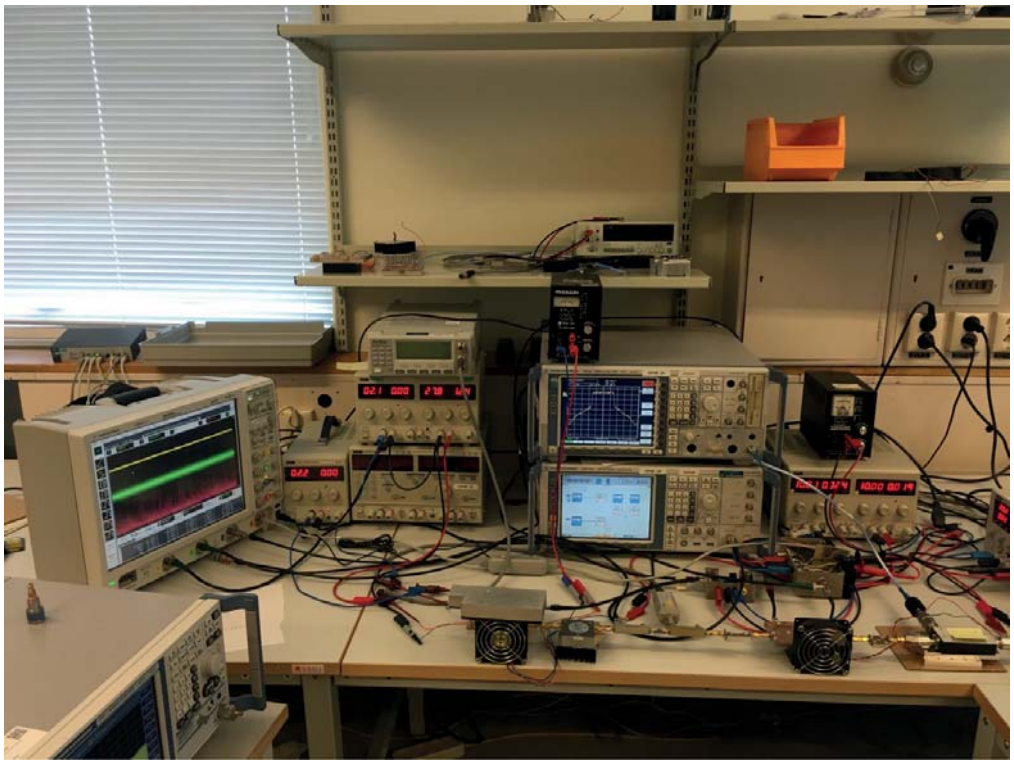

Figure B.3: Large signal measurement setup.

Appendix C

Envelope of the 16-QAM signal and the bias and the supply voltage waveforms

C.1 Envelope of the input signal and the PGT bias waveform

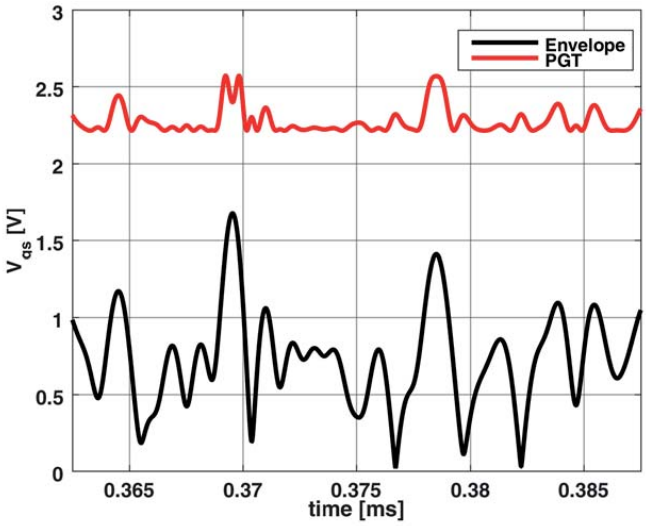

Figure C.1: Envelope of the 16-QAM signal at the input of the DUT (not at the intrinsic gate) and the PGT bias voltage waveform.

C.2 Envelope of the output signal and drain supply voltage waveforms of different techniques (ET, PET, 2nd order PET, AET and APT)

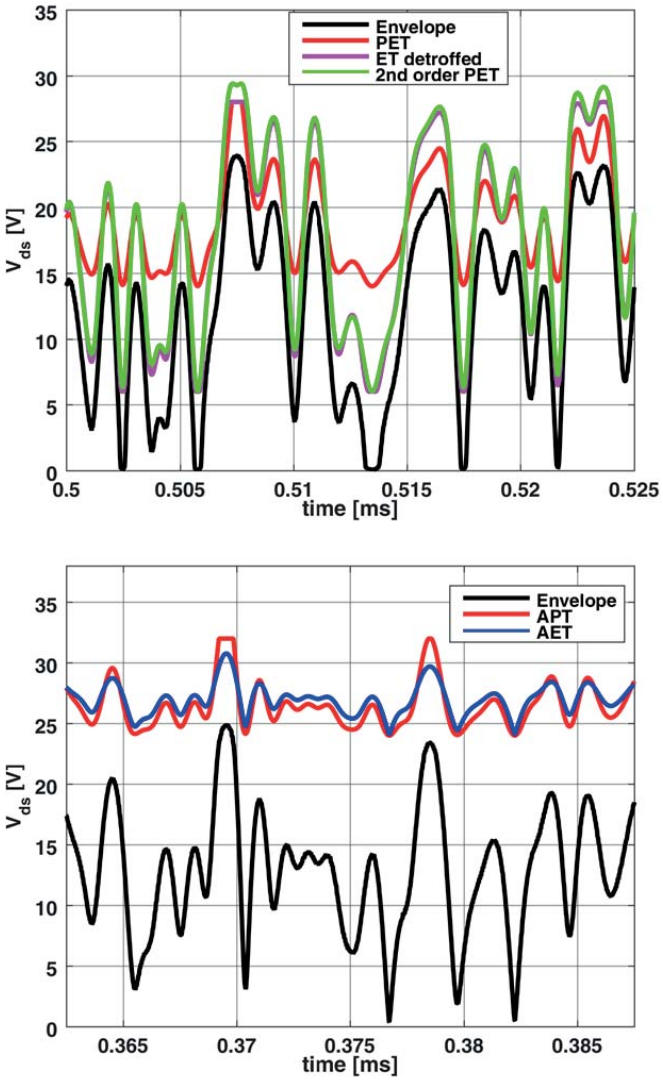

Figure C.2: Approximated intrinsic envelope of the output 16-QAM signal (on both figures). The drain supply voltage waveforms of the PET, detroughed ET and the 2nd order PET as the approximation of the ET (upper figure). The drain supply voltage waveforms of the AET and the APT techniques (lower figure).

Appendix D

List of Papers with Clarification of the Author's Contribution and Appended Papers

The following papers are appended to this thesis.

Paper I

D. Gecan, M. Olavsbraten and K. M. Gjertsen, "Investigation of the practical output load impedance sensitivity of a 10 W GaN device subject to gate bias variation," *2016 IEEE Topical Conference on Power Amplifiers for Wireless and Radio Applications (PAWR)*, Austin, TX, 2016, pp. 45-48.

The author designed the fixture for the device under test, calibrated the measurement setup and performed the measurements. The results have been discussed with M. Olavsbråten and Karl M. Gjertsen.

Paper II

D. Gecan, M. Olavsbråten and K. M. Gjertsen, "Investigation of linearity improvement with dynamic gate bias technique for flat gain or phase of an 10 W GaN HEMT power amplifier," 2016 IEEE/ACES International Conference on Wireless Information Technology and Systems (ICWITS) and Applied Computational Electromagnetics (ACES), Honolulu, HI, 2016, pp. 1-2.

The author performed measurements of the power amplifier for the behavioural model, wrote a simulation code in Matlab, performed the simulation and analysed the results. The results have been discussed with M. Olavsbråten and Karl M. Gjertsen. The power amplifier has been designed by the author in collaboration with M. Olavsbråten.

Paper III

D. Gecan, M. Olavsbraten and K. M. Gjertsen, "Comprehensive investigation of a dynamic gate biasing technique for linearity improvement based on measurement of a 10 W GaN HEMT power amplifier," *2016 24th Telecommunications Forum (TELFOR)*, Belgrade, 2016, pp. 1-3.

The author performed measurements of the power amplifier for the behavioural model, wrote a simulation code in Matlab, performed the simulations for various tracking functions and analysed the results. The results have been discussed with M. Olavsbråten and Karl M. Gjertsen. The power amplifier has designed by the author in collaboration with M. Olavsbråten.

Paper IV

D. Gecan, M. Olavsbråten and K. M. Gjertsen, "Measured linearity improvement of 10 W GaN HEMT PA with dynamic gate biasing technique for flat transfer phase," 2016 IEEE MTT-S International Microwave Symposium (IMS), San Francisco, CA, 2016, pp. 1-4.

The author wrote a code in Matlab to control the measurement equipment, performed the measurements for various tracking functions and analysed the results. The results have been discussed with M. Olavsbråten and Karl M. Gjertsen. The power amplifier has been designed by the author in collaboration with M. Olavsbråten.

Paper V

D. Gecan, K. M. Gjertsen and M. Olavsbråten, "Novel Metric Describing Total Nonlinearity of Power Amplifier With a Corresponding Figure of Merit for Linearity Evaluation and Optimization," in IEEE Microwave and Wireless Components Letters, vol. 27, no. 1, pp. 85-87, Jan. 2017.

The idea has been proposed by Karl M. Gjertsen. The elaboration of the proposed idea has been elaborated by the author and discussed with Karl M. Gjertsen and M. Olavsbråten. The Matlab code for the instrument control and tracking function optimization has been written by the author. All the measurements have been performed by the author.

Paper VI

D. Gecan, M. Olavsbraten and K. M. Gjertsen, "Investigation of the gate bias voltage influence on linearity performance of the ET and AET 10 W GaN HEMT PAs," 2016 24th Telecommunications Forum (TELFOR), Belgrade, 2016, pp. 1-3.

The author performed measurements and wrote the Matlab code for instrument control and result analysis. The results have been discussed with M. Olavsbråten and Karl M. Gjertsen. The power amplifier has been designed by the author in collaboration with M. Olavsbråten.

Paper VII

D. Gecan, M. Olavsbraten and K. M. Gjertsen, " Auxiliary Power Tracking Technique for Linearity Improvement of a 10 W GaN HEMT PA with and without Power Gate Tracking," *2017 IEEE Topical Conference on Power Amplifiers for Wireless and Radio Applications (PAWR)*, Phoenix, AZ, 2016

The author wrote the Matlab code for the instrument control, tracking function optimisation and performed the measurements. The results have been discussed with M. Olavsbråten and Karl M. Gjertsen. The power amplifier has been designed by the author in collaboration with M. Olavsbråten.

The following papers are not appended to this thesis.

Paper VIII

M. Olavsbråten and D. Gecan, "Bandwidth Reduction for Supply Modulated RF PAs Using Power Envelope Tracking," in *IEEE Microwave and Wireless Components Letters*, vol. 27, no. 4, pp. 374-376, April 2017.

The theory has been elaborated by M. Olavsbråten. The author performed the measurements and wrote the Matlab script for the instrument control.

Appendix E

Published Papers

Paper I: Investigation of the practical output load impedance sensitivity of a 10 W GaN device subject to gate bias variation

Is not included due to copyright

Paper II: Investigation of linearity improvement with dynamic gate bias technique for flat gain or phase of an 10 W GaN HEMT power amplifier

Is not included due to copyright

Paper III: Comprehensive investigation of a dynamic gate biasing technique for linearity improvement based on measurement of a 10 W GaN HEMT power amplifier

Is not included due to copyright

Paper IV: Measured linearity improvement of 10 W GaN HEMT PA with dynamic gate biasing technique for flat transfer phase

Is not included due to copyright

Paper V: Novel Metric Describing Total Nonlinearity of Power Amplifier With a Corresponding Figure of Merit for Linearity Evaluation and Optimization

Is not included due to copyright

Paper VI: Investigation of the gate bias voltage influence on linearity performance of the ET and AET 10 W GaN HEMT PAs

Is not included due to copyright

Paper VII: Auxiliary Power Tracking Technique for Linearity Improvement of a 10 W GaN HEMT PA with and without Power Gate Tracking

Is not included due to copyright